


Free-electron–light interactions in nanophotonics

Cite as: Appl. Phys. Rev. **10**, 011303 (2023); <https://doi.org/10.1063/5.0118096>

Submitted: 03 August 2022 • Accepted: 15 December 2022 • Published Online: 18 January 2023

 Charles Roques-Carmes,  Steven E. Kooi,  Yi Yang, et al.

COLLECTIONS

 This paper was selected as Featured



View Online



Export Citation



CrossMark

ARTICLES YOU MAY BE INTERESTED IN

[Nucleic acid nanostructures for in vivo applications: The influence of morphology on biological fate](#)

Applied Physics Reviews **10**, 011304 (2023); <https://doi.org/10.1063/5.0121820>

[Adhesive tapes: From daily necessities to flexible smart electronics](#)

Applied Physics Reviews **10**, 011305 (2023); <https://doi.org/10.1063/5.0107318>

[Advanced fiber in-coupling through nanoprinted axially symmetric structures](#)

Applied Physics Reviews **10**, 011401 (2023); <https://doi.org/10.1063/5.0127370>



Applied Physics Reviews

Special Topic: Materials and Technologies
for Bioimaging and Biosensing

Submit Today!

Free-electron-light interactions in nanophotonics

Cite as: Appl. Phys. Rev. **10**, 011303 (2023); doi: [10.1063/5.0118096](https://doi.org/10.1063/5.0118096)

Submitted: 3 August 2022 · Accepted: 15 December 2022 ·

Published Online: 18 January 2023



View Online



Export Citation



CrossMark

Charles Roques-Carmes,^{1,a)}  Steven E. Kooi,²  Yi Yang,^{1,3,4}  Nicholas Rivera,^{3,5}  Phillip D. Keathley,¹ 
John D. Joannopoulos,^{2,3}  Steven G. Johnson,⁶  Ido Kaminer,⁷  Karl K. Berggren,¹  and Marin Soljačić^{1,5} 

AFFILIATIONS

¹Research Laboratory of Electronics, MIT, Cambridge, Massachusetts 02139, USA

²Institute for Soldier Nanotechnologies, MIT, Cambridge, Massachusetts 02139, USA

³Department of Physics, MIT, Cambridge, Massachusetts 02139, USA

⁴Department of Physics, University of Hong Kong, Hong Kong, China

⁵Department of Physics, Harvard University, Cambridge, Massachusetts 02138, USA

⁶Department of Mathematics, MIT, Cambridge, Massachusetts 02139, USA

⁷Department of Electrical and Computer Engineering, Technion, Haifa 32000, Israel

^{a)} Author to whom correspondence should be addressed: chrc@mit.edu

ABSTRACT

When impinging on optical structures or passing in their vicinity, free electrons can spontaneously emit electromagnetic radiation, a phenomenon generally known as cathodoluminescence. Free-electron radiation comes in many guises: Cherenkov, transition, and Smith–Purcell radiation, but also electron scintillation, commonly referred to as incoherent cathodoluminescence. While those effects have been at the heart of many fundamental discoveries and technological developments in high-energy physics in the past century, their recent demonstration in photonic and nanophotonic systems has attracted a great deal of attention. Those developments arose from predictions that exploit nanophotonics for novel radiation regimes, now becoming accessible thanks to advances in nanofabrication. In general, the proper design of nanophotonic structures can enable shaping, control, and enhancement of free-electron radiation, for any of the above-mentioned effects. Free-electron radiation in nanophotonics opens the way to promising applications, such as widely tunable integrated light sources from x-ray to THz frequencies, miniaturized particle accelerators, and highly sensitive high-energy particle detectors. Here, we review the emerging field of free-electron radiation in nanophotonics. We first present a general, unified framework to describe free-electron light–matter interaction in arbitrary nanophotonic systems. We then show how this framework sheds light on the physical underpinnings of many methods in the field used to control and enhance free-electron radiation. Namely, the framework points to the central role played by the photonic eigenmodes in controlling the output properties of free-electron radiation (e.g., frequency, directionality, and polarization). We then review experimental techniques to characterize free-electron radiation in scanning and transmission electron microscopes, which have emerged as the central platforms for experimental realization of the phenomena described in this review. We further discuss various experimental methods to control and extract spectral, angular, and polarization-resolved information on free-electron radiation. We conclude this review by outlining novel directions for this field, including ultrafast and quantum effects in free-electron radiation, tunable short-wavelength emitters in the ultraviolet and soft x-ray regimes, and free-electron radiation from topological states in photonic crystals.

Published under an exclusive license by AIP Publishing. <https://doi.org/10.1063/5.0118096>

TABLE OF CONTENTS

I. INTRODUCTION	2	C. Recent milestones enabled by nanophotonics	6
A. Free-electron–light interaction mediated by nanophotonic structures	3	II. TYPOLOGY OF FREE-ELECTRON RADIATION	8
1. Grazing-angle interaction zone	4	A. Coherent vs incoherent cathodoluminescence	8
2. Impact interaction zone	5	B. A unifying picture of coherent cathodoluminescence in arbitrary nanophotonic environments	8
B. Fundamental discoveries in free-electron physics	6	1. Cherenkov radiation	9

2. Smith–Purcell radiation	10
3. Transition radiation	11
4. Coherent excitation of surface plasmon polaritons (SPPs) by free electrons	11
C. Fundamental bounds for coherent cathodoluminescence	11
D. Incoherent cathodoluminescence (electron scintillation)	12
III. CONTROL AND ENHANCEMENT OF CATHODOLUMINESCENCE WITH NANOPHOTONICS	12
A. Cathodoluminescence in electron microscopes	12
1. Cathodoluminescence spectroscopy and polarimetry techniques	12
2. Probing electron–light interactions in ultrafast electron microscopes	14
3. Free-electron analogs	14
B. Controlling free-electron radiation in nanophotonic structures	14
1. Angular and spectral control	14
2. Polarization control	15
3. Spatial control	16
C. Enhancing free-electron–light interactions in nanophotonics	16
1. Coherent cathodoluminescence	16
2. Incoherent cathodoluminescence and scintillation	16
3. Nanophotonic scintillators for x- and γ -ray detection	17
IV. FUTURE PERSPECTIVES	17
A. Quantum effects	17
1. Recoil effects	17
2. Quantum interference and wavelshaping effects	19
3. High-order effects in quantum electrodynamics	19
B. Ultrashort-wavelength emitters	19
C. Nanophotonic dielectric laser accelerators	21
D. Inverse-designed free-electron radiators and accelerators	21
E. Free-electron lasing in nanophotonic structures and other exotic effects	22
F. Topological effects in free-electron radiation	22
G. Non-equilibrium emission processes with free electrons	22
H. Fully integrated on-chip systems	23
V. CONCLUSION	23

NOMENCLATURE

BIC	Bound state in the continuum
BZ	Brillouin zone
CL	Cathodoluminescence
CR	Cherenkov radiation
EELS	Electron energy-loss spectroscopy
ICL	Incoherent cathodoluminescence
NIR	Near-infrared

PhC	Photonic crystal
PINEM	Photon-induced near-field electron microscopy
SPP	Surface plasmon polariton
SPR	Smith–Purcell radiation
TR	Transition radiation
UV	Ultraviolet

I. INTRODUCTION

The interaction of free electrons with light and matter is a century-old field of research that has had profound implications in electron microscopy, radiation sources, and high-energy particle detection. At the heart of this field lies a few fundamental discoveries, unveiling various conditions in which free electrons can convert part of their energy into photons.^{1–5} On the other hand, over the past two decades, nanophotonics has emerged as a platform to control photonic modes at the nanoscale, by patterning materials at scales comparable to the photon wavelength. The recent merger of these two fields has spurred new applications and fundamental discoveries.^{6–32} This review is dedicated to (1) provide a general understanding of free-electron–light interactions mediated by nanophotonic structures; (2) highlight recent theoretical and experimental developments in the field; and (3) outline future prospects for fundamental research and novel applications.

How can charged particles emit light? This fundamental question has driven much development in theoretical and experimental physics in the 20th century. Perhaps, the original interest in this question can be traced back to early discoveries in radioactivity, where luminescence from liquids was used to detect the presence of radioactive substances.^{33,34} Later on, emission processes, such as the Cherenkov effect, were extensively used to track and detect particles.^{35–38} Therefore, the understanding of radiation processes from charged particles, such as free electrons, has evolved in tandem with some of the most profound discoveries of modern physics, such as quantum electrodynamics and particle detection within and beyond the standard model.^{37,39} Concepts from free-electron radiation have also permeated throughout many fields of physics, from nonlinear optics to gravitational physics.⁴⁰ Other forms of spontaneous emission induced by free-electron (de)acceleration—which are not covered in this review—have received a lot of interest, especially in the context of free-electron lasers.^{41,347}

Much more recently, nanophotonics has become a paramount framework and technology, enabling, among other things, the design of novel light sources, detectors, and devices controlling the polarization, spectral, and angular distribution of light.^{42,43} A hallmark of nanophotonics is the design of nanostructured materials (metasurfaces,⁴⁴ photonic crystals,^{42,45} resonators,^{46,47} etc.) to tailor the interaction of light with matter, either by shaping light propagation at the nanoscale or by controlling emission from atoms and molecules. Historically, plasmonics played a paramount role in the development of free-electron physics, as it was realized early on that free electron beams could be utilized to excite and study plasmonic modes in metallic thin films and nanostructures.^{7,9,48,49}

Free electrons and other types of charged high-energy particles usually carry large kinetic energies compared to the energies of optical photons often controlled with nanophotonics and can, in principle, emit photons with any energy below the kinetic energy of the electron (including at optical frequencies). The perspective of enhancing and controlling free-electron radiation with nanophotonics, thus, applies to wide spectral ranges.

There has been a recent surge of interest in research at the intersection of free-electron physics and nanophotonics.^{28,29} If this research is successful, nanophotonics-enhanced free-electron light sources could cover the entire electromagnetic spectrum, with controllable polarization, spectral, spatial, and angular properties. This perspective is all the more attractive for regions of the electromagnetic spectrum where sources are scarce, inefficient, bulky, and/or expensive [such as THz, deep ultraviolet (UV), and x-rays], enabling novel lab-on-chip applications. Unveiling novel regimes of free-electron radiation in nanophotonic systems would also open the way to enhanced beam diagnosis and detection tools, such as Cherenkov and scintillation detectors, that are ubiquitous in many domains of modern science and engineering.^{35–38,50,51} Such detectors could, for instance, leverage various effects in nanophotonics to significantly increase their sensitivity and strongly discriminate signals from various incident particles.^{52,53}

The inverse effects have also attracted a great amount of attention: in nanostructures absorbing energy from powerful lasers, particles can be accelerated, forming the basis for highly compact particle accelerators that may even one day fit on a chip.^{22,54,55} Nanophotonic particle accelerators exhibit much higher damage threshold and acceleration gradient than conventional linear accelerators and their compact form factor opens the perspectives of point-of-care radiation medicine and table-top high-energy electron microscopes. One should expect other areas of nanophotonics, such as topological photonics and design optimization (via inverse design and topology optimization), to have an equivalently important impact on nanophotonics-enhanced free-electron physics. In this context, we wish to provide a unified picture of free-electron radiation in nanophotonic structures, highlighting physical processes to control and enhance radiation, thereby enabling some of the applications mentioned above.

In all of the above-mentioned applications, recent works^{56–64} have highlighted the possibility of shaping the quantum properties of free electrons and the emitted radiation. This branch of work could also open the way to novel sources of quantum light with controllable properties.

Previous works reviewed experimental results in electron–light interactions, providing frameworks to calculate electron energy loss spectroscopy (EELS) and cathodoluminescence (CL) in classical and quantum regimes.²⁸ More recent reviews highlighted spectroscopy techniques combining the unprecedented combination of high space, energy, and time resolution enabled by electron beams, with a focus on quantum and ultrafast effects.²⁹

In this review, we highlight the role of nanophotonics in free-electron physics and electron–light interactions. We show how one can control and enhance the interaction of electron beams with photonic modes for various types of free-electron radiation physics. We first give a high-level overview of several types of free-electron radiation processes, followed by a historical timeline of the field of free-electron physics, and an outline of some of the recent achievements enabled in this field by nanophotonics. In Sec. II A, we then revisit the typology of free-electron radiation with a general formalism accounting for most types of coherent (Secs. II B 1–II B 4) and incoherent cathodoluminescence (Sec. II D). With building blocks of the formalism outlined in Sec. II, we revisit several types of free-electron radiation as a form of interaction between a free electron and specific photonic eigenmodes in a nanophotonic structure. We also connect our formalism to recent works on calculating bounds for free-electron radiation

and energy loss in nanophotonics (Sec. II C). In Sec. III, we review experimental methods and considerations to observe and quantify such effects (Sec. III A) and describe nanophotonic techniques to control (Sec. III B) and enhance (Sec. III C) (coherent and incoherent) cathodoluminescence. We then outline several exciting perspectives at the intersection of nanophotonics and free-electron physics in Sec. IV. We conclude this review in Sec. V by summarizing our main findings, progress in the field, and future applications of this active field of research.

A. Free-electron–light interaction mediated by nanophotonic structures

Free electrons can emit light in many different ways. Radiation generally occurs when the electron (with charge q and propagating at velocity \mathbf{v}) interacts with a structure or medium supporting photonic modes such that energy-momentum conservation is satisfied. In general, one can predict which modes are excited by a free electron by considering the phase-matching condition:⁶⁵

$$\omega = \mathbf{v} \cdot \mathbf{k}, \quad (1)$$

where ω is the photon frequency and \mathbf{k} is its wavevector. This condition requires that the electron velocity and the mode phase velocity coincide. From this formula, many situations in free-electron radiation can be readily analyzed. For example, one immediate consequence of Eq. (1) is that in free space, free-electron radiation from uniformly moving particles is prohibited. It would require the electron to move at the phase velocity of light in vacuum. Unless stated otherwise, in the following, we will consider *point* electrons propagating in rectilinear motion defined by \mathbf{v} in three-dimensional space. This is in contrast to *sheet* electrons, which can be considered in two-dimensional problems as a mathematical convenience that reduces computational complexity. In the latter case, the transverse component of the momentum in Eq. (1) can be neglected.

Nanophotonic structures with various geometries and symmetries enable the control of the dispersion relation $\omega(\mathbf{k})$. In particular, because of the ability of these structures to reduce the phase velocity of light, they enable radiation in situations where unstructured materials may not. In periodic media, Bloch modes generally have an infinite Fourier series of components at wavevectors given by $\mathbf{k} = \mathbf{k}' + \mathbf{G}$, where \mathbf{k}' lies in the first Brillouin Zone (BZ) and \mathbf{G} is a reciprocal lattice vector. This means that Eq. (1) can be satisfied at arbitrary small velocities \mathbf{v} , which is why Smith–Purcell radiation (SPR)—an effect we discuss extensively in this review—has no low-velocity cutoff. Another important consequence of Eq. (1) is that for structures that break translation symmetry (e.g. a photonic crystal defect cavity or a plasmonic nanoparticle), photonic modes have all possible wavevectors, allowing photon emission into any localized mode. The ease of phase-matching free electrons with nanoparticles is of historical significance, since it accelerated the development of research at the intersection of nanophotonics and free-electron physics.⁶ Another example in which translation-symmetry-breaking is important is in transition radiation, discussed below, where the interface between two materials is chiefly responsible for the emitted light.

A typical interaction of an electron beam with a sample is shown in Fig. 1. A beam of electrons interacts with a sample in two distinct

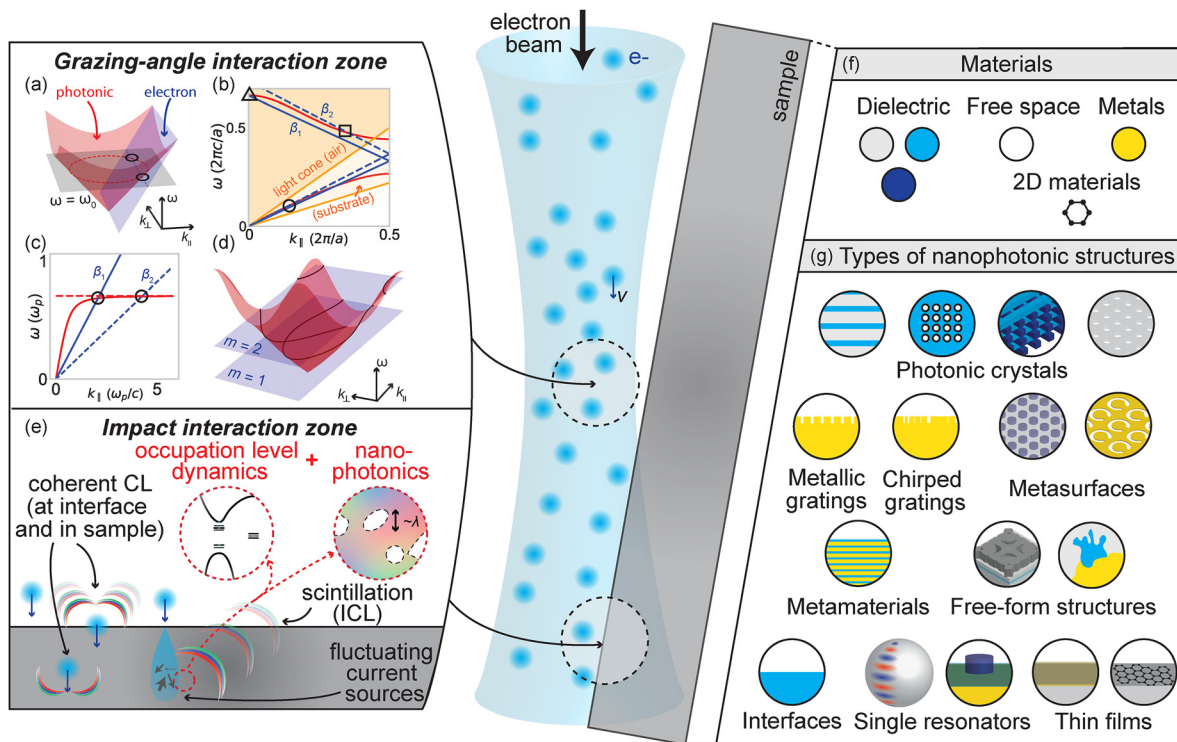


FIG. 1. Overview of free-electron radiation in nanophotonics. Schematic of an electron beam interacting with a sample. Radiation can occur from events in the “grazing-angle interaction zone” (a)–(d) or in the “impact interaction zone” (e). In this review, we discuss interactions of free-electrons with nanophotonic structures made of materials as listed in (f) and of geometries as listed in (g). In (a)–(d), the electrons’ surfaces/lines are shown in blue and photonic mode band structures are shown in red. (a) Schematic band structure of Cherenkov radiation in uniform medium. The black plane represents an isofrequency plane with intersections of red and blue surfaces shown as dashed lines. (b) Schematic band structure of free electrons interacting with a one-dimensional periodic photonic crystal (PhC) slab waveguide. Free electrons propagating at velocity β_1 (full line) can excite guided modes (circles) and symmetry-protected bound states in the continuum (triangle). Free electrons propagating at velocity β_2 (dashed line) can excite guided modes (circles) and leaky resonances (square). (c) Dispersion plot of plasmon polariton (SPP) excitation by free electrons flying above a vacuum-metal interface. Free electrons propagating at various speeds can excite modes of various energies under the cutoff ($\omega_p/\sqrt{2}$). (d) Dispersion plot of free-electron radiation in a two-dimensional periodic PhC. Electron planes with various radiation orders $m \in \mathbb{N}$ can intersect the photonic band structure. (e) In the impact interaction zone, emission can occur at the boundary between vacuum and sample [resulting in transition radiation (TR)]; by excitation of photonic modes after penetration in the sample; or from emitters in the sample excited in the electron energy loss volume (shown in blue). Emission from fluctuating current sources can be modeled by taking into account their occupation level dynamics and the nanophotonic environment in which they emit.^{27,66}

manners, corresponding to the grazing-angle and impact interaction zones. We now proceed to discuss each of these two zones separately.

1. Grazing-angle interaction zone

In the grazing-angle interaction zone, the phase-matching condition from Eq. (1) allows us to predict which photonic modes are excited by free electrons, given prior knowledge of the photonic modes, as shown in Figs. 1(a)–1(d). This general principle accounts for the excitation of localized and extended modes, in various photonic environments.

More specifically, as shown in Figs. 1(a)–1(d), electrons passing in the vicinity of photonic structures can transfer some of their energy into available modes. Examples of such interactions include Cherenkov radiation from free electrons propagating in a uniform medium [Fig. 1(a)]; excitation of guided, radiative, and bound states in the continuum (BIC) modes in photonic crystals (PhC) [Fig. 1(b)]; excitation of surface plasmon polaritons (SPP) localized at

metal–dielectric interfaces [Fig. 1(c)]; and excitation of a superposition of Bloch modes in a two-dimensional PhC [Fig. 1(d)].

In a bulk medium, free electrons propagating faster than the phase velocity of light in the medium can excite photonic modes [such that the velocity component of the photon phase velocity is equal to the electron velocity, as per Eq. (1)]. In a non-dispersive dielectric, such an electron thereby emits Cherenkov radiation, a “shock wave” of light.^{2,34,67,68} In Fig. 1(a), the free-electron plane (defined as $\omega = |\mathbf{v}|k_{\parallel}$) intersects the light cone (defining bulk medium plane waves) only above a certain threshold velocity $\beta = 1/n$ (where $\beta = v/c$ is the reduced velocity). At a given frequency [isofrequency plane shown in black in Fig. 1(a)], the intersection of the two surfaces (consisting of two points at $\pm k_{\perp}$) defines the angle of emission (see Sec. II B 1 for more details).

When propagating in periodic media, free electrons can spontaneously emit photons in the form of Bloch modes.⁴ The folded free-electron line (for sheet electrons) or plane (for point electrons) can intersect photonic bands at various locations in the BZ. Two such

scenarios are shown in Figs. 1(b) and 1(d) for the case of a one-dimensional PhC slab (interacting with a sheet electron) and a two-dimensional PhC (interacting with a point electron). In both cases, free electrons can excite modes from several bands at the same time, resulting in complex emission processes. In PhC slabs, guided modes and leaky resonances can be excited, and even modes with diverging quality factors (so-called BIC⁶⁹). Emission patterns in the two-dimensional case can exhibit even richer physics, given that radiation arises as a superposition of multiple modes with various group velocities.⁸

Other types of spatially extended modes, such as SPPs, phonon polaritons, and other surface waves, can be excited by free electrons flying in their vicinity (for SPPs, typically, parallel to the interface between a metal and a dielectric).

The excitation of SPPs with free electrons was originally proposed by Ritchie.⁵ The typical dispersion relation converging asymptotically to $\omega_p/\sqrt{2}$ (where ω_p is the plasma frequency) intersects the electron dispersion at various (ω, k_{\parallel}) as a function of the electron velocity. Such a dispersion relation is shown in Fig. 1(c) for the case of a sheet electron.

Historically, whispering gallery modes in nanospheres played an important role in the development of free-electron physics. To illustrate this fact, one can consider the development of monochromators in electron microscopes down to \sim meV energy dispersion regimes, which enabled the selective excitation of few modes of interest via phase-matching.^{70,71} It was first proposed that free electrons could lose energy and induce radiation from metallic and dielectric nanoparticles, suggesting the use of electron microscopy to image high-Q whispering gallery modes in such structures, first realized in a monochromated electron microscope.⁷⁰ This technique then found applications in imaging other high-Q photonic modes, e.g., in photonic crystal cavities⁷² and dielectric microfibers modes for broadband coupling.⁷³

Finally, the excitation of phonon polaritons by free electrons has been a topic of intense recent research, motivated by pioneering theoretical work.^{74–77} The development of atomic-wide electron beams with \sim meV energy resolution made possible the imaging of atomic-scale vibrations and surface phonon polariton spectroscopy in the mid-infrared. These techniques have recently enabled the imaging of bulk and surface vibrational modes in nanostructures,⁷⁸ subatomic movements in nanostructures,⁷⁹ three-dimensional vectorial mapping of surface phonon polaritons,⁸⁰ in addition to spatiotemporal dynamics of wavepacket propagation⁸¹ and nanoscale confinement effects in hexagonal boron nitride.⁸²

2. Impact interaction zone

In the impact interaction zone, one way in which electrons can radiate is the transition radiation (TR), which occurs when an electron crosses the interface between two media with distinct electromagnetic properties. From an electromagnetic perspective, TR originates in the continuity relation of the fields at the interface.²⁸ This effect might still be explained in terms of the excitation of photonic modes by a free-electron current source, using the image charge formalism (see Sec. II B 3).

Beyond the simple TR effect, the more general family of impact interaction effects appear in almost all experiments, whenever some fraction of the incoming electrons penetrates into the sample. In this

impact interaction zone, the electron kinetic energy can be transferred to the material, allowing subsequent emission processes.

Those emission processes can be understood as arising from fluctuating current sources associated with bound polarization (e.g., from excited electrons in defects, excitons, etc.). Such bound polarization is qualitatively similar to electrons in atoms or molecules, and thus, their light emission (and nanophotonic shaping perspective) is understood from the perspective of bound-electron radiation engineering, which is a dominant paradigm in nanophotonics currently. Therefore, in this process, the phase-matching condition does not describe the coupling of free electrons with light. However, photonic engineering can still be used to enhance and control radiation.

This type of radiation is commonly referred to as incoherent cathodoluminescence (ICL). Since this process is equivalent to what is referred to as scintillation in other fields of physics (e.g., as observed with x-rays, γ -rays,⁸³ α and β particles⁸⁴), we will refer to this effect as “electron scintillation” as well, to highlight their common physical origin and similarity. Scintillation is a complex “multi-physics” process spanning several disparate length, time, and energy scales. The key steps in scintillation can be summarized as follows: (1) ionization of electrons in the sample by the pump electrons followed by production and diffusion of secondary electrons;⁸⁵ (2) establishment of a non-equilibrium steady-state of bound electrons;^{86,87} and (3) recombination, leading to light emission (when the recombination is radiative).

The first step of the process usually involves the excitation of a bulk plasmon (with material-dependent energy 20–30 eV), which then decays very rapidly (fs time scales) into a few hot electron–hole pairs.^{85,88} Electron microscopy has recently unveiled key physical mechanisms in ICL, revealing the possibility of photon bunching at low current densities⁸⁹ and imaging excitation pathways with nanometer resolution.⁹⁰

The final step of light emission is particularly complex in nanophotonics environments, as it results from fluctuating, spatially distributed dipoles with a non-equilibrium distribution function. The final step also hints at the feasibility of enhancing and controlling ICL with nanophotonics. Moreover, such ICL is often ubiquitously present in experimental studies of CL, and much analysis is typically devoted to attributing signals to CL vs ICL/scintillation.⁹¹

To conclude this preliminary overview of light emission mechanisms in electron microscopy, we first note that the discrepancy between grazing-angle and impact interaction zones is introduced in this review for convenience of discussion. Photonic excitations can also be triggered from penetrating electron paths [one simple example is Cherenkov radiation (CR) from electrons propagating in the bulk after penetration]. The distinction between surface and bulk emission processes was discussed in previous work.⁹²

We also note that there exist additional free-electron radiation processes, such as bremsstrahlung (“braking” radiation), that arises from abrupt deceleration. We do not focus on these processes in this review because their enhancement or shaping with nanophotonics structures has not been (yet) demonstrated. In contrast, free-electron radiation effects, such as parametric x-ray and coherent bremsstrahlung, are discussed below to highlight their connections to the wider family of diffraction radiation phenomena that can be affected by nanophotonics. We do, however, discuss connections between the previously mentioned acceleration/deceleration effects (in both

interaction zones) and other forms of “diffraction radiation,”⁹³ such as parametric x-ray emission and coherent bremsstrahlung.

B. Fundamental discoveries in free-electron physics

The fundamental physics of radiation by free-electrons (without nanophotonics) has been known for decades in the context of macroscopic electrodynamics and high-energy physics. The fundamental physics of electron–light interaction has a long history, dating back to the early 1900s and has resulted in several cornerstone discoveries in fundamental physics.

Perhaps, the most celebrated of those effects is CR, given its many analogs in other systems,⁴⁰ applications in nonlinear optics,^{94–98} high-energy particle detectors,³⁷ dosimetry, medical imaging, and therapy.⁵¹ The original observation of CR was reported by Cherenkov² and Vavilov⁹⁹ from secondary (Compton) electrons in a liquid irradiated by γ -rays. Shortly thereafter, the observation was confirmed by a series of observations and theoretical predictions by Cherenkov, Vavilov, Frank, and Tamm.^{100–102} Cherenkov, Frank, and Tamm were awarded the Nobel Prize in Physics in 1958 for the “discovery and the interpretation of the Cherenkov effect” (a few years after Vavilov had passed away). Tamm insisted in his Nobel lecture¹⁰³ that the effect should rather be named the “Vavilov–Cherenkov effect,” to highlight the contribution of Vavilov. Ginzburg later noted (regretfully) that the name “Vavilov” had been dropped in most instances.³⁴ CR is discussed in greater depth in Sec. II B 1.

TR was originally proposed by Ginzburg and Tamm in 1945.^{3,104} The original observation was reported by Goldsmith and Jelly in 1959 in the visible by bombarding metallic surfaces with 1 MeV protons. Significant important contributions to the field of CR and TR were reported in the few decades following their original discovery, such as TR calculations from metallic thin films¹⁰⁵ discovery of the anomalous Doppler effect in the Cherenkov cone,^{53,106,107} and quantum recoil corrections to the Cherenkov effect.^{61,67,68} Both techniques became mainstay technologies in high-energy particle detector experiments.^{35–38} Free-electron injection into a metal can also lead to the generation of SPPs. This fundamental discovery was first proposed by Ritchie in 1957⁵ and experimentally observed for the first time in 2006.^{9,49}

Scintillation (from various high-energy particles, such as x-rays, free electrons, and α -particles) was originally discovered as a diagnosis and detection tool in early works on gemology and radioactivity. Early works by Hittorf (reported in Ref. 108) and later Crookes¹ reported ICL from various stones, including diamonds. The first reported scintillator detector was invented by Crookes in 1903 to detect α -particles, following original observations of light emission from phosphorescent powders in cathode-ray tubes in 1879.¹ Developments in optical amplification devices made scintillator detectors widely available for applications in radiology, electron microscopy, and high-energy particle detection.⁵⁰ Interestingly, the first x-ray images following Röntgen’s discovery were not performed with scintillators, but rather radiation-sensitive photographic film,¹⁰⁹ which required very long exposure and acquisition times. Scintillators became the workhorse detection technique in x-ray imaging around the 1990s with the emergence of digital detectors.¹¹⁰ ICL, or equivalently free-electron scintillation, has remained a technique of interest in gemology¹¹¹ and semiconductor physics,¹¹² with applications in cathode-ray tube instruments.¹¹³ ICL, and scintillation and their applications to nanophotonics are discussed in Sec. II D.

All of the original observations discussed up to this point were performed with bulk media and high-energy electrons. The first occurrence of free-electron radiation in structured media was done in 1953 by Smith and Purcell who observed visible radiation from ≈ 300 keV electrons flying above a metallic diffraction grating.⁴ The effect, now coined as SPR, is also sometimes referred to as a form of diffraction radiation.⁹³ SPR has found direct applications in microwave electronics¹¹⁴ and is considered as a promising platform for noninvasive particle beam diagnosis.¹¹⁵ SPR is discussed in greater depth in Sec. II B 2.

The core of this review is to discuss recent developments in nanophotonics that have enabled a plethora of new effects and a new framework to understand free-electron emission. Specifically, we discuss how the interplay of free-electron physics (and more generally high-energy physics in the case of scintillation) has enabled the control and enhancement of the above-mentioned emission effects.

C. Recent milestones enabled by nanophotonics

A historical timeline of free-electron radiation, from the discovery of its fundamental building blocks to recent effects enabled by nanophotonics, is shown in Fig. 2. The first wave of discoveries in the field of free-electron radiation happened in the years between 1870 and 1953. In this period, the fundamental mechanisms were first observed and explained. What we have seen in the past 10–20 years is a second wave of discoveries, mostly driven by the possibilities and new concepts emerging from the field of nanophotonics.¹¹⁶

Around the turn of the 21st century, advances in nanofabrication triggered a renewal of interest in understanding light propagation in patterned materials on the scale of optical wavelengths.⁴³ In particular, the birth of PhCs enabled an abundance of techniques to control photonic properties in engineered materials.^{42,45} The field of nanophotonics recently found applications in free-electron physics, as a way to control and enhance radiation from free electrons. Alternatively, free electron beams can be used as diagnostic tools to probe photonic properties of nanostructures.^{28,29}

Perhaps the most obvious, yet much awaited application of nanophotonics in free-electron physics is the miniaturization of free-electron-driven radiation sources.^{14,15,17,19,20,117,118} Specifically, nanophotonic structures have been shown to allow visible radiation from relatively slow electrons ($\beta < 0.2$, which can be generated and accelerated on chip-scale distances), and to eliminate emission threshold in CR.^{19,119,120} This effort has also been bolstered by advances in integrated free-electron sources such as field emitter arrays.^{121–123}

More generally, nanophotonics offers a convenient platform to control and enhance radiation by engineering the interaction of electron beams with photonic modes.^{21,124–128} Some regimes of electron emission forbidden in most macroscopic media¹²⁹ are realizable in some specific nanophotonic structures, such as backward CR in PhC.^{8,53}

One of the most promising advantages of free-electron radiation is its wide tunability and the available wavelength ranges, from microwave to x-ray radiation. This tunability is achieved via structural and electron beam engineering. This is in contrast with wavelength tunability in, e.g., laser sources, which typically requires the sometimes painstaking development of new materials emitting at the wavelength of interest. Specifically, nanophotonic structures pumped by free-electron beams have been shown to emit photons in hard-to-reach regimes, such as UV,^{119,130–133} soft x-ray,²³ THz,¹³⁴ and mm-wave.¹³⁵

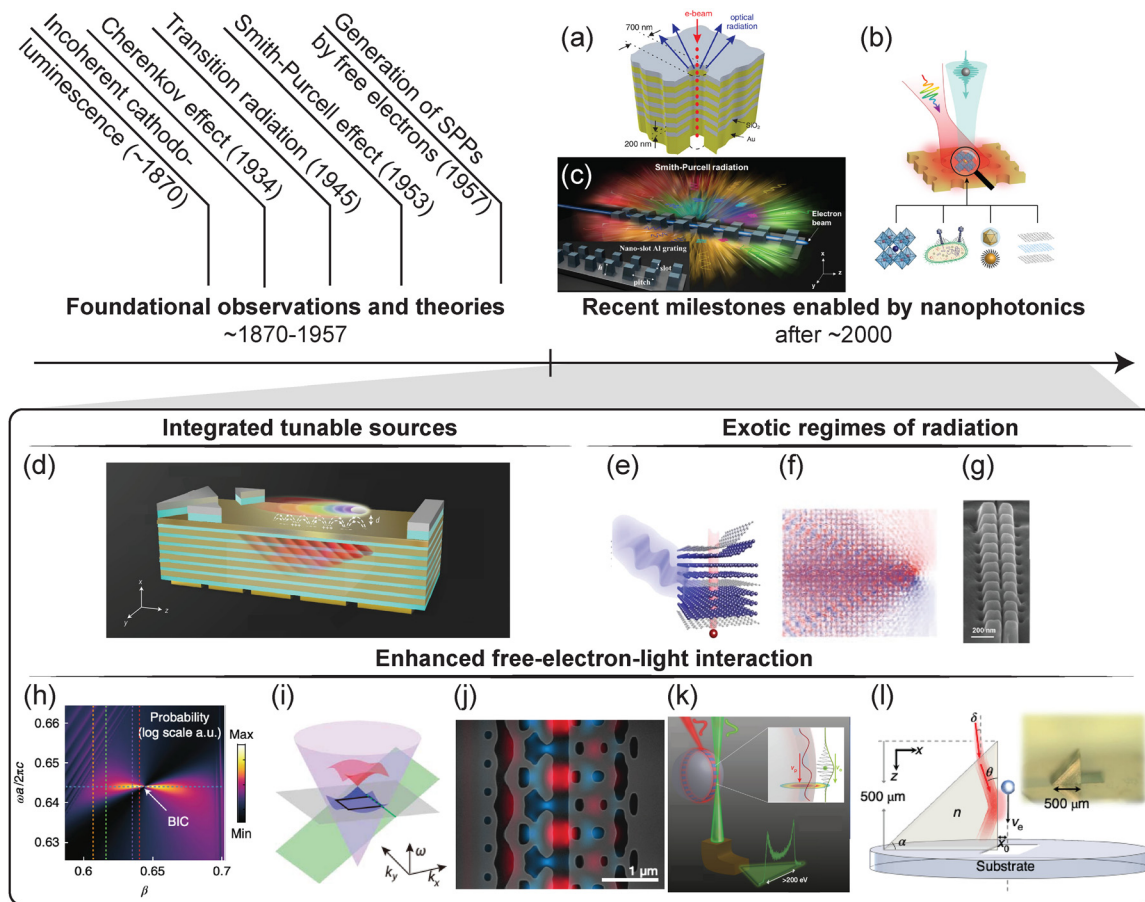


FIG. 2. Historical timeline: from fundamental discoveries to novel applications enabled by nanophotonics. The field of free-electron-light interactions was enabled by a few late-19th and 20th-century fundamental discoveries and theoretical proposals such as incoherent cathodoluminescence, CR, TR, SPR, and excitation of SPPs by free electrons. (a)–(m) Recent advances in nanophotonics have enabled the demonstration of several new effects and technologies relying on those fundamental effects. (a) Light well: tunable electron beam source. Reprinted with permission from Adamo *et al.*, *Phys. Rev. Lett.* **103**, 113901 (2009). Copyright 2009 the American Physical Society.¹⁴ (b) Ultrafast multidimensional spectroscopy and microscopy in a transmission electron microscope (TEM), such as perovskite materials, frozen cells, quantum dots, and two-dimensional materials. Reproduced with permission from Wang *et al.*, *Nature* **582**, 50–54 (2020). Copyright 2020 Springer Nature.²⁵ (c) and (g) Deep ultraviolet SPR enabled by nano-slot aluminum grating. Adapted with permission from Ye *et al.*, *Optica* **6**, 592–597 (2019). Copyright 2019 The Optical Society.¹³⁰ (d) Thresholdless integrated Cherenkov emitter in a hyperbolic metamaterial. Reproduced with permission from Liu *et al.*, *Nat. Photonics* **11**, 289–292 (2017). Copyright 2017 Springer Nature.¹⁹ (e) Tunable x-ray generation from van der Waals heterostructures. Reproduced with permission from Shentcis *et al.*, *Nat. Photonics* **14**, 686–692 (2020). Copyright 2020 Springer Nature.²³ (f) Backward Cherenkov emission in PhCs. Reproduced with permission from Luo *et al.*, *Science* **299**, 368–371 (2003). Copyright 2003 AAAS.⁸ (h) Bound state in the continuum enhancement of free-electron emission. Reproduced with permission from Yang *et al.*, *Nat. Phys.* **14**, 894–899 (2018). Copyright 2018 Springer Nature.²¹ (i) Flatband resonance enhancement of free-electron emission. Reproduced with permission from Yang *et al.*, *Nature* **613**, 42–47 (2023). Copyright 2023 Springer Nature.¹²⁴ (j) Inverse-designed electron accelerator. Reproduced with permission from Sapra *et al.*, *Science* **367**, 79–83 (2020). Copyright 2020 AAAS.²² (k) Resonant interaction between an electron beam and a photonic resonator. Reproduced with permission from Kfir *et al.*, *Nature* **582**, 46–49 (2020). Copyright 2020 Springer Nature.²⁴ (l) Phase-matched interaction between a free-electron beam and a light wave. Reproduced with permission from Dahan *et al.*, *Nat. Phys.* **16**, 1123–1131 (2020). Copyright 2020 Springer Nature.¹³⁷

Free electrons provide a versatile platform to access parts of the electromagnetic spectrum where few sources are available, utilizing the radiation control and enhancement techniques mentioned above.

Given the nanometer scale spatial resolution of electron beams in most electron microscopes, free-electron radiation has been considered as a spectroscopic probe to study nanophotonic structures.^{28,29,136} Free electrons can also interact with nanophotonic structures over extended interaction lengths, thereby achieving stronger coupling strengths, enabling regimes of multi-photons stimulated emission and

absorption by a single electron,¹³⁷ and electron acceleration in integrated dielectric laser accelerators.²²

Some of the above-mentioned applications have been enabled by recent advances in ultrafast electron microscopy, where electron-beam and optical excitation of the sample can be modulated in time down to attosecond pulses,^{138–141} thereby unveiling quantum properties of electron–light interactions.^{142–144} In particular, in photon-induced near-field electron microscopy^{145–147} (PINEM), one can probe near-field non-equilibrium properties of physical systems with unprecedented

time and spatial resolution. The recent introduction of nanophotonics in PINEM has enabled the implementation of cavity quantum electrodynamics^{24,25} with free electrons, the generation of electron vortex beams,¹⁴⁸ the coherent control of electron beam statistics,¹⁴⁹ electron beam modulation with silicon photonics,¹⁵⁰ coincidence electron-photon detection,^{90,151} and strong coupling in the single-photon-single-electron regime.¹⁵²

II. TYPOLOGY OF FREE-ELECTRON RADIATION

In this section, we describe the basic organizing principles of this review, which help to sort out the different effects under a general formalism that highlights the role and prospects of nanophotonics in this field.

A. Coherent vs incoherent cathodoluminescence

All of the effects in the grazing-angle interaction and impact interaction zones have a common physical origin: they result from the coherent interaction between the photonic eigenmodes of the structure and a current source $\mathbf{J}(\mathbf{r}, t)$ (describing the particle trajectory). The current distribution can be equivalently described in time and frequency domain. In the following, we consider a trajectory of the form $\mathbf{r}(t) = \mathbf{v}t$ (with the initial position at $t = 0$ taken to zero without loss of generality):

$$\begin{aligned} \mathbf{J}(\mathbf{r}, t) &= q\mathbf{v}\delta(\mathbf{r} - \mathbf{v}t), \\ \mathbf{J}(\mathbf{r}, \omega) &= q\hat{\mathbf{r}}_{\parallel}\delta(\mathbf{r}_{\perp})e^{i\omega r_{\parallel}/v}, \end{aligned} \quad (2)$$

where q is the electron charge. The particle propagates along the linear trajectory defined by the velocity vector $\mathbf{v} = v\hat{\mathbf{r}}_{\parallel}$. The unit vector parallel to \mathbf{v} is $\hat{\mathbf{r}}_{\parallel}$ and the orthogonal space is denoted as $\{\hat{\mathbf{r}}_{j,\perp}\}_{j=1,\dots,N-1}$ (where N is the dimensionality of space). Given the mismatch in energies between the incoming electron (>1 keV in most settings) and the emitted photon energy [few eV's in the visible to near-infrared (NIR)], one can often safely neglect the quantum emission recoil and therefore consider the trajectory to be unaffected by radiation processes.

This current source can be plugged into Maxwell's equations in free space, resulting in an evanescent near field,¹⁵³ which can be scattered by the structure.^{28,29} This observation also led to the application of fundamental bounds on free-electron radiation and energy loss (derived in Sec. II C and Ref. 21). Said differently, the current source (representing the free electron) is performing work on the system and some of which results in radiation.

The current distribution in Eq. (2) can be modeled in Maxwell's equations in several ways, depending on the type of numerical solver. For instance, in finite-difference time-domain solvers, it can be modeled as an array of dipoles "turned on" sequentially at a speed corresponding to the flight of the electron.^{20,118} Alternatively, it can be directly injected as a line current in frequency domain (with Bloch periodic boundary conditions to model periodic systems).^{21,154}

Coherent CL effects are often considered in opposition to ICL, which originates from stochastic energy losses in the material. Because of the stochastic nature of the process, emitted photons lose their coherence with respect to the incoming electron. Instead of the deterministic current distribution from Eq. (2), one models ICL as radiation from a stochastic current distribution, whose current-current correlations are prescribed as

$$\langle J_j^-(\mathbf{r}_1, \omega)J_k^+(\mathbf{r}_2, \omega) \rangle \equiv 2\pi TS_{jk}(\mathbf{r}_1, \mathbf{r}_2, \omega), \quad (4)$$

with $S_{jk}(\mathbf{r}_1, \mathbf{r}_2, \omega) = \sum_{\alpha,\beta} J_j^{z\beta}(\mathbf{r}_1)J_k^{\beta\alpha}(\mathbf{r}_2) \times f_{\alpha}(1 - f_{\beta})\delta(\omega - \omega_{\alpha\beta})$, and T is a normalization time. In this spectral function, f_{α} is the occupation factor of microscopic state α with energy E_{α} , $J^{z\beta}$ represents the matrix element of the current density operator $\mathbf{J} \equiv \frac{e}{m}\psi^{\dagger}(-i\hbar\nabla)\psi$, and $\omega_{\alpha\beta} = [E_{\alpha} - E_{\beta}]/\hbar$. The current density matrix and the occupation functions can depend on position, as they depend on the electron energy loss density.

Direct calculation of radiation from the stochastic current source described in Eq. (4) is a computationally expensive problem, as is known in the context of thermal emission.¹⁵⁵ Such calculations would indeed require the sampling of a three-dimensional current distribution, whose correlations partially depend on the microscopics and electron energy loss dynamics. Therefore, it is strongly beneficial to resort to more efficient numerical methods, leveraging electromagnetic reciprocity, to make such calculations tractable in three dimensions.²⁷

The distinction between coherent and incoherent CL is also linked to the final quantum state in which the sample is left after radiation.²⁸ In the following, we show how CR, TR, SPR, and other coherent CL effects arise from the coherent interaction of the current distribution from Eq. (2) with photonic eigenmodes. We also show how the stochastic current distribution from Eq. (4) can radiate ICL in arbitrary nanophotonic environments and computational techniques to calculate it efficiently.

B. A unifying picture of coherent cathodoluminescence in arbitrary nanophotonic environments

Considering the current source in Eq. (2) as a source in Maxwell's equations, one can calculate radiation from a moving free electron in arbitrary nanophotonic media. We expand the Green dyadic tensor—relating currents to fields linearly as

$$\mathbf{E}(\mathbf{r}, \omega) = i\omega\mu_0 \int d\mathbf{r}' \mathbf{G}(\mathbf{r}, \mathbf{r}', \omega)\mathbf{J}(\mathbf{r}', \omega)$$

—over its set of eigenmodes⁴³ $\{\mathbf{F}_m(\mathbf{r}, \omega)\}_m$:

$$\mathbf{G}(\mathbf{r}, \mathbf{r}', \omega) = c^2 \sum_m (\mathbf{F}_m(\mathbf{r}, \omega) \otimes \mathbf{F}_m^*(\mathbf{r}', \omega))g(\omega, \omega_m), \quad (5)$$

where $g(\omega, \omega_m) = (\omega^2 - \omega_m^2 - 2i\omega_m\gamma_m)^{-1}$. The eigenmodes \mathbf{F}_m are normalized such that $\int_V \frac{1}{2\omega_m} \frac{d}{d\omega} (\epsilon(\omega)\omega^2) |\mathbf{F}_m(\mathbf{r}, \omega)|^2 = 1$. The main assumption in deriving this equation are small losses and weak dispersion, which are valid in most cases we consider in this work, and can be relaxed further by using the dyadic Green tensor directly⁶³ (without referring to a mode expansion). Similar modal expansions have been used to calculate EELS and CL in nanophotonics.^{156–159}

The total energy radiated by a dipole can be calculated as an integral in frequency domain,¹⁶⁰ and we get the following expression, which corresponds to the electron energy lost by interacting with nanophotonic modes:

$$\begin{aligned} U &= \overbrace{\frac{\mu_0 q^2 c^2}{\pi}}^{\text{prefactor}} \int dr_{\parallel} dr'_{\parallel} \text{Im} \int d\omega \omega \\ &\times \sum_m \underbrace{(\hat{\mathbf{r}}_{\parallel} \cdot \mathbf{F}_m(r_{\parallel}, \mathbf{r}_{\perp}, \omega))(\hat{\mathbf{r}}_{\parallel} \cdot \mathbf{F}_m^*(r'_{\parallel}, \mathbf{r}_{\perp}, \omega))}_{\text{mode-electron overlap}} \\ &\times \underbrace{e^{i\omega(r'_{\parallel} - r_{\parallel})/v}}_{\text{phase-matching}} \underbrace{g(\omega, \omega_m)}_{\text{spectral dependence}}. \end{aligned} \quad (6)$$

Equation (6) already highlights the main physical parameters relevant to understanding all effects in coherent CL, and we therefore refer to it as the “master equation.” The prefactor is always proportional to q^2 , which underlines possible radiation enhancements by considering highly charged particles (such as heavy ions¹⁶¹) More generally, the q^2 dependence offers a mechanism to distinguish between particles with elementary charge q (such as electrons, protons, etc.) and nuclei with charge Zq (where Z is the atomic number). For instance, even CR from fully ionized helium is four times stronger than that of hydrogen isotopes and elementary charges.³⁴ In heavier materials, the larger discrepancy can be used to “count” the energy of each incoming particle.³⁸

The rest of the expression is summed over all photonic modes indexed by m which may, in principle, contribute to radiation. The photonic mode-electron overlap highlights the importance of the spatial overlap between the photonic mode and the electron beam (since \mathbf{F}_m is evaluated at the fixed location \mathbf{r}_\perp perpendicular to the axis of propagation of the electron). Radiation might also be enhanced by considering extended interactions over lengths such that $\mathbf{F}_m(\mathbf{r}_\parallel, \mathbf{r}_\perp, \omega)$ remains large over the polarization parallel to the electron trajectory.

Further physical considerations can be made to evaluate the mode-electron overlap. The mode profile $\mathbf{F}_m(\mathbf{r}_\parallel, \mathbf{r}_\perp, \omega)$ has a given polarization distribution, but only the polarization along the beam propagation contributes to emission. The spatial dependence of the field profile results in evanescent coupling strengths in many scenarios, as will be made evident for the excitation of SPPs and electromagnetic bounds on coherent CL (Secs. II B 4 and II C).

The spectral dependence of the emitted energy is encoded in $g(\omega, \omega_m)$, such that $\text{Im}(g) \approx \pi\delta(\omega^2 - \omega_m^2) \approx \frac{\pi}{2\omega_m}\delta(\omega - \omega_m)$ in the limit of small losses (where Im denotes the imaginary part). Therefore, radiation in eigenfrequencies of the photonic structure are strongly enhanced.

The term labeled “phase-matching” in the master equation [Eq. (6)] only contributes partially to the phase-matching condition described in Eq. (1) and is complemented by a phasor of the form $e^{ik_\parallel r_\parallel}$ from the mode-electron overlap term, which for instance appears in systems exhibiting translational invariance (see below). Their combination

yields the phase-matching relation from Eq. (1). To further outline the physical importance of phase-matching, we consider a specific mode with longitudinal wavevector k_\parallel , such that

$$\mathbf{F}_m(\mathbf{r}_\parallel, \mathbf{r}_\perp, \omega) = e^{ik_\parallel r_\parallel} \mathbf{f}_m(\mathbf{r}_\perp, \omega).$$

This yields a version of the master equation where the phase-matching condition is evident:

$$U \propto \sum_m \underbrace{|\hat{\mathbf{r}}_\parallel \cdot \mathbf{f}_m(\mathbf{r}_\perp, \omega_m)|^2}_{\text{mode-electron overlap}} \overbrace{\Lambda^2 \text{sinc}^2\left(\left(\frac{\omega_m}{v} - k_\parallel\right)\Lambda\right)}^{\text{phase-matching}}, \quad (7)$$

where $\text{sinc}(x) = \sin(x)/x$ is the sinc function, and Λ is the length of interaction. The phase-matching term becomes a Dirac delta function for large interaction lengths Λ , thereby highlighting the critical importance of phase-matching in physical settings with extended interactions. Compared to Eq. (6), this equation also highlights the spectral dependence of the radiation, which is determined by the photonic eigenfrequencies $\omega_m(\mathbf{k})$. This compact form also hints at a geometric method to calculate the emitted power by (1) considering the intersection of the band structure dispersion $\omega_m(\mathbf{k})$ with the electron plane $\mathbf{k} \cdot \mathbf{v} = k_\parallel v$ and (2) weighting each intersection by the mode-electron overlap term in Eq. (7). We described in Sec. I A how such a method can be used to predict radiation in various radiation events occurring in the grazing-angle interaction zone in the introduction, for CR in bulk media and PhCs, SPR, and excitation of SPPs.

To gain further physical insight with this formalism, we must consider specific photonic environments, which will be described by various eigenmode distributions, and are discussed in Secs. II B 1–II B 4.

1. Cherenkov radiation

CR in its simplest embodiment occurs in a homogeneous dielectric medium (of index n) and consists in the spontaneous emission of plane waves by a charged particle [see Fig. 3(a)]. Its description, in the

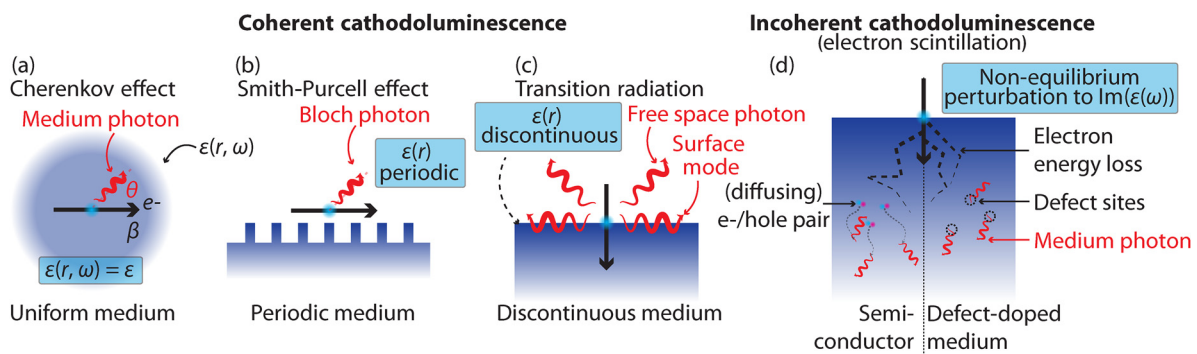


FIG. 3. Examples of spontaneous emission from free electrons. Free electrons can emit photons spontaneously in several manners. (a) CR: a free electron propagating in a bulk medium at a speed larger than the speed of light in the medium $[c/\text{Re}(\sqrt{\epsilon})]$. (b) SPR: in a periodic medium, free electrons can emit a Bloch photon. (c) TR: when going through a discontinuous interface between two media (such that $\epsilon(r)$ is discontinuous), free electrons can emit a surface plasmon at the interface. (d) ICL, also known as electron scintillation, occurs in materials with radiating energy levels, such as in semiconductors or in defect-doped media. A free electron impinging on the material can convert part of its energy into a cascade of secondary electrons and excite radiating sites, such as diffusing electron–hole pairs or excited states in implanted defects. In such materials, optical emission can be modeled as a small (perturbative) non-equilibrium loss function $\text{Im}[\epsilon(\omega)]$ at the emission wavelength. This review focuses on types of spontaneous emission that have been enhanced or controlled using nanophotonics. Other types of spontaneous emission from free electrons, not covered in this review, include bremsstrahlung, betatron radiation, and undulator radiation.

language of Sec. II A and the master equation, can be understood in terms of plane wave eigenmodes of a medium of index n . The dispersion relation is $\omega_k = c|\mathbf{k}|/n$. Plugging this expression into the master equation [Eq. (6)], we can get the famous *Frank–Tamm formula*¹⁰⁰ for the spectral density per unit propagation length, shown in the Subsection 1 of the Appendix. Emission is only allowed for superluminal electrons, which is equivalent to the phase-matching condition from Eq. (1) in a bulk medium.

Quantum corrections to this formalism can be introduced, taking into account recoil,^{67,68} non-perturbative effects with heavy ions,¹⁶¹ the particle’s spin and orbital angular momentum,⁶¹ reduced dimensionality,¹⁵² or emission from hot electrons in two-dimensional materials.¹⁶²

2. Smith–Purcell radiation

SPR is a natural extension of CR to periodic media as the spontaneous emission of Bloch photons⁶³ [see Fig. 3(b)], which we use as eigenmodes in the expansion from Eq. (5). We first consider the case of a one-dimensional periodic structure (period L) along the direction of electron propagation. Eigenmodes can be described by the band index m and reciprocal lattice vector G in the first BZ, such that $\mathbf{F}_{m,k_{\parallel}} = \sum_G \mathbf{c}_{m,k_{\parallel}}^G(\mathbf{r}_{\perp}) e^{-ir_{\parallel}(G+k_{\parallel})/\sqrt{L}}$, where $\mathbf{c}_{m,k_{\parallel}}^G$ are coefficients of the mode’s Fourier expansion.

We then get the following expression for the energy spectral density:

$$\frac{1}{L} \frac{dU}{d\omega} = \frac{\mu_0 q^2 c^2}{2} \sum_m \sum_G \left| \hat{\mathbf{r}}_{\parallel} \cdot \mathbf{c}_{m,k_{\parallel}}^G(\mathbf{r}_{\perp}) \right|^2 \delta(\omega - \omega_{m,k_{\parallel}}). \quad (8)$$

The δ function in Eq. (8) gives us a geometric way of predicting which Bloch modes are excited by the electron beam, by considering the intersection of the band structure $\omega_{m,k_{\parallel}}$ with $\omega = k_{\parallel}v$. This method generalizes well to higher dimensions where the electron “line” becomes a plane in the band structure representation [see Figs. 1(b) and 1(d) for some example band structures]. The phase-matching condition also sets the dispersion relation, known as the Smith–Purcell relation,

$$\lambda = \frac{L}{m} \left(\frac{1}{\beta} - \cos \theta \right), \quad (9)$$

where λ is the photon wavelength, and m the Bloch mode index. The emission angle θ is measured, as in the case of CR, with respect to the electron propagation direction.

This simple relation enables us to make quick predictions of the radiation spectrum (in the absence of resonant enhancement), knowing the structure periodicity along the electron trajectory. Several observations of SPR from various periodicities and electron energies are shown in Fig. 4, on a background corresponding to the wavelength predicted by Eq. (9) with $\theta = \pi/2$ and $m = 1$. The original observation from Smith and Purcell was performed with $\beta \approx 0.78 - 0.8$. The relatively large grating pitch they used should have resulted in radiation in the short-wave infrared at normal emission direction, but they measured visible radiation at a shallower angle $\theta \approx 20^\circ$.

Early work on SPR was essentially focused on metallic structures.¹⁶³ More recent work used electrons in similar energy ranges, pushing radiation into the near-UV regime with higher diffraction orders.¹⁶⁴ With the goal of integrating Smith–Purcell emitters into

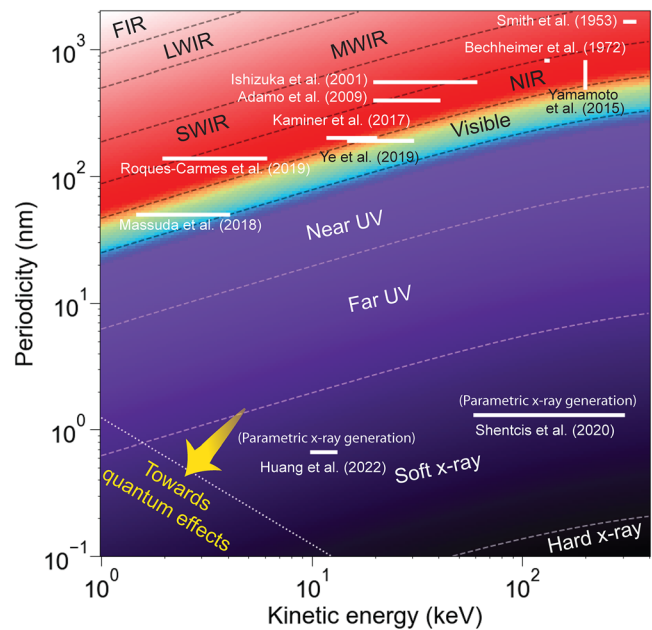


FIG. 4. Overview of progress in Smith–Purcell emitters. Each straight thick white line corresponds to a reported experimental observation, starting from the original observation from Smith and Purcell* (top right corner). The overview highlights recent progress enabled by nanophotonics toward high-frequency radiation (visible and ultraviolet) with short-pitch gratings and/or low-energy electrons (<10 keV). The background color corresponds to the emitted wavelength “color” at normal incidence $\theta = 90^\circ$.^{4,14,20,23,117,118,130,164,173–175} In some Refs. 130 and 173, the main reported result comes from a higher-order Smith–Purcell peak, which is why the work appears in a longer wavelength domain (e.g., Ref. 130 reports radiation in the deep ultraviolet with up to third-order SPR). In some other references (e.g., Ref. 4), radiation is measured at an angle closer to $\theta = 0^\circ$, therefore reporting shorter wavelengths than what is displayed here. In Refs. 23 and 175, free electrons emit soft x-ray photons via parametric x-ray radiation or coherent bremsstrahlung. UV: ultraviolet; NIR: near infrared; SWIR: short wave infrared; MWIR: mid wave infrared; LWIR: long wave infrared; FIR: far infrared. “Quantum effects” denote the region where recoil effects become observable, delimited by $\lambda(\theta = 90^\circ) = \lambda_e$, where $\lambda_e(\theta = 90^\circ)$ is the emission wavelength at normal incidence, and λ_e the de Broglie wavelength of the electron.

optoelectronic devices, recent effort has been targeted at reducing the electron kinetic energy and periodicity, to retain emission in the NIR to regimes. [We note that SPR was also observed with relativistic electrons (Ref. 348).] This effort has been enabled by recent progress in nanofabrication, namely, the capability of fabrication sub-100 nm periodic structures with electron-beam lithography.²⁰ Some works even reported emission from electron beams generated on-chip by field emitters¹¹⁷ and/or with integrated all-silicon structures.¹¹⁸ The prospect of generating radiation deeper in the UV remains an exciting perspective, with recent work demonstrating SPR in the UV with $\beta \approx 0.24 - 0.33$ and leveraging higher-order diffraction modes.¹³⁰ Beyond the technological promise of integrated and tunable UV emitters, short-wavelength SPR also exhibits quantum recoil effects in low-energy and short-period settings.¹⁶⁵ While demonstrations of short-wavelength SPR have been limited to the near UV, other free-electron radiation effects, such as coherent bremsstrahlung and parametric x-ray radiation, being similar in some respects to SPR, are amenable to generation of x-ray radiation. In these effects, the electron

flies in a “structured” medium consisting of a crystalline lattice of atoms, such that the period is on the ångström scale. Those techniques offer an interesting platform to generate x-ray photons with moderately relativistic electrons.^{166–171} We highlight recent work^{23,172} to reveal the similarities and differences between SPR and the previously mentioned x-ray emission techniques.

Many theoretical studies focused on SPR and CR in 2D, where the structures are assumed to be invariant along the third dimension and the electron beam is assumed to be a “sheet” beam. In higher dimensions, the point-like nature of the electron must be considered, and the photonic band structure gives greater flexibility in tuning the coupling between the electron and photonic modes. Considering the case of a three-dimensional periodic PhC, we get the following expression, as previously reported in Ref. 160:

$$\frac{dU}{d\omega dl} = \frac{q^2}{8\pi^2 \epsilon_0} \sum_{m,\mathbf{G}} \int_{\partial S} dk \frac{|\mathbf{c}_{m,\mathbf{k}}^{\mathbf{G}}(\omega) \cdot \hat{\mathbf{r}}_{\parallel}|^2}{|\nabla_{\mathbf{k}_{\perp}} \omega_{m,\mathbf{k}}|}, \quad (10)$$

where ∂S is the contour defined by $\omega = \omega_{m,\mathbf{k}}$. This formula shows that the radiated power is proportional to the Fourier coefficient $|\mathbf{c}_{n,\mathbf{k}}^{\mathbf{G}}(\omega) \cdot \hat{\mathbf{r}}_{\parallel}|$, describing the coupling of the current density with the electromagnetic field at the electron location. Also, the emitted power is proportional to the inverse of the transverse group velocity. This suggests a path to strongly enhance emission from electrons using engineered bands in PhCs.^{21,124,160}

3. Transition radiation

To describe transition radiation within the same framework, we consider the simplified case of a charge impinging at normal incidence on a perfect conductor [see Fig. 3(c)] and resort to the introduction of an image charge with opposite charge and velocity. The current distribution $\mathbf{J}(\mathbf{r}, \omega)$ is modified accordingly and its emission in free space is considered. Doing so, we get the spectral distribution shown in Subsection 2 of the Appendix, first derived by Ginzburg and Tamm.⁶⁷

This relation can be extended to interfaces between two media with finite permittivities,^{67,176} radiation into waveguides,¹⁷⁷ and metallic thin films.¹⁰⁵ Resonant transition radiation, the coherent interference of multiple TR emission in a multilayered medium, has also been considered as a promising platform for high-energy particle detectors^{52,53} and x-ray emission.¹⁷⁸ Though considered as an extension of TR at a single interface, we note that resonant TR has a dispersion relation similar to that of SPR.¹⁷⁹

4. Coherent excitation of surface plasmon polaritons (SPPs) by free electrons

SPPs can be excited by free electrons^{9,19,152,180–184} either when impinging on metals or when grazing the interface, with first observations reported in Refs. 9 and 152, respectively. This phenomenon is observed even in the absence of corrugation at the surface and can be understood with our formalism, when considering SPP eigenmodes. For concreteness, we consider the case of an interface between two media $\epsilon_1 > 0$ and ϵ_2 , with the electron propagating in ϵ_1 . The lower branch of the SPP mode is shown in Fig. 1(c) for a Drude-like metal $\epsilon_2 = 1 - (\omega_p/\omega)^2$ (where ω_p is the plasma frequency). The energy emitted by the free electron per unit length is derived and shown in Subsection 3 of the Appendix.

As expected from the master equation [Eq. (6)], the exponential decay of the field at the interface results in a factor $\exp(-2|k_{\perp}|r_{\perp})$, arising from the mode-electron overlap evaluated along the electron trajectory. As with other effects in the grazing-angle interaction zone, one can predict which SPP modes are excited by an electron with velocity reduced β by identifying the intersection of the dispersion relation with the electron line¹⁸¹ $\omega(k_{\parallel}) = vk_{\parallel}$. Analogs of this effect have been observed in systems supporting Dyakonov surface waves¹⁸⁵ and hyperbolic dispersion.¹³⁰

C. Fundamental bounds for coherent cathodoluminescence

Another perspective that the field of nanophotonics brought to research on free-electron radiation is the idea of setting electromagnetic bounds from first principles. Nanophotonics research led to the formulation of universal bounds on various photonic processes,¹⁸⁶ such as scattering and absorption,¹⁸⁷ focusing,¹⁸⁸ Raman scattering,¹⁸⁹ and near-field optical response.¹⁹⁰ The same approach was applied in Ref. 21 to propose a universal bound on free-electron radiation and energy loss. Such bounds represent the maximal amount of power that could be scattered or absorbed by an optimal structure excited by free electrons and enclosed in a given volume.

Coherent CL can be interpreted as a scattering problem and is therefore amenable to recent work on electromagnetic bounds.²¹ Intuitively, the scattering problem can be bounded by a convex optimization problem, whose solution is obtained by calculating variational derivatives of the incident fields.²¹ [The incident evanescent field is generated in free space by the current distribution²⁸ $\mathbf{J}(\mathbf{r}, \omega)$.] Maximal radiation and energy loss powers can then be derived²¹ for an arbitrary “scatterer” (corresponding to the sample inducing coherent CL) with susceptibility $\chi(\mathbf{r}, \omega) = \epsilon(\mathbf{r}, \omega) - 1$ and volume V as

$$P_{\tau} \leq \frac{q^2 \zeta_{\tau}}{8\epsilon_0 \omega \pi^2} \int_V d\mathbf{r} \underbrace{\frac{|\chi|^2}{\text{Im}\chi}}_{\text{material}} \overbrace{\left(k_{\perp}^4 K_0^2(k_{\perp} \rho) + k_{\perp}^2 k_{\parallel}^2 K_0^2(k_{\perp} \rho) \right)}^{\text{geometry}}, \quad (11)$$

where $\tau \in \{\text{rad}, \text{loss}\}$, $\zeta_{\text{loss}} = 1$, $\zeta_{\text{rad}} = \eta(1 - \eta) \leq 1/4$ (with η the ratio of radiative to total energy loss), $k_{\parallel} = \omega/v$, and $k_{\perp} = \sqrt{k_{\parallel}^2 - k^2} = k/\beta\gamma$ (with γ the Lorentz factor). K_n is the n th order modified Bessel function of the second kind.

The power bounds from Eq. (11) apply to the non-retarded or retarded regimes, and only assume the absence of gain in the optical medium. This expression also highlights the main physical parameters of interest to maximize radiation from free electrons: the material factor $|\chi|^2/\text{Im}\chi$, which reflects the influence of material choice, depending on the wavelength of interest; the electron velocity β and Lorentz factor γ appearing in the impact parameter $k_{\perp} \rho$ in the integral. Approximations of this bound²¹ explicit the role of the minimum distance between the electron trajectory and the scatterer d , such that the relevant length scale of interaction is set by $k_{\perp} d = kd/\beta\gamma$. At large beam-sample distances, the bound decays exponentially $\propto e^{-2k_{\perp} d}$, which matches the dependence from Eq. (A10).

The analytical bound also reveals several interesting physical behaviors. Namely, there exists a regime of near-field interaction between the beam and the structure where slow electrons are favored

(i.e., they radiate more efficiently). Recent works also highlighted the possibility of strong interactions between slow electrons and plasmonic near fields.^{191–193} This supports recent interest in developing on-chip sources of free-electron radiation,^{20,118,130} where electron beams can be precisely aligned to nanophotonic structures (e.g., gratings for SPR) to control the beam-sample coupling.

Another interesting feature is the apparent divergence of the bound in the limit of small losses, which suggests mechanisms to strongly enhance free-electron radiation with high-Q resonances, a path which we discuss in Sec. III C 1.

D. Incoherent cathodoluminescence (electron scintillation)

All of the previous types of radiation were forms of coherent CL, which naturally give themselves into control via shaping of the photonic eigenmodes, as we explained in the previous paragraphs. We now consider the case of ICL, or electron scintillation, and propose ways to control and enhance this form of radiation. The method we propose here is readily transferable to scintillation from other types of high-energy particles, such as x- and γ -rays.

ICL is usually observed when a beam of electrons is bombarding a material directly (and is therefore occurring in the impact interaction zone), as depicted in Fig. 3(d). Energy is then lost by the electron beam, which can be transferred to radiative sites (electron-hole pairs in semiconductors, or defect states in a doped medium), which subsequently radiate in a nanophotonic environment described by the eigenmode expansion from Eq. (5).

We can calculate the emitted energy by the stochastic current distribution in Eq. (4), and for simplicity, make the assumption that the current correlations are local, isotropic, and real-valued $S_{ij}(\mathbf{r}_1, \mathbf{r}_2, \omega) = \delta_{ij}\delta(\mathbf{r}_1 - \mathbf{r}_2)S(\mathbf{r}_1, \omega)$, a condition that can be straightforwardly relaxed.¹⁹⁴ ICL is, in general, described by the light emission from this non-equilibrium steady-state distribution. This assumption is corroborated by the fact that energy deposition occurs on picosecond time scales, which are effectively instantaneous relative to the excited-state depletion time scales (typically nanoseconds).^{29,87} We then get

$$\frac{d\langle U \rangle}{d\omega} = \frac{\pi T}{\epsilon_0} \sum_m \int d\mathbf{r} |\mathbf{F}_m(\mathbf{r}, \omega)|^2 S(\mathbf{r}, \omega) \delta(\omega - \omega_m). \quad (12)$$

This expression makes explicit the way in which ICL (where the light emission results from spontaneous emission) can be controlled by photonic shaping via the eigenmodes $\mathbf{F}_m(\mathbf{r}, \omega)$. It is also apparent that ICL can be enhanced by optimizing the overlap between a given eigenmode and the current correlation function $S(\mathbf{r}, \omega)$ (for example, by optimizing the overlap between the photonic eigenmode and the energy-loss density of the high-energy particles).

Another formulation of ICL can be obtained by using electromagnetic reciprocity and the Green's function directly (instead of its eigenmode expansion), yielding the following expression for the power spectrum per unit solid angle and frequency:²⁷

$$\frac{dP^{(i)}}{d\omega d\Omega} = \frac{\pi}{\epsilon_0 \omega} \times S(\omega) \times \left[V_{\text{eff}}^{(i)}(\omega, \Omega) / \lambda^3 \right], \quad (13)$$

where we also assumed that the current correlations are uniform and isotropic in the material (corresponding for example to uniform energy loss), and $V_{\text{eff}}^{(i)}(\omega, \Omega) = \int_{V_s} d\mathbf{r} |\mathbf{E}^{(i)}(\mathbf{r}, \omega, \Omega)|^2 / |\mathbf{E}_{\text{inc}}^{(i)}(\omega, \Omega)|^2$.

Equation (13) states that the ICL spectrum, under this approximation, is a simple product of a microscopic factor, set by the non-equilibrium steady-state distribution function $S(\omega)$,^{27,66} and an effective absorption volume V_{eff} , which is only determined by the (structured) optical medium surrounding the emitting sites.

Equation (13) enables a key simplification thanks to electromagnetic reciprocity, which relates the following two quantities: (1) the emitted ICL from the structure (at a given frequency ω , direction Ω , and polarization i) and (2) the intensity of the field induced in the sample $[|\mathbf{E}^{(i)}(\mathbf{r}, \omega, \Omega)|^2]$ by sending a plane wave at it {of frequency ω , propagating along direction Ω [with field $\mathbf{E}_{\text{inc}}^{(i)}(\omega, \Omega)$] into the structure, and polarization i }. This expression opens the path to efficient numerical methods for ICL and scintillation in three dimensions and arbitrary nanophotonic environments.²⁷

III. CONTROL AND ENHANCEMENT OF CATHODOLUMINESCENCE WITH NANOPHOTONICS

Section II suggested several ways in which one can control CL with engineered nanophotonic structures. In this section, we describe several methods to experimentally measure (coherent and incoherent) CL from nanophotonic structures in electron microscopes; we also review experimental demonstrations and nanophotonic techniques to control and enhance CL.

A. Cathodoluminescence in electron microscopes

It is worth noting that CL in electron microscopes was an already-established technique before the 2000s, given its widespread use in gemology and materials science.¹¹¹ The transfer of this technique to the characterization of nanophotonic structures enabled the observation of electron-light interactions in nanophotonic structures via direct spectroscopic techniques (measuring CL) and indirect electron measurement techniques (EELS).

1. Cathodoluminescence spectroscopy and polarimetry techniques

Apart from optical-CL instruments—in which an electron beam is generated under moderate vacuum via discharge in a chamber (small enough to be mounted on a standard optical microscope)—most modern CL instruments are based on a scanning electron microscope (SEM) or a (scanning) transmission electron microscope [(S)TEM]. Figure 5 illustrates representative types of SEM- and TEM-based CL instruments. In all instruments, the light generated by the interaction of a focused electron beam with a sample is out-coupled (with free space collection optics or an optical fiber). Collection optics that have been used for CL measurement and characterization include parabolic mirrors (for angular resolution) and objective lenses (for spatial resolution). Depending on how the light is collected and what additional components are utilized, a wide range of measurements can be performed from obtaining spatially resolved spectral information to angular, polarization, and even time-sensitive detection. Alternatively, placing the nanostructures on the tip of a fiber enables to directly collect the radiation through the fiber, a technique shown to enhance the evanescent field of the free electrons interacting with a nanostructure.²⁰¹ It has also been demonstrated that the evanescent field of free electrons can be amplified as electrons fly over a plasmonic surface.²⁰² Having to pass through a window to exit a vacuum chamber can limit

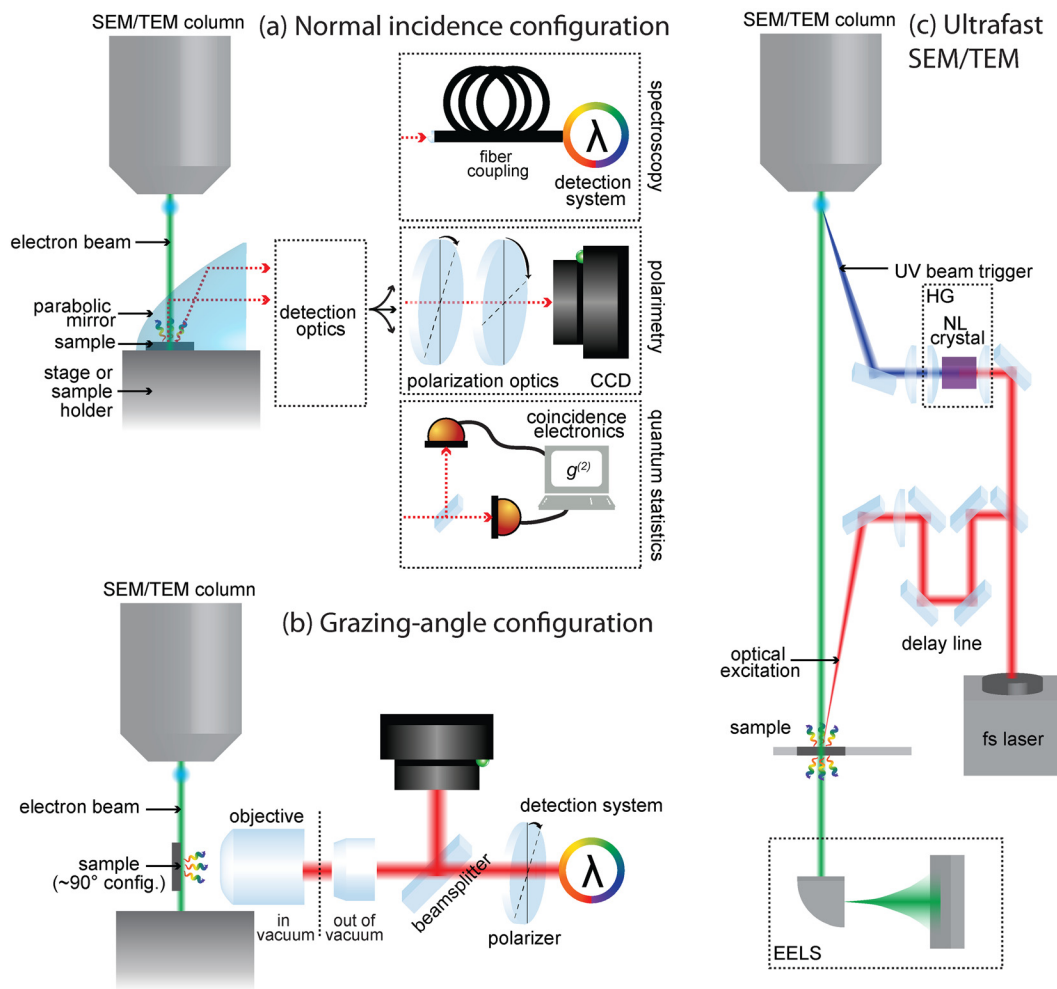


FIG. 5. Probing electron-light interactions in scanning and transmission electron microscopes. The figure illustrates example systems that represent the wide range of experimental capabilities in modern electron microscopy for measuring free-electron-light interactions in nanophotonics. (a) Normal incidence configuration in a scanning (transmission) electron microscope.^{89,127,194–196} An electron beam impinges on a sample through a hole in a parabolic mirror. Light emitted by the sample upon bombardment is collected with a parabolic mirror. Light can be (1) spectrally resolved with a spectral detection system; (2) analyzed with polarization optics before being detected by a CCD camera; or (3) analyzed with a Hanbury Brown–Twiss setup to measure intensity correlations. The electron beam might be triggered by an ultrafast laser or a beam blinder²⁹ [similar to ultrafast SEM/TEM shown in (c)]. (b) Grazing-angle configuration.^{20,21,27,118,124,174,198} Sample is mounted in a 90° configuration. Light emitted from the sample is collected with an objective and imaged on a CCD. Light is also coupled to a spectrometer. Spatial resolution is obtained within the CCD field of view. (c) Ultrafast scanning (transmission) electron microscope setup.^{24,25,88,137–140,142,145,148–150,199} An electron beam is triggered by an ultraviolet pulse generated via a HG (harmonic generation) setup with a NL (nonlinear) crystal pumped by a femtosecond laser. A delay line is used to control the time delay between the optical excitation of the sample and the beam trigger. EELS is also used to measure the electron beam dispersion. CL measurement techniques, as shown in (a) and (b) can be incorporated into such setups.^{88,200}

the detectable wavelength range. An extensive review of current CL measurement techniques was recently published.¹³⁶

Relevant to this review, we highlight selected papers detailing different experimental methods useful for nanophotonic applications of CL. The use of tightly focused electron beams allows for collecting spectral information directly from nanoscale samples with spatial resolution limited by the size of the focused electron beam. CL found applications in plasmonics,^{6,7,9,11–13,48,49,203–210} photonics,^{211,212} semiconductors,^{213–215} electron-beam lithography,²¹⁶ and tomographic reconstruction.²¹⁷ Additionally, the combination of spatial and spectral resolution can be combined to measure the dispersion of CL

effects such as SPR.^{20,21,118,174} Methods were also proposed to disentangle several types of emission from farfield measurements.²¹⁸ Inspired by the early days of radio, it has been shown that a nanoscopic dipole Herzian antenna acts as an efficient emitter of visible light when an electron beam is injected in the dipole gap.²⁰³

Thermal measurements can also be performed with CL, such as nanoscale thermometry and thermal transport measurements both in low current conditions (where sample heating is avoided) and higher current conditions²¹⁹ (where electron beam induced heating is present). Other electron-beam induced effects such as phase transitions in gallium nanoparticles at picojoule excitation energies have also been

observed. Transformations between coexisting structural phases are accompanied by continuous changes in the nanoparticle film's reflectivity²²⁰ and luminescence,²²¹ which may be used for modulating light and optical data storage. Promising new techniques for resolving and hyperspectrally mapping picometric movements by detecting secondary electron emission from the edge of the nanostructure in an electron microscope⁷⁹ might also be realized via cathodoluminescence microscopy in the future.

Next, phase-sensitive imaging measurements were performed utilizing both angle-resolved CL and hyperspectral angle-resolved cathodoluminescence to characterize the far-field phase signal from scattering off of plasmonic nanostructures allowing for the reconstruction of the angle-dependent phase distributions²²² and the coupling between nanoparticles and SPPs.²²³ Similar techniques were used in the Fourier domain to determine the emission polarization properties of sub-wavelength structures like optical nanoantennas.²²⁴ CL measurements have also been used to directly image plasmonic modes in annular nanoresonators, ultrathin plasmonic strip antennas, and metallic thin films,^{11,13,16} and to measure the statistics of the emitted light.^{89,197,225–227} Finally, CL measurements can be employed to characterize photonic band structures and measure the local density of states in nanostructured metallic, semiconductor, and dielectric materials.^{228–231}

2. Probing electron-light interactions in ultrafast electron microscopes

Several TEM-based CL instruments are similar to their SEM analogs, as shown in Figs. 5(a) and 5(b). For instance, collecting mirrors can be used to couple light out of the TEM vacuum chambers. The presence of two collecting mirrors can even allow the measurement of backward and forward radiation independently in some commercial systems.^{232–235} A TEM analog of the spectrally/spatially resolved SEM CL setup was also built,^{125,236} with a low-numerical-aperture objective outside the vacuum chamber and an additional rotation degree of freedom to measure radiation at various angles. An interesting advantage of TEM-based solutions is the availability of EELS, which allows the measurement of electron energy loss and gain after interacting with a sample. EELS provides a method to probe near-field electron-light interactions and is complementary to CL measurement techniques.²⁹ Since EELS is directly related to the photonic local density of states,²³⁰ tomographic techniques have been demonstrated to reconstruct the full three-dimensional local density of states in nanoparticles.²³⁷

Several techniques have been developed to add time-resolved measurements to the field of SEM- and TEM-based CL. This field has also been inspired by the techniques developed for ultrafast TEM in the Zewail group.^{238,239} Currently, time-resolved CL involves modifications to the electron beam emitter to generate electron pulses by the use of ultrashort laser pulses or by using fast electrostatic beam blanking to modulate a continuous electron beam. An example of a time-resolved TEM instrument is shown in Fig. 5(c), wherein an ultrafast laser is used to generate short time duration electron pulses from the electron source. The ultrafast laser can also be used to excite or probe the sample as a function of the of arrival of the electron pulse. Alternatively, instruments with beam blanking devices located after the electron source can provide time-resolved measurements, albeit at a lower time resolution than the laser-driven emitters. One example of

a beam blanking measurement is found in Ref. 240, where a modified standard SEM with beam blanking electronics was used to produce electron pulses in the 80–90 ps duration range. This provided sufficient time resolution to characterize the spontaneous emission decay rate in a cerium-doped yttrium aluminum garnet sample.²⁴⁰

3. Free-electron analogs

Physical analogs of free electrons are convenient platforms to observe some of the above-mentioned physical phenomena. There are many free-electron analogs in the context of CR, since it is a general wave phenomenon, with analogs in classical and quantum electromagnetics, superfluid hydrodynamics, and classical hydrodynamics.⁴⁰ In electromagnetics, CR can also be observed with superluminal polarization waves in SPP,²⁴¹ quantum cascade lasers,⁹⁸ solitons in optical fibers,^{94–97} and superluminal domain perturbations in rapidly time-modulated systems.^{242–245} Synchrotron-like radiation has also been observed by nonlinear polarization induced in a metasurface.²⁴⁶

Most of the physical effects discussed in this review are typically observed from electron beams generated in electron microscopes, with kinetic energies from few keV to hundreds of keV. Analogs of those effects have been predicted with hot electrons in graphene for CR¹⁶² and two-dimensional electrons in a driving field for SPR in the THz regime.²⁴⁷

Some of those analog systems have been utilized as a test bed for novel physical phenomena. In particular, metamaterial-loaded and slot waveguides have been used to directly emulate the propagation of an electron beam.^{248–252} The slot waveguide platform was first used to demonstrate backward Cherenkov radiation,²⁴⁹ an intriguing effect which has otherwise not been demonstrated in free-electron experiments. They have also been used to demonstrate polarization control in SPR²⁵⁰ and, in combination with helical metastructures, SPR vortex beams.^{253,254}

B. Controlling free-electron radiation in nanophotonic structures

1. Angular and spectral control

The spectral-angular distribution of coherent CL effects is, to first order, embedded into their dispersion relation [e.g., Eq. (9) for SPR]. When free electrons emit in a nanophotonic medium, certain spectral and angular components of the radiative fields can be selectively enhanced. The possibility of selective enhancement is evident in periodic structures, where the emitted energy is proportional to the overlap between the electron trajectory and Fourier components of the photonic modes [as in Eqs. (8) and (10)]. The shaping of the spectral-angular distribution via photonic engineering has been the focus of many recent works in coherent CL. Certain notable results are shown in Fig. 6.

It was first proposed by Van den Berg that even perfect reflectors with sinusoidal corrugations could significantly alter the angular distribution of SPR.²⁶¹ Controlling the emission direction can also be achieved by exciting plasmonic resonances in periodic metallic gratings with a free electron.¹²⁶ SPR spectral-angular shaping has also been proposed and demonstrated with engineered grating profiles,¹²⁵ resulting in multi-peaked spectra, and aperiodic gratings.²⁶²

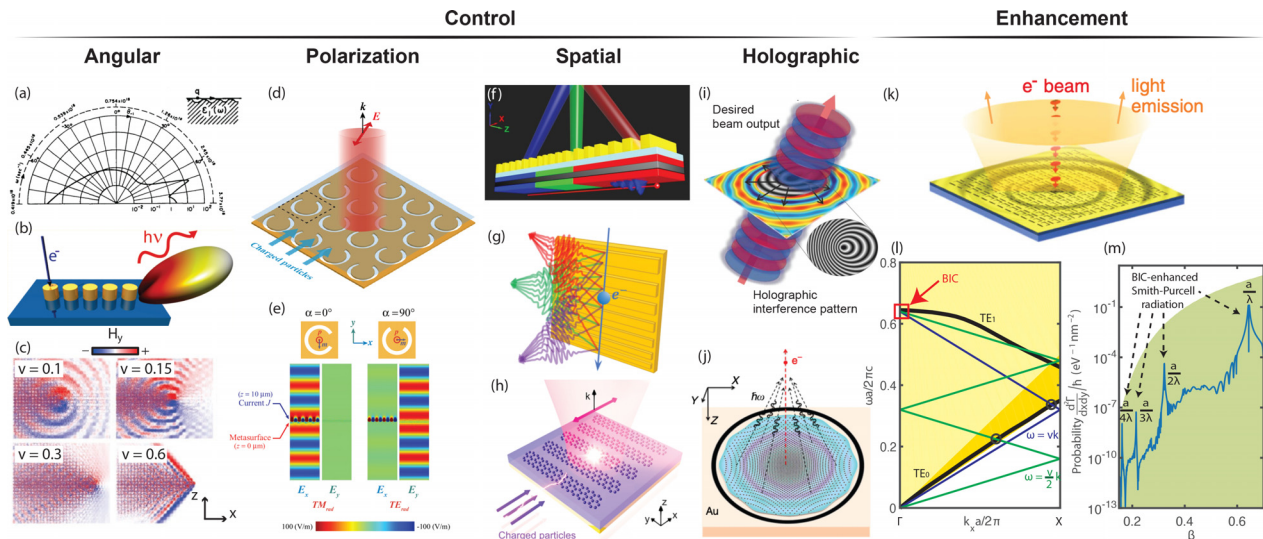


FIG. 6. Controlling and enhancing coherent cathodoluminescence with nanophotonics. Angular control: (a) Angular SPR distribution in a metallic grating with permittivity profile shown as inset. The sharp peak at $\theta = 71^\circ$ is where the surface-plasmon mode is excited strongly. Adapted with permission from Chuang *et al.*, *J. Opt. Soc. Am. A* **1**, 672–676 (1984). Copyright 1984 The Optical Society.¹²⁶ (b) Angular control of CL emission in plasmonic Yagi-Uda antennas. Reproduced from Coenen *et al.*, *Appl. Phys. Lett.* **99**, 143103 (2011), with the permission of AIP Publishing.¹²⁷ (c) Distribution of radiated magnetic field from free electron propagating in PhC. Inset shows the value of v used in simulation (in units of c). Reproduced with permission from Luo *et al.*, *Science* **299**, 368–371 (2003). Copyright 2003 AAAS.⁸ Polarization control: (d) SPR polarization control with Babinet metasurfaces. (e) SPR electric-field distributions from C-apertures. (d) and (e) Reprinted with permission from Wang *et al.*, *Phys. Rev. Lett.* **117**, 157401 (2016). Copyright 2016 the American Physical Society.²⁵⁵ Spatial control: (f) Schematic representation of a chirped grating acting as a SPR lens. Reproduced with permission from Lai *et al.*, *Sci. Rep.* **7**, 11096 (2017). Copyright 2017 Authors, licensed under a Creative Commons Attribution (CC BY) License.²⁵⁶ (g) Focused Smith–Purcell emission by a free-electron-driven metalens: free electrons passing in close proximity to a metagrating with a chirped period emit a converging wavefront, with different wavelengths converging at different positions. Reproduced with permission from Karnieli *et al.*, *Nano Lett.* **22**, 5641–5650 (2022). Copyright 2022 Authors, licensed under a Creative Commons Attribution (CC BY) License.²⁵⁷ (h) Graphene metasurfaces offer a playground to control the amplitude, phase, and polarization of SPR. Reprinted with permission from Su *et al.*, *Nano Lett.* **6**, 1947–1954 (2019). Copyright 2019 American Chemical Society.²⁵⁸ (i) Schematic of a free-electron holographic light source, a universal approach allowing generation of light with prescribed wavelength, direction, and topological charge via point-excitation of holographic metasurfaces. Reproduced with permission from Li *et al.*, *Nat. Commun.* **7**, 13705 (2016). Copyright 2016 Authors, licensed under a Creative Commons Attribution (CC BY) License.²⁵⁹ (j) Formation of focused broadband transition radiation in interaction of an electron beam with an engineered planar lens. The structure is designed to effectively mimic a porous hemispherical geometry. Reproduced with permission from Talebi *et al.*, *Nat. Commun.* **10**, 599 (2019). Copyright 2019 Authors, licensed under a Creative Commons Attribution (CC BY) License.²⁶⁰ Enhancement: (k) Electron-beam-driven collective metamaterial light source concept: highly localized electron beam excitation at the center of a metamaterial array leads, via the strong coupling among metamolecules, to the collective oscillation of many cells and thereby the emission of a free-space light beam. Reprinted with permission from Adamo *et al.*, *Phys. Rev. Lett.* **109**, 217401 (2012). Copyright 2012 the American Physical Society.¹⁷ (l) Calculated TE band structure of a two-dimensional PhC slab (black solid lines) in the Γ -X direction. The area shaded in light and dark yellow indicates the light cone of air and silica, respectively. The electron lines (blue for velocity v , and green for $v/2$) can phase match with either the guided modes (circle) or high-Q resonances near a BIC (red square). (m) Probability of free-electron-induced photon emission in a two-dimensional PhC slab as a function of reduced electron velocity. Strong enhancement of SPR matched phase-matched to BIC and analytical limit accounting for material losses (shaded green). (l) and (m) Reproduced with permission from Yang *et al.*, *Nat. Phys.* **14**, 894–899 (2018). Copyright 2018 Springer Nature.²¹

Localized electron beam excitation can also be leveraged to achieve directional emission in single resonators²⁶³ (selectively exciting and interfering multipolar modes) and plasmonic Yagi antennas excited by free electrons.¹²⁷

The control of radiative angular distribution has also been proposed in CR in PhC⁸ and resonant TR in multi-layer structures.^{52,53} It was demonstrated for TR in elliptical plasmonic bull’s eye targets.²⁶⁴

2. Polarization control

Coherent CL effects are strongly linearly polarized, with limited tunability of the polarization angle. For instance, the polarization angle in SPR is set by the propagation direction of the electron beam. The control of the linear polarization angle and the generation of spin angular momentum in CL has therefore received recent interest, with some notable works shown in Figs. 6(d) and 6(e).

In CR, small components of circular polarization can be acquired when considering spin-polarized electron beams.^{61,265} With unpolarized electron beams, metasurfaces on waveguides have been proposed as platforms to generate circularly polarized CR.²⁶⁶ Because of its potential applications in spectroscopy, the generation of circularly polarized TR light in the mm-wave regime was realized by interfering its forward and backward components²⁶⁷

In particular, SPR is highly polarized along the direction of the electron beam (a feature which has been known since its original discovery⁴). Recent work using cross-coupled electric and magnetic dipoles in THz Babinet metasurfaces suggested a path to steer the angle of linear polarization.^{128,255,268} In principle, graphene metasurfaces can also be utilized to generate circular polarization states in the THz regime.²⁵⁸ More recently, an experimental demonstration was provided by exciting cross-polarized resonances in a PhC.¹²⁴ The generation and control of SPR with orbital angular momentum (vortex

beams) could also be achieved with holographic gratings.²⁶⁹ Full control of the optical angular momentum (spin and angular) in SPR could also find applications in on-chip spectroscopy, but its realization has remained elusive thus far.

3. Spatial control

As coherent CL relies on the excitation of photonic eigenmodes, phase relationships between different wave vector components are constrained, which prevents the control of the radiation far-field profile. With the promise of on-chip electron-driven light sources, there has been a growing interest in manipulating the far-field spatial distribution of emitted radiation in CL. If successful, this effect could be leveraged to realize integrated sources and collimators into a single component, with some notable works shown in Figs. 6(f)–6(h).

The design of a CR lens was first proposed by adjusting the boundary of the Cherenkov target based on ray optics considerations to concentrate light into a focal spot.^{270,271} Given the well-defined spectral-angular relation in SPR, a natural design for a SPR concentrator is a chirped grating (with decreasing pitch along the beam trajectory). That way, the emission angle is tuned along the direction of propagation or, equivalently, a thin-lens-like phase modulation is imparted to light generated via SPR. This concept was first proposed theoretically and demonstrated numerically for concentrators working at single wavelengths^{125,256} and exhibiting strong chromatic aberrations. Alternatively, graphene metasurfaces can also generate converging SPR in the THz regime.²⁵⁸ Recently, signatures of SPR lensing have been reported²⁵⁷ using a chirped grating design.

The most general type of far-field wavefront engineering, holography, has also been proposed using tailored nanophotonic structures [see Figs. 6(i), and 6(j)].²⁵⁹ This method relies on the controlled interference of transition radiation, generated by a focus electron beam, with an interference holographic mask. This enables the generation of light with prescribed wavelength, direction, divergence, and topological charge via point-excitation of CL holography in plasmonic^{222,259,272} and dielectric²⁷³ metasurfaces. Free-electron holographic light sources offer a universal approach to generate light with prescribed wavelength, direction, divergence and topological charge via point-excitation of holographic metasurfaces with an electron beam. Finally, inspired by transformation optics, several nanophotonic structure designs have been demonstrated to realize broadband focusing of transition radiation,²⁶⁰ vortex light beams,²⁷⁴ and more generally structured light from free electrons.³² Such structures have been proposed as platforms to measure time-energy correlation functions in electron microscopes, paving the way toward attosecond electron-based spectroscopy techniques.²⁷⁵

C. Enhancing free-electron-light interactions in nanophotonics

1. Coherent cathodoluminescence

The existence of fundamental bounds on CL, as presented in Sec. II C, begs the following question: could one enhance coherent CL with nanophotonics to achieve emission efficiencies approaching such bounds?

The possibility of resonant enhancement in electron–light interaction is highlighted in the phase-matching relation Eq. (1). Emission

into phase-matched photonic modes is selectively enhanced by adjusting the electron velocity. This concept has been proposed to enhance SPR by coupling electrons to photonic²⁷⁶ and plasmonic resonances,¹²⁶ and CR in PhCs.⁸ Resonant enhancement of the electron–light interaction is also observed in an increase in PINEM signal when exciting photonic resonances.^{24,25}

Specifically, one can design a resonance mode of interest in metamaterials and excite it with a beam of free electrons. In particular, localized free-electron-beam excitation can create a low-divergence spatially coherent free-space light beam that bears similarity with laser light through coherent collective oscillation of an ensemble of coupled metamolecules.¹⁷

An interesting feature of the general bound from Eq. (11) is its apparent divergence in the limit of small losses. Recently, the use of BICs²⁷⁷ was theoretically proposed as a new mechanism for enhanced SPR: coupling of electrons with BICs.²¹ Such photonic modes have the extreme quality factors of guided modes but are, crucially, embedded in the radiation continuum, with no resulting SPR into the far field. Figure 6(j) shows that by tuning the electron velocity (here, a sheet electron beam translationally invariant along the y direction), one can achieve strong emission enhancements (such as in CL into a guided mode), while keeping the radiative coupling into a continuum resonance. This enhancement technique also requires a large modal overlap between the BIC and the electron near field [see Fig. 6(i)]. This enhancement mechanism is in line with the upper limits from Eq. (11), since the enhancement is limited by the material's non-zero losses at the emission wavelengths. Nevertheless, it has been theoretically shown that BIC-enhanced coupling enables the radiation intensity to closely approach this upper limit at several resonant velocities. In the presence of an absorptive channel, the maximum enhancement occurs at a small offset from the BIC where the Q -matching condition is satisfied.

Photonics can also provide CL enhancement via band structure engineering in periodic structures. Specifically, the perspective of enhancing SPR and CR was first proposed in two-dimensional periodic PhCs, where the intersection of the electron plane with photonic band structures can be manipulated.¹⁶⁰ In particular, it was predicted that bands with vanishing transverse components of the group velocity would display strong emission enhancement; this has been suggested recently as a platform to realize full phase-matching of point electrons with photonic modes (with a continuum of phase-matched transverse modes). Recent experimental demonstration of resonant enhancement from flatbands also shows their potential in enhancing electron–light interactions.¹²⁴

2. Incoherent cathodoluminescence and scintillation

The process of light emission from fluctuating current sources in samples pumped by high-energy particles is called ICL (for free-electron pumps) or scintillation (for x - and γ -ray pumps). From the multi-physics picture illustrated in Fig. 1(e), there appears to be at least two ways to enhance it: (1) control of the available emitting states in the electronic band structure (material engineering) and (2) control of the nanophotonic environment (nanophotonic engineering).

a. Material engineering. ICL can be enhanced by engineering the electronic band structure of emitting materials and specifically

available defect states or bandgap to make bright emitters. Such techniques are also ubiquitous in the context of brighter and faster x-ray scintillator development, which rely on the development of new materials⁵⁰ (typically, with large atomic numbers, high density, and doped with rare earth elements to emit strongly in the UV–NIR).

In the context of ICL, two-dimensional materials and van der Waals heterostructures have received particular attention, given their bright emission properties and exceptional nanophotonic properties.^{280,281} Specifically, bright UV emission from hexagonal boron nitride has been demonstrated, with emission patterns reminiscent of a lasing behavior.¹³³ Such substrates were then integrated into handheld devices to demonstrate their applicability to sanitization¹³¹ [see Figs. 7(c) and 7(d)]. Those achievements have been enabled by the control of hexagonal boron nitride's excitonic properties, by growing crystals under high pressure and temperature. Recent work utilized ICL as a probe of the material's properties down to the few-layer regime.²⁸²

In semiconductors, the emission process is similar to LEDs, and the electron–hole pair recombination probability limits the emission efficiency. In van der Waals heterostructures, engineering of the excitonic properties of an ICL emitter can be realized, for instance, by “sandwiching” a transition metal dichalcogenide monolayers between two layers of hexagonal boron nitride, resulting in several orders of magnitude ICL enhancement.²⁷⁸

Another common method for enhancing ICL and scintillation is by fabricating semiconductor quantum dots whose small dimensions cause quantum confinement of the excited charge carriers, resulting in larger dipoles and enhanced emission rates.²⁸³

b. Nanophotonic engineering. The other way to enhance ICL and scintillation is to engineer the nanophotonic environment in which the fluctuating current sources from Eq. (4) radiate. The possibility of nanophotonic enhancement can be explained by Eqs. (12) and (13).

Scintillation and ICL being in essence spontaneous emission, they can be enhanced with nanophotonics in two distinct ways: (1) via direct enhancement of the rate of spontaneous emission by shaping the density of optical states^{66,284} [as evident from the eigenmode formulation in Eq. (12)] or (2) through improved light extraction from bulk scintillators [as evident from the far-field formulation in Eq. (13)]. The prospect of enhancing scintillation through the local density of states as well as the prospect of large scintillation enhancements, by either mechanism, had remained unrealized until recently.²⁷

A recent demonstration of enhanced ICL from self-trapped hole defects in silica is shown in Fig. 7(e), where the emitted ICL from a defect transition emitting around ~ 700 nm is enhanced and spectrally shaped. This is enabled by the presence of several high-Q photonic resonances due to the PhC patterning at the surface of the scintillator. In the same work, ICL is used as a spectroscopic probe of the nonlinear microscopic dynamics accounting for competing emission processes. Given the generality of Eqs. (12) and (13), we note that similar techniques can be used to enhance emission from a stochastic ensemble of emitters, which could find applications beyond ICL and scintillation: in thermal radiation,^{87,285–287} LEDs,²⁸⁸ and photoluminescence.²⁸⁸

3. Nanophotonic scintillators for x- and γ -ray detection

Our approach highlights the common physical origin of ICL (from free electrons) and scintillation from x- and γ -rays. In a broader

context scintillators are used for applications across medical imaging, nondestructive testing, and night vision technologies.⁵⁰ This analogy holds especially for low-energy x-rays whose penetration depths are comparable to electrons in SEM and TEM.

The possibility of nanophotonic scintillation enhancement for x- and γ -ray application was recently revived by the availability of large-scale deposition and patterning techniques compatible with state-of-the-art scintillators in x-ray and nuclear imaging. Early work demonstrated enhanced light extraction provided by a PhC coating atop a bulk scintillator^{279,289–294} [see Fig. 7(i)]. It was then realized that x-ray scintillation could be enhanced via local photonic density of state enhancement in multi-layered structure, a convenient platform to also shape the scintillation angular emission profile.⁶⁶ Taking a step forward, a general framework for scintillation in nanophotonics was proposed,²⁷ with experimental demonstrations of both enhancement mechanisms in two distinct platforms (ICL and x-ray scintillation). The perspective of using such nanophotonic scintillators for x-ray imaging was demonstrated in the same work [see Figs. 7(j) and 7(k)].

IV. FUTURE PERSPECTIVES

In this section, we outline several research directions, which we believe will significantly flourish in the next few years. In particular, we highlight the use of nanophotonics in enabling these novel applications of (quantum) electron–light interactions.

A. Quantum effects

Much of the content of this review can be understood in purely classical terms: in terms of solutions to the classical Maxwell's wave equation in a dielectric medium, with a source $\mathbf{J}(\mathbf{r}, \omega)$ (a moving electron). Even in the case of ICL (scintillation), the radiation may be understood in terms of radiation from classically non-deterministic current sources, although the correlations of the current sources may be dictated by the quantum statistics of the radiating currents (e.g., Bose–Einstein or Fermi–Dirac statistics). Nowadays, there is a great deal of effort in theoretically predicting, as well as experimentally isolating, genuinely quantum mechanical effects in free-electron radiation, which may not be described in terms of the classical wave equation with a source. In this section, we give a brief outline of the different types of quantum effects that can emerge in free-electron radiation. For more discussion of such effects (with different emphasis), we refer the reader to Refs. 59 and 63.

1. Recoil effects

As discussed in Sec. II, much of the spectral and angular properties of coherent cathodoluminescence may be understood from the phase-matching relation Eq. (1). This phase-matching, while naturally following from the classical Maxwell's equations, can also be understood in quantum mechanical terms. Taking the emitted photon to have a four-momentum $k = \hbar(\omega, \mathbf{k})$ and the electron to have its own [initial (*i*)/final (*f*)] four-momentum $p_{i,f} = (E_{i,f}, \mathbf{p}_{i,f})$, with E the electron energy and \mathbf{p} the electron momentum—one finds that the phase-matching condition is nothing other than an approximate solution to the energy-momentum conservation condition $p_i = p_f + k$: under the approximation that the electron energy and momentum change only weakly due to the emission. For almost all cases in electron–photon interactions in nanophotonics, this approximation is very accurate,

Enhancing incoherent cathodoluminescence (electron scintillation)

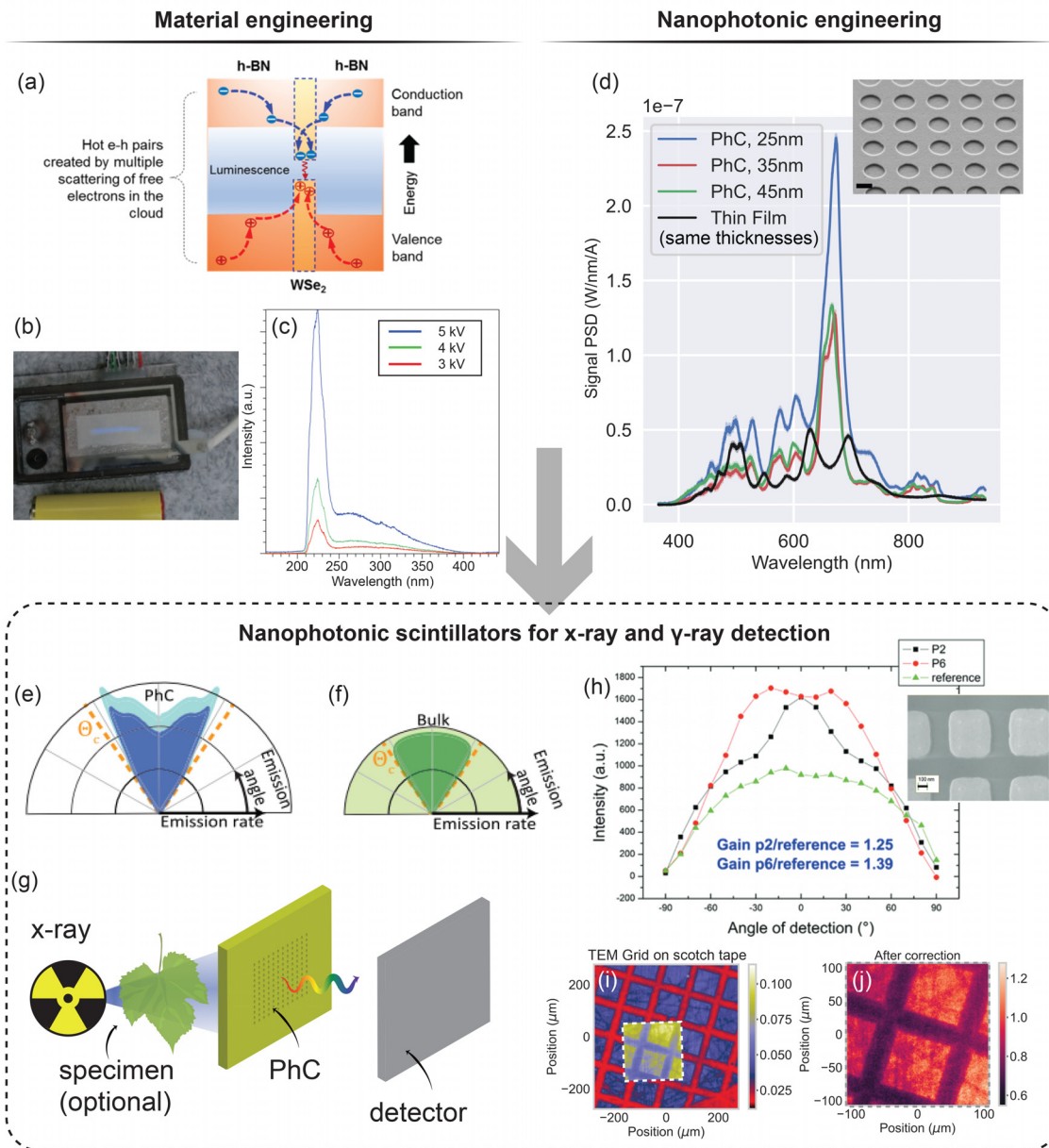


FIG. 7. From shaping incoherent cathodoluminescence (ICL) to nanophotonic scintillators. (a) Nearly monochromatic cathodoluminescence can be observed from monolayers of chalcogenide semiconductor in a van der Waals heterostructure when it is sandwiched between layers of boron nitride with a higher energy gap. Reprinted with permission from Zheng *et al.*, *Nano Lett.* **17**, 6475–6480 (2017).²⁷⁸ Copyright 2017 American Chemical Society. (b) Photograph of a prototype far-ultraviolet plane-emission device in operation. (c) Output spectra show a dominant peak at 225 nm. This broad far-ultraviolet band is a result of superposition of excitonic bands from 215 to 227 nm. The weak tail from 250 to 400 nm is a result of impurities and defect states. (b) and (c) Reproduced with permission from Watanabe *et al.*, *Nat. Photonics* **3**, 591–594 (2009). Copyright 2009 Springer Nature.¹³¹ (d) ICL signal from self-trapped holes defect in silicon-on-insulator wafer for various PhCs and thin film geometries. Inset shows SEM image of PhC with etch depth 35 nm (scale bar 200 nm). (e) Angular distribution from a multilayer scintillator. (f) Angular distribution from bulk scintillator. (e) and (f) Reprinted with permission from Kurman *et al.*, *Phys. Rev. Lett.* **125**, 040801 (2020). Copyright 2020 the American Physical Society.⁸⁵ (g) Schematic of PhC scintillators for x-ray applications. (h) Measured scintillation angular distribution from scintillators with dielectric antireflection coatings. Inset: scanning electron micrograph of sample P6 (scale bar 100 nm). Samples “P2” and “P6” refer to two different designs of antireflection coatings on scintillators. Reproduced with permission from Knapitsch *et al.*, *Int. J. Mod. Phys. A* **29**, 1430070 (2014).²⁷⁹ Copyright 2014 World Scientific. (i) X-ray scan of a TEM grid glued to tape using a PhC scintillator on YAG:Ce. The yellow bright area corresponds to the PhC pattern. (j) Flat-field corrected image from (i). (d), (i), and (j) Reproduced with permission from Roques-Carmes *et al.*, *Science* **375**, abm9293 (2022). Copyright 2022 AAAS.²⁷

since the typical energy of the photon (≈ 1 eV), is quite small compared to that of the electron (in excess of ≈ 1 keV). The main regimes in which the recoil approximation may break down are: low electron energies,^{165,175,298} high photon energies,^{295,296,299} and near velocity thresholds⁶¹ (between which the emission is kinematically forbidden or allowed). All three of these regimes have been subject of theoretical investigation: as of this writing, clear quantum recoil effects in coherent CL have not been observed (for SPR, the region where such quantum effects should arise is shown in Fig. 4).

2. Quantum interference and waveshaping effects

Another way by which quantum effects can alter light emission by electrons is through electron waveshaping. One might imagine that controlling the wavefunction of the emitting electron will control the emitted radiation in much the same way that controlling the shape of the current density in Maxwell's equations controls the radiation. The situation in quantum mechanics is more subtle, as the wavefunction of the electron does not represent a smeared out charge density. If it did, one could imagine that simply expanding or compressing the electron wavefunction transverse to its motion would change its radiation (e.g., by Cherenkov or Smith–Purcell emission): tunable transverse coherent size has shown that the intensity does not depend on the electron wavefunction.²³⁶ In fact, the transverse size had no influence on the emitted radiation, as first predicted for CR.⁶¹ Despite this, the shape of the electron wavefunction *can* alter the radiation, under specific circumstances: namely, if the emitted photon has enough symmetries broken. For example, in a recent experiment involving EELS, it was found that the electron energy-loss spectrum could be modified by shaping the electron wavefunction to have its symmetry be compatible with different localized (plasmonic) modes of a structure.¹⁴⁰ Namely, the electron could lose energy primarily through a dipolar mode of the structure (of one energy) when the electron wavefunction had a certain symmetry, and lose energy primarily through a quadrupolar mode (of a different energy) when the electron had a different symmetry. This shows the influence of the electron wavefunction on plasmon emission.

The key constraint that enables the dependence on the wavefunction is that the measurement system performs post-selection on the electron (by conditioning the measurement on the electron state). Without electron post-selection, the radiation intensity is independent of the electron wavefunction.^{59–61} Unlike with the radiation intensity, other properties of the radiation such as coherence can be modified by shaping the electron wavefunction. This was first predicted in Ref. 56, showing that the pulse duration of CR depends on the electron wavefunction. Building on this concept, electron wavefunction shaping was proposed as a method to control the quantum states of free-electron radiation.^{57,300}

Recent theoretical work has also shown how the emission of high-energy photons such as x-rays can be controlled through quantum interference effects.⁵⁸ In that work, it was shown how quantum interference of amplitudes could lead to strong control over phenomena such as bremsstrahlung radiation, where an electron emits radiation after scattering off of an external (Coulomb) potential. In particular, two different initial electron states can scatter into the same final electron and emitted photon states, leading to quantum interference. Such interference can only occur when the external potential

breaks sufficient symmetries to enable both transitions to conserve energy and momentum simultaneously. Beyond this, the effect of the electron wavefunction on the entanglement structure of the emitted radiation has been explored theoretically in other examples of coherent CL (e.g., CR).⁶¹ Reference 62 also showed the existence of phase correlations between the emitted CL field and the electron-modulating laser in the quantum-optical regime.

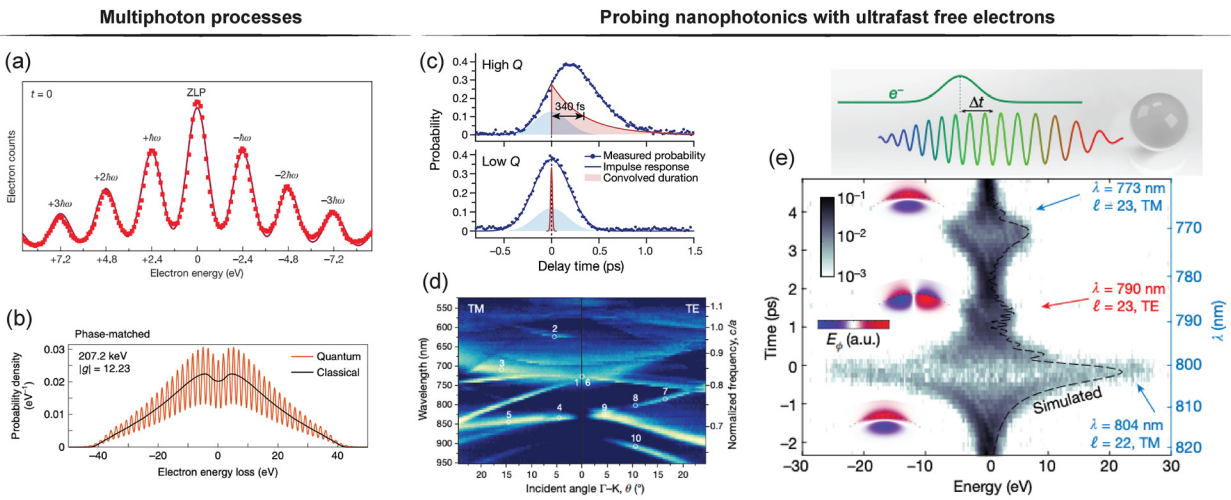
3. High-order effects in quantum electrodynamics

A third class of important effects, which are now a rich and vibrant field on their own, is related to strong-field interactions, in which an electron can interact with a strong external field, leading to absorption or stimulated versions of coherent CL (see Fig. 8). For the types of fields that are now typical in such experiments, an electron can emit and absorb multiple (even hundreds) of quanta from the external field, leading to a large number of quantized peaks in the electron energy loss/gain spectrum of the post-interaction electron.¹³⁷ Since the first observations of this effect in 2009,¹⁴⁵ which forms the basis for PINEM, this effect has been observed and extended in many guises and has been exploited for imaging electromagnetic fields in materials with high spatial (nanometer) resolution and high temporal (sub-picosecond) resolution.^{25,137–140,142,146,148,199} Of particular note is that the electron energy spectrum after the interaction is sensitive to the quantum statistics of the field,³⁰¹ as recently demonstrated in Ref. 149 to distinguish between thermal and coherent light. Such effects form the basis for the extension of quantum optics to free electrons. High-order processes have also been proposed in CR from heavy ions, resulting in modified emission angles and suppression of radiation pathways close to the threshold.¹⁶¹ More recently, quantum regimes of interactions between free electrons and photons were observed at much lower energies in a SEM.³⁰²

B. Ultrashort-wavelength emitters

Free electrons are ideal platforms to generate high-energy radiation, since they carry large kinetic energies (in the keV to MeV range in most electron microscopes) that can be converted into electromagnetic radiation. Among the effects we have discussed in this review, SPR displays the most evident wavelength tunability, via the incident electron velocity and the structure periodicity. In Fig. 4, we highlighted recent work toward SPR from low-energy (sub-keV) electrons and short-wavelength photons. Specifically, there has been excitement around achieving tunable SPR in the UV.³⁰³ There has been renewed interest in using SPR to generate UV light, with recent experimental demonstrations down to a wavelength of 230 nm. The perspective of generating UV light with SPR is especially promising for sanitization applications.³⁰⁴

Generation of much shorter wavelength radiation has been reported in crystals, whose structure is naturally “modulated” at Ångström scales. Recently, such effects found renewed interest in van der Waals heterostructures pumped by free electrons emitting soft x-ray light,²³ with enhanced functionality demonstrated in Ref. 305. The ability to control coherent CL with engineered nanostructures is especially exciting for short-wavelength radiation generation, given the unavailability of efficient focusing optics in this wavelength range. Therefore, the ability to concentrate coherent CL has received specific



Controlling electron beams with nanophotonics

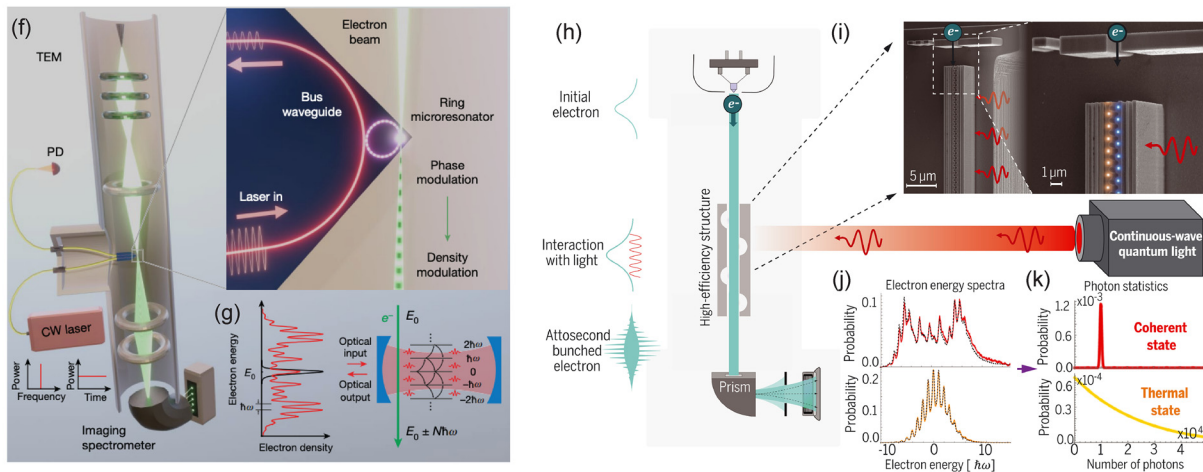


FIG. 8. Quantum and ultrafast free-electron-light interactions. (a) Electron energy loss spectra (EELS) of carbon nanotubes irradiated with an intense fs laser pulse at two different delay times. The energy spectrum at coincidence of the two pulses ($t=0$ fs) displays the zero-loss peak (ZLP) and multiple quanta of photon absorption/emission. Reproduced with permission from Barwick *et al.*, *Nature* **462**, 902–906 (2009). Copyright 2009 Springer Nature.¹⁴⁵ (b) Electron energy loss spectrum for a perfectly phase-matched interaction between a free-electron and a photonic near field along a prism. Reproduced with permission from Dahan *et al.*, *Nat. Phys.* **16**, 1123–1131 (2020). Copyright 2020 Springer Nature.¹³⁷ (c) Experimental (dots) and simulated (solid curve) probabilities of the electron-cavity-photon interaction as a function of delay time, enabling the measurement of photonic Q-factors. (d) Band structure measured by scanning over incident laser angles and wavelengths. Each data point in the map is a separate EELS measurement of the electron-light interaction at zero delay time. (c) and (d) Reproduced with permission from Wang *et al.*, *Nature* **582**, 50–54 (2020). Copyright 2020 Springer Nature.²⁵ (e) Probing multiple nanophotonic resonances with EELS and a chirped pulse. The color maps present the relevant azimuthal component of the electric field. Reproduced with permission from Kfir *et al.*, *Nature* **582**, 46–49 (2020). Copyright 2020 Springer Nature.²⁴ (f) Rendering of the experimental setup to achieve continuous-wave modulation of an electron beam. Inset: magnified interaction region with the electron beam passing a microresonator. CW, continuous wave; PD, photodiode. (g) Left: during interaction with the laser-driven cavity mode, the initially narrow electron spectrum (black) develops discrete sidebands at integer multiples of the photon energy (red). Right: in a cavity quantum electrodynamics depiction, the cavity photons induce transitions between the free-electron energy ladder states. (f) and (g) Reproduced with permission from Henke *et al.*, *Nature* **600**, 653–658 (2021). Copyright 2021 Authors, licensed under a Creative Commons Attribution (CC BY) License.¹⁵⁰ (h) CW modulation of electron wave functions in transmission electron microscopy. (i) Highly efficient electron-light interaction facilitated by an inverse-designed silicon-photonic nanostructure (scanning electron microscope image), consisting of a Bragg mirror and a periodic channel that achieves quasi-phase-matching of electron and quantum light. (j) The electron energy spectrum after the interaction with two types of light states: coherent and thermal. (k) The corresponding photon statistics reconstructed from the measured spectra. (h)–(k) Reproduced with permission from Dahan *et al.*, *Science* **373**, eabj7128 (2021). Copyright 2021 AAAS.¹⁴⁹

attention recently, with proposals in the near-UV¹²⁵ and x-ray regime.^{172,306}

Pumping of wide-bandgap materials with free electrons is another way to generate bright UV light. In particular, hexagonal

boron nitride was proposed as a bright UV emitter, exhibiting lasing behavior,¹³³ and the possibility of being integrated in compact devices.¹³¹ The existence of a large catalogue of wide-bandgap semiconductors,³⁰⁷ in addition to the availability of nanophotonic

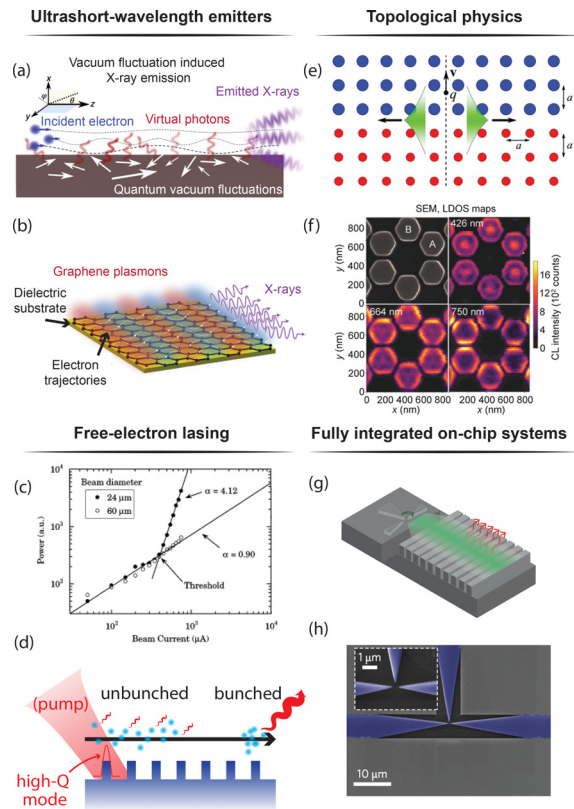


FIG. 9. Future prospects in free-electron radiation. (a) A beam of electrons traveling in the near field of a nanophotonic structure and interacting with its vacuum field can emit x-rays. Reproduced with permission from Rivera *et al.*, *Nat. Phys.* **15**, 1284–1289 (2019). Copyright 2019 Springer Nature.²⁹⁵ (b) Compton scattering with graphene plasmons to produce short-wavelength output radiation. Reproduced with permission from Wong *et al.*, *Nat. Photonics* **10**, 46–52 (2016). Copyright 2016 Springer Nature.²⁹⁶ (c) Detected power vs electron beam current in an experiment demonstrating super-radiant SPR. Reprinted with permission from Urata *et al.*, *Phys. Rev. Lett.* **80**, 516–519 (1998). Copyright 1998 the American Physical Society.¹³⁴ (d) Proposal for free-electron lasing in nanophotonic structures. An electron beam interacting with a high-Q photonic mode can self-bunch. The use of an optical pump can enable the observation of stimulated emission from free electrons. (e) TR between two PhCs, resulting in the excitation of edge and bulk modes. Reprinted with permission from Yu *et al.*, *Phys. Rev. Lett.* **123**, 057402 (2019). Copyright 2019 the American Physical Society.²⁹⁷ (f) Spatially resolved cathodoluminescence spectroscopy of topological modes in a hexagonal photonic lattice of silicon Mie resonators. Reprinted with permission from Peng *et al.*, *Phys. Rev. Lett.* **122**, 117401 (2019). Copyright 2019 the American Physical Society.²²⁹ (g) Fully integrated on-chip Smith–Purcell silicon radiator, consisting of a silicon field emitter array and a silicon nanograting. Reproduced with permission from Roques-Carnes *et al.*, *Nat. Commun.* **10**, 3176 (2019). Copyright 2019 Authors, licensed under a Creative Commons Attribution (CC BY) License.¹¹⁸ (h) Planar molybdenum electron emitter used for on-chip Cherenkov emission from hyperbolic metamaterials. Reproduced with permission from Liu *et al.*, *Nat. Photonics* **11**, 289–292 (2017). Copyright 2017 Springer Nature.¹⁹

enhancement and shaping,²⁷ and the theoretical possibility of large conversion efficiencies,⁸⁵ makes UV ICL a particularly promising research direction.

Other ways, such as scattering of electrons with graphene SPPs^{296,299,308} [see Fig. 9(a)] and virtual vacuum photons²⁹⁵

[see Fig. 9(b)] have been proposed to generate table-top x-ray sources pumped by free electrons.

C. Nanophotonic dielectric laser accelerators

The time-reversal process of free-electron emission generation is particle acceleration. Similarly, nanophotonic development leads to new designs, device miniaturization, and performance improvement in particle accelerators.^{309–313}

A channel for electron propagation usually has to be defined for accelerators; this limits the current applied to the device. To address this issue, a multi-channel accelerator structure was proposed,³¹⁴ which naturally transforms the seminal dual-grating accelerating structure into PhCs, thus allowing device designs via 2D and 3D band structure engineering. The use of photonic flatband proposed for enhancing SPR¹²⁴ can be used in reverse to aid in optical localization and enhancement of electron acceleration without the need for electron channels, thus allowing more electrons to interact with accelerator devices.

Experimentally, an inverse-designed (see section below), waveguide-integrated, microscale dielectric laser accelerator was fabricated and tested, showing acceleration gradients around 30 MeV/m in a recent demonstration.²² Meanwhile, electron phase space control was realized via introducing phase discontinuity (similar to a lattice dislocation) in a high-aspect ratio, silicon-based, integrated structure,³¹³ indicating the possibility for particle acceleration of confined beams to the MeV range with minimal particle loss over extended distances. Quantized peaks in electron energy spectra have also been observed in dielectric laser accelerators, revealing the quantum nature of such devices.⁶⁴

D. Inverse-designed free-electron radiators and accelerators

Computational inverse design has now penetrated every single field of nanophotonics.^{315,316} Free-electron radiation will be no exception. In general, inverse design enables the automatic discovery of nanophotonics structures that are locally optimal for a pre-defined objective function. Among the various inverse-design techniques available, topology optimization is one of the most popular, given the many degrees of freedom it can investigate, while remaining computationally tractable, thanks to efficient gradient calculation methods (such as the adjoint method³¹⁵ and automatic differentiation techniques³¹⁷). Topology optimization enables the inverse design “pixel by pixel” of various nanophotonic components, such as metasurfaces,³¹⁸ multiplexers,³¹⁹ and nonlinear frequency converters,³²⁰ while taking into account fabrication constraints.³²¹

Topology optimization has recently been utilized to discover optimal nanophotonic structures as free-electron radiators, nanophotonic scintillators,²⁷ radiators, and accelerators.^{22,322} Several features of free-electron radiation make it amenable to inverse design. First, electron–light interaction lends itself to closed-form expressions describing radiation and acceleration processes (such as the total emitted power in a range of angles, frequencies, and polarizations; or the particle acceleration gradient). Those expressions are enabled by the modeling of electron–light interactions mediated by the current sources from Eqs. (2) and (4). Second, numerical methods are available in the time- and frequency-domains to calculate those expressions and their

respective gradients efficiently, either via the adjoint method or via automatic differentiation algorithms. This enables the implementation of efficient gradient-based discovery of complex nanophotonic structures interacting efficiently with free electrons. We also expect that recent efforts in inverse design for free-electron physics will bolster interest in fully differentiable multi-physics pipelines, integrating electron trajectories and energy loss, microscopic dynamics, and nanophotonics.²⁷

E. Free-electron lasing in nanophotonic structures and other exotic effects

As discussed earlier in this review, the various coherent mechanisms by which a free electron can emit light (e.g., CR, SPR, TR) can be thought of as elementary processes of spontaneous emission in which an electron transitions to a state of lower kinetic energy while emitting a quantized mode of Maxwell's equations (a photonic quasiparticle⁶³) whose properties (e.g., energy, momentum, polarization, and other quantum numbers) strongly control the observed properties of the emission. From this “quantum” perspective of free-electron radiation, the general principles of quantum mechanics determine that an electron should be able to absorb photonic quasiparticles (leading to inverse processes, such as inverse CR⁵²³) and also *stimulatedly emit* photonic quasiparticles—leading to amplification and lasing phenomena.⁵²⁴

Although we have used quantum arguments to infer the possibility of stimulated emission and free-electron lasing, much of the known phenomena can be described classically. In fact, the “stimulated emission” of light by a beam of classical electrons simply corresponds to net deceleration of a beam of electrons in an applied electromagnetic field: by energy conservation, the lost energy of the electrons goes into the field (into photons). Meanwhile, “absorption” of photons by the electrons corresponds to net acceleration.

Net stimulated emission by a beam of electrons forms the basis for a number of developed and developing technologies. In the microwave domain, these effects form the basis for established high-power microwave sources such as traveling wave tubes and klystrons used in space communication systems.^{325,326} In traveling wave tubes and klystrons, such “lasing” is largely based on SPR. In the x-ray domain, amplification has also been achieved based on the collective interactions of a dense beam of electrons with a spatially periodic magnetic field.³²⁷ In such systems, the electrons can amplify their own spontaneous emission, when the density of the electron beam is sufficiently high.

As of this writing, free-electron lasing based on coherent CL in nanophotonic systems is yet to be observed, despite reported signatures of super-radiance at THz frequencies,¹³⁴ shown in Fig. 9(c). Such observations represent not only a logical step in the development of compact and integrated free electron radiation sources, but may also grant some practical advantages. Compared to CL, the coherence of the lasing field should be quite high [especially in architectures based on an optical feedback cavity,^{41,328} such as a PhC resonance,^{329,330} as shown in Fig. 9(d)].

Finally, other unconventional effects in free-electron radiation, such as backward CR, remain unobserved as of this writing. Originally predicted in left-handed materials,^{8,129,248,331,332} and then in PhCs,⁸ this effect has not been observed yet with free electrons (despite observations using free-electron analogs²⁴⁹) The observation of this effect in nanophotonics with free electrons could open a way to novel high-energy particle detector designs.

F. Topological effects in free-electron radiation

Topological photonics^{333,334} has undergone rapid development over the past decade. So far, optical excitations have been mostly employed for these studies. In Sec. III C 1, we have shown that photonic topological features, such as BICs^{21,335} and flatbands,¹²⁴ can be used for boosting radiation generation from free electrons. In the following, we outline other opportunities at the intersection between free-electron nanophotonics and topological photonics.

Several recent advances show that free electrons can serve as probes for photonic topology. In Ref. 229, the local density of states and the band structure of a topological PhC were mapped out via CL techniques, as shown in Fig. 9(f). In Ref. 297, highly relativistic electron beams were used to excite the domain-wall edge states of a quantum-spin-Hall-like metamaterial, where localization to the edge was identified [see Fig. 9(e)]. In Ref. 336, free electrons were proposed for resolving the optically driven phase transition of a graphene-dielectric metamaterial. In addition, it is worth mentioning that photonic topological properties can also be potentially adapted, in turn, for diagnosing the location, energy, and duration of charged particle beams.

Furthermore, free electrons can serve as pumps for photonic topology. It has been shown that free electron beams can drive nonreciprocity in metallic waveguides, therefore giving rise to unidirectionally propagating modes.³³⁷ Because the free electron velocity can be substantially higher than that in solids, the bandwidth of the resulting unidirectionality could be dramatically increased.

Some of the free-electron analogs mentioned earlier in this review could be adequate platforms to demonstrate physical effects which require hard-to-realize photonic topological states in the visible regime such as chiral edge states³³⁸ and Weyl points.³³⁹

G. Non-equilibrium emission processes with free electrons

The recent development of a general framework to predict non-equilibrium radiation phenomena such as scintillation (or ICL) reveals the sensitive dependence of the scintillation spectrum on the non-equilibrium distribution of the excited electrons generated by the high-energy electron beam.²⁷ In particular, the radiated photons can inherit the non-equilibrium statistical properties of the excited electrons and holes generated in the scintillation process. Consider an interesting example which has yet to be observed in scintillation: when electrons and holes in semiconductors are produced by a high-energy pump, the electrons and holes quickly relax into a non-equilibrium quasi-steady state which can be described by quasi-Fermi levels for the electrons and holes which are different. In such a case, the radiated photons must (by detailed balance) experience an effective chemical potential dictated by the difference between the electron and hole chemical potentials.^{86,87} This is of course in complete contrast to thermal radiation, in which the photons have no chemical potential. More broadly, by controlling the energy of the high-energy electron pump, different non-equilibrium distributions of electrons and holes can be conceivably created, shaping the quantum statistical properties of the radiated photons. The ability to achieve this would represent a new way to control the quantum optical properties of photons. Such effects could be measured through second-order intensity correlation ($g^{(2)}$) measurements, as applied to ICL,^{89,227} where it was shown that for low enough electron-currents, the radiation could show signatures of

antibunching, indicating single-photon emission, or signatures of bunching, indicating super-Poissonian statistics, depending on the material.

H. Fully integrated on-chip systems

The use of compact nanoscale structures to convert energy from free electrons into radiation has spurred interest into realizing fully on-chip systems. This perspective is enabled by the realization of on-chip electron emitters, such as field emitter arrays.^{121–123,340} Such devices can realize focused electron beams, in continuous wave or pulsed regimes, with relatively low kinetic energies (from few tens of keV to few hundreds of eV).

It was first realized that Smith–Purcell and Cherenkov systems could be fully integrated on chip,^{117,341–343} thereby enabling integrated, tunable light emitters. One of the additional advantages of fully integrated systems is the ability to precisely align the electron emitter with nanophotonics structures, thereby optimizing free-electron emission. One such device is shown in Fig. 9(g), with a recent design of electron emitter shown in Fig. 9(h). Recent work focused on the realization of all-silicon Smith–Purcell emitters¹¹⁸ and on-chip systems emitting CR from hyperbolic metamaterials.¹⁹ The realization of fully integrated electron accelerator devices has also been the focus of much research recently.^{22,54,55,313,344}

With the development of vacuum packaging techniques,³⁴⁵ in addition to high-voltage DC-DC converters³⁴⁶ for lab-on-chip applications, such integrated systems could be realized in a scalable way and be compatible with CMOS fabrication processes.

V. CONCLUSION

In conclusion, we have provided a review of the fundamental physics and applications of free-electron interactions with nanophotonic structures, with an emphasis on nanophotonic mechanisms to enhance and shape free-electron radiation. We first proposed a general classical framework to model cathodoluminescence as the excitation of photonic eigenmodes by the free-electron current density. This excitation can be coherent, as is the case for all coherent CL effects, or partially incoherent, as is the case for ICL and scintillation. This framework enabled us to re-derive fundamental formula in free-electron physics and to provide a unified method to shape and enhance CL. It also enabled us to derive fundamental bounds on electromagnetic radiation from free electrons in arbitrary nanophotonic environments.

Those methods have been confirmed and observed thanks to the development of experimental methods to observe and characterize light emission from free electrons in nanophotonic structures. Specifically, we reviewed the development of CL and EELS measurement techniques in SEM and (ultrafast) TEM. The several experimental methods we reviewed have enabled the measurement of all optical properties of interest: spectral, angular, time, spatial, polarization distributions, and quantum correlations. They can also be complemented by measurement of the electron properties with EELS.

Finally, we shared our enthusiasm for a few ways in free-electron radiation enabled by nanophotonics, namely, the emerging fields of ultrafast, topological, and quantum effects in electron microscopy, the design of ultrashort-wavelength emitters pumped by free electrons, miniaturized particle accelerators, novel inverse-design techniques applied to free-electron emitters, and the aspiration to reach stimulated emission and lasing by free electrons in nanophotonics. While

the realization of some of those effects might still be a few years ahead of us, we believe that the strong interest from our community has already demonstrated the potential of nanophotonics in controlling and enhancing CL. Future developments in the field might unlock some of the most promising prospects in free-electron physics, such as the realization of widely tunable integrated light sources from x-rays to mm-wave, particle accelerators, and high-energy particle detectors. They should find direct applications across particle detection and acceleration, electron microscopy, dosimetry, water sanitization, medical imaging, and therapy.

ACKNOWLEDGMENTS

The authors would like to thank Nikolay I. Zheludev, Kevin MacDonald, and Liang Jie Wong for their helpful comments on the review. This material is based on work supported in part by the U.S. Army Research Laboratory and the U.S. Army Research Office through the Institute for Soldier Nanotechnologies under contract W911NF-18-2-0048. This material is also, in part, based on work supported by the Air Force Office of Scientific Research under awards FA9550-20-1-0115 and FA9550-21-1-0299. Y.Y. acknowledges the support from the start-up fund of the University of Hong Kong and the National Natural Science Foundation of China Excellent Young Scientists Fund (HKU 12222417).

AUTHOR DECLARATIONS

Conflict of Interest

The authors have no conflicts to disclose.

Author Contributions

Charles Roques-Carnes wrote the manuscript with inputs from Steven Earl Kooi, Yi Yang, Nicholas Rivera, and Phillip D. Keathley. All authors read and reviewed the final manuscript.

Charles Roques-Carnes: Conceptualization (lead); Data curation (lead); Formal analysis (lead); Writing – original draft (lead); Writing – review & editing (lead). **Marin Soljagic:** Supervision (lead). **Steven Earl Kooi:** Writing – original draft (supporting); Writing – review & editing (supporting). **Yi Yang:** Writing – original draft (supporting); Writing – review & editing (supporting). **Nicholas Rivera:** Writing – original draft (supporting); Writing – review & editing (supporting). **Phillip Keathley:** Supervision (supporting). **John Dimitris Joannopoulos:** Supervision (supporting). **Steven G Johnson:** Supervision (supporting). **Ido Kaminer:** Supervision (supporting). **Karl K. Berggren:** Supervision (supporting).

DATA AVAILABILITY

The data that support the findings of this study are available within the article and upon request for Fig. 4.

APPENDIX: UNIFIED THEORY OF COHERENT CATHODOLUMINESCENCE

In this Appendix, we provide more details on the derivation of emitted power densities for coherent CL. We then re-derive emblematic formulas of the field for CR, TR, and excitation of SPPs.

We derive our theory in the context of classical electrodynamics, with the analogy of a moving free electron as a time-dependent current source. We consider the case of a moving electron of charge q propagating along the linear trajectory defined by the speed vector $\mathbf{v} = v\hat{\mathbf{r}}_{\parallel}$, which is described by the current distribution of Eqs. (2) and (3).

This expression of the current in Fourier domain already highlights the existence of preferred field wavevectors to which the electron beam will couple to, which is the essence of the phase-matching condition shown in Eq. (1). The nanophotonic environment is described by the Green's function expansion shown in Eq. (5).

The total energy radiated by a dipole can be calculated as an integral in frequency domain as follows:¹⁶⁰

$$U = -\frac{1}{\pi} \text{Re} \left(\int d\omega \int d\mathbf{r} \mathbf{J}^*(\mathbf{r}, \omega) \mathbf{E}(\mathbf{r}, \omega) \right). \quad (\text{A1})$$

We then get the master equation shown in Eq. (6), which describes all coherent CL effects considered in this review. In the Subsections 1–3 of the Appendix, we provide more details on its application the cases of CR, TR, and excitation of SPPs.

1. Cherenkov radiation

CR in its simplest embodiment occurs in a homogeneous dielectric environment and consists in the spontaneous emission of plane waves by a charged particle [see Fig. 3(a)]. Its description entails eigenmodes as plane waves of the form $\mathbf{F}_k(\mathbf{r}, \omega) = \frac{e^{i\mathbf{k}\cdot\mathbf{r}}}{\sqrt{V\tilde{\epsilon}}} \hat{\mathbf{e}}_k$, in a uniform medium of refractive index $n = \sqrt{\tilde{\epsilon}}$ with polarization vector $\hat{\mathbf{e}}_k$ orthogonal to \mathbf{k} , and $\tilde{\epsilon} = (2\omega k)^{-1} \frac{d}{d\omega} (\omega^2 \epsilon(\omega))|_{\omega=\omega_k}$. The dispersion relation is $\omega_k = c|\mathbf{k}|/n$. We also make the following adjustment $\sum_m \rightarrow \int V \frac{d\mathbf{k}}{(2\pi)^3}$. Injecting this expression into Eq. (6), we get the Frank–Tamm formula¹⁰⁰ for the spectral density per unit propagation length as follows:

$$\frac{dU}{d\omega dl} = \frac{\mu_0 q^2}{4\pi} \omega \sin^2 \theta \Theta(\beta n - 1), \quad (\text{A2})$$

with Θ the Heaviside function [$\Theta(x) = 1$ if $x > 0$, otherwise $\Theta(x) = 0$]. Here, the Cherenkov angle is defined such as $\cos \theta = (\beta n)^{-1}$. The Heaviside function defines the well-known Cherenkov threshold $\beta n > 1$, which is equivalent to satisfying the phase-matching condition from Eq. (1) in a bulk medium.

2. Transition radiation

To describe transition radiation within the same framework, we consider the simplified case of a charge impinging at normal incidence on a perfect conductor [see Fig. 3(c)]. We resort to the introduction of an image charge with opposite charge and velocity $(-q, -\mathbf{v})$. The current distribution $\mathbf{J}(\mathbf{r}, \omega)$ is modified accordingly and its emission in free space is considered. The current distribution is given by

$$\mathbf{J}(\mathbf{r}, t) = q\mathbf{v}[\delta(\mathbf{r} - \mathbf{v}t) + \delta(\mathbf{r} + \mathbf{v}t)] \quad \text{for } t < 0, \quad (\text{A3})$$

$$\mathbf{J}(\mathbf{r}, t) = 0 \quad \text{for } t > 0, \quad (\text{A4})$$

and its Fourier transform

$$\mathbf{J}(\mathbf{r}, \omega) = q\hat{\mathbf{r}}_{\parallel} \delta(\mathbf{r}_{\perp}) e^{-i\omega\sigma(r_{\parallel})\frac{1}{v}}, \quad (\text{A5})$$

with σ the sign function. Utilizing the free space mode expansion as in the case of Cherenkov radiation, we get the following spectral distribution, first derived by Ginzburg and Tamm:⁶⁷

$$\frac{dU}{d\omega d\Omega} = \frac{\mu_0 q^2 \beta^2 c}{4\pi^3} \frac{\sin^2 \theta}{(1 - \beta^2 \cos^2 \theta)^2}. \quad (\text{A6})$$

3. Coherent excitation of SPPs by free electrons

Excitation of SPPs is often considered in tandem with TR, since it typically occurs at the interface between two media supporting SPP. This phenomenon is observed even in the absence of corrugation at the surface because the electron point nature enables coupling directly to the SPP modes. Our formalism captures this effect by considering emission into the SPP modes rather than free space modes as before.

For simplicity, we consider an electron flying parallel to a planar interface at $r_{\perp} = 0$ (reduced to a 2D problem). We consider the simplified case of a lossless interface between a dielectric (relative permittivity $\epsilon_1 > 0$) and a metal (relative permittivity $\epsilon_2 < 0$). The p -polarized modes take the following form [in the $(r_{\parallel}, r_{\perp})$ basis]:

$$\mathbf{F}_{1,\mathbf{k}}(\mathbf{r}) \propto \begin{pmatrix} 1 \\ -\sqrt{-\frac{\epsilon_1}{\epsilon_2}} \end{pmatrix} e^{-|k_{1,\perp}|r_{\perp}} e^{-ik_{\parallel}r_{\parallel}}, \quad (\text{A7})$$

$$\mathbf{F}_{2,\mathbf{k}}(\mathbf{r}) \propto \begin{pmatrix} 1 \\ -\sqrt{-i\frac{\epsilon_1}{\epsilon_2}} \end{pmatrix} e^{-|k_{2,\perp}|r_{\perp}} e^{-ik_{\parallel}r_{\parallel}}. \quad (\text{A8})$$

The following dispersion relation:

$$k_{\parallel}^2 = \frac{\epsilon_1 \epsilon_2}{\epsilon_1 + \epsilon_2} \frac{\omega^2}{c^2}, \quad \text{and} \quad k_{\perp,i}^2 = \frac{\epsilon_i^2}{\epsilon_1 + \epsilon_2} \frac{\omega^2}{c^2}. \quad (\text{A9})$$

We obtained the following expression for the energy emitted by the free electron per unit length:

$$\frac{dU}{d\omega dl} \propto \frac{q^2 \mu_0 c}{2\pi^2} \sqrt{\frac{-\epsilon_1^2}{\epsilon_1 + \epsilon_2}} e^{-2|k_{\perp}|r_{\perp}}, \quad (\text{A10})$$

with the phase-matching condition:

$$\omega = vk_{\parallel} = \beta \sqrt{\frac{\epsilon_1 \epsilon_2}{\epsilon_1 + \epsilon_2}} \omega, \quad (\text{A11})$$

which can be solved graphically by finding the intersection of the SPP's dispersion and the electron line $\omega = vk_{\parallel}$. Such an intersection always exists for the lower branch (corresponding to the excitation of a SPP).

REFERENCES

- W. Crooke, "XVI. Contributions to molecular physics in high vacua. Magnetic deflection of molecular trajectory—Laws of magnetic rotation in high and low vacua—Phosphorogenic properties of molecular discharge," *Philos. Trans. R. Soc. London* **170**, 641–662 (1879).

- ²P. A. Cherenkov, "Visible light from clear liquids under the action of gamma radiation," *Dokl. Akad. Nauk SSSR* **2**, 451 (1934).
- ³V. Ginzburg and I. Frank, "Radiation of a uniformly moving electron due to its transition from one medium into another," *Zh. Eksp. Teor. Fiz.* **9**, 353–362 (1945).
- ⁴S. J. Smith and E. M. Purcell, "Visible light from localized surface charges moving across a grating," *Phys. Rev.* **92**, 1069 (1953).
- ⁵R. H. Ritchie, "Plasma losses by fast electrons in thin films," *Phys. Rev.* **106**, 874 (1957).
- ⁶F. J. García de Abajo, "Relativistic energy loss and induced photon emission in the interaction of a dielectric sphere with an external electron beam," *Phys. Rev. B* **59**, 3095 (1999).
- ⁷N. Yamamoto, K. Araya, and F. J. García de Abajo, "Photon emission from silver particles induced by a high-energy electron beam," *Phys. Rev. B* **64**, 205419 (2001).
- ⁸C. Luo, M. Ibanescu, S. G. Johnson, and J. D. Joannopoulos, "Cherenkov radiation in photonic crystals," *Science* **299**, 368–371 (2003).
- ⁹M. V. Bashevoy, F. Jonsson, A. V. Krasavin, N. I. Zheludev, Y. Chen, and M. I. Stockman, "Generation of traveling surface plasmon waves by free-electron impact," *Nano Lett.* **6**, 1113–1115 (2006).
- ¹⁰J. T. Van Wijngaarden, E. Verhagen, A. Polman, C. E. Ross, H. J. Lezec, and H. A. Atwater, "Direct imaging of propagation and damping of near-resonance surface plasmon polaritons using cathodoluminescence spectroscopy," *Appl. Phys. Lett.* **88**, 221111 (2006).
- ¹¹M. V. Bashevoy, F. Jonsson, K. F. MacDonald, Y. Chen, and N. I. Zheludev, "Hyperspectral imaging of plasmonic nanostructures with nanoscale resolution," *Opt. Express* **15**(18), 11313–11320 (2007).
- ¹²E. J. R. Vesseur, R. De Waele, M. Kuttge, and A. Polman, "Direct observation of plasmonic modes in Au nanowires using high-resolution cathodoluminescence spectroscopy," *Nano Lett.* **7**, 2843–2846 (2007).
- ¹³C. E. Hofmann, E. J. R. Vesseur, L. A. Sweatlock, H. J. Lezec, F. J. G. De Abajo, A. Polman, and H. A. Atwater, "Plasmonic modes of annular nanoresonators imaged by spectrally resolved cathodoluminescence," *Nano Lett.* **7**, 3612–3617 (2007).
- ¹⁴G. Adamo, K. F. MacDonald, Y. H. Fu, C. M. Wang, D. P. Tsai, F. J. García De Abajo, and N. I. Zheludev, "Light well: A tunable free-electron light source on a chip," *Phys. Rev. Lett.* **103**, 113901 (2009).
- ¹⁵G. Adamo, K. F. MacDonald, Y. H. Fu, D. P. Tsai, F. J. García De Abajo, and N. I. Zheludev, "Tunable electron-beam-driven nanoscale light source," *J. Opt. A: Pure Appl. Opt.* **12**, 024012 (2010).
- ¹⁶E. S. Barnard, T. Coenen, E. J. R. Vesseur, A. Polman, and M. L. Brongersma, "Imaging the hidden modes of ultrathin plasmonic strip antennas by cathodoluminescence," *Nano Lett.* **11**, 4265–4269 (2011).
- ¹⁷G. Adamo, J. Y. Ou, J. A. So, S. D. Jenkins, F. Deaangelis, K. F. MacDonald, E. Diafabrizio, J. Ruostekoski, and N. I. Zheludev, "Electron-beam-driven collective-mode metamaterial light source," *Phys. Rev. Lett.* **109**, 217401 (2012).
- ¹⁸I. Kaminer, S. Kooi, R. Shiloh, B. Zhen, Y. Shen, J. López, R. Remez, S. A. Skirlo, Y. Yang, J. D. Joannopoulos, A. Arie, and M. Soljačić, "Spectrally and spatially resolved Smith–Purcell radiation in plasmonic crystals with short-range disorder," *Phys. Rev. X* **7**, 011003 (2017).
- ¹⁹F. Liu, L. Xiao, Y. Ye, M. Wang, K. Cui, X. Feng, W. Zhang, and Y. Huang, "Integrated Cherenkov radiation emitter eliminating the electron velocity threshold," *Nat. Photonics* **11**(5), 289–292 (2017).
- ²⁰A. Massuda, C. Roques-Carmes, Y. Yang, S. E. Kooi, Y. Yang, C. Murdia, K. K. Berggren, I. Kaminer, and M. Soljačić, "Smith–Purcell radiation from low-energy electrons," *ACS Photonics* **5**, 3513 (2017).
- ²¹Y. Yang, A. Massuda, C. Roques-Carmes, S. E. Kooi, T. Christensen, S. G. Johnson, J. D. Joannopoulos, O. D. Miller, I. Kaminer, and M. Soljačić, "Maximal spontaneous photon emission and energy loss from free electrons," *Nat. Phys.* **14**, 894–899 (2018).
- ²²N. V. Sapra, K. Y. Yang, D. Vercrucy, K. J. Leadle, D. S. Black, R. J. England, L. Su, R. Trivedi, Y. Miao, O. Solgaard, R. L. Byer, and J. Vučković, "On-chip integrated laser-driven particle accelerator," *Science* **367**, 79–83 (2020).
- ²³M. Shentcis, A. K. Budniak, X. Shi, R. Dahan, Y. Kurman, M. Kalina, H. Herzig Sheinfux, M. Blei, M. K. Svendsen, Y. Amouyal, S. Tongay, K. S. Thygesen, F. H. Koppens, E. Lifshitz, F. J. García de Abajo, L. J. Wong, and I. Kaminer, "Tunable free-electron x-ray radiation from van der Waals materials," *Nat. Photonics* **14**(11), 686–692 (2020).
- ²⁴O. Kfir, H. Lourenço-Martins, G. Storeck, M. Sivis, T. R. Harvey, T. J. Kippenberg, A. Feist, and C. Ropers, "Controlling free electrons with optical whispering-gallery modes," *Nature* **582**(7810), 46–49 (2020).
- ²⁵K. Wang, R. Dahan, M. Shentcis, Y. Kauffmann, A. Ben Hayun, O. Reinhardt, S. Tseses, and I. Kaminer, "Coherent interaction between free electrons and a photonic cavity," *Nature* **582**, 50–54 (2020).
- ²⁶A. Nussupbekov, G. Adamo, J. K. So, L. Wu, Y. D. Chong, and L. J. Wong, "Enhanced photon emission from free electron excitation of a nanowell," *APL Photonics* **6**, 096101 (2021).
- ²⁷C. Roques-Carmes, N. Rivera, A. Ghorashi, S. E. Kooi, Y. Yang, Z. Lin, J. Beroz, A. Massuda, J. Sloan, N. Romeo, Y. Yu, J. D. Joannopoulos, I. Kaminer, S. G. Johnson, and M. Soljačić, "A framework for scintillation in nanophotonics," *Science* **375**, abm9293 (2022).
- ²⁸F. J. García De Abajo, "Optical excitations in electron microscopy," *Rev. Mod. Phys.* **82**, 209–275 (2010).
- ²⁹A. Polman, M. Kociak, and F. J. García de Abajo, "Electron-beam spectroscopy for nanophotonics," *Nat. Mater.* **18**, 1158–1171 (2019).
- ³⁰N. Talebi, "Interaction of electron beams with optical nanostructures and metamaterials: From coherent photon sources towards shaping the wave function," *J. Opt.* **19**, 103001 (2017).
- ³¹T. Coenen, S. V. d. Hoedt, and A. Polman, "A new cathodoluminescence system for nanoscale optics, materials science, and geology," *Microscopy Today* **24**, 12–19 (2016).
- ³²J. Christopher, M. Taleb, A. Maity, M. Hentschel, H. Giessen, and N. Talebi, "Electron-driven photon sources for correlative electron-photon spectroscopy with electron microscopes," *Nanophotonics* **9**, 4381–4406 (2020).
- ³³M. Curie, *Radio-Active Substances* (Chemical News Office, 1904).
- ³⁴V. L. Ginzburg, "Radiation by uniformly moving sources (Vavilov–Cherenkov effect, transition radiation, and other phenomena)," *Phys.-Usp.* **39**, 973–982 (1996).
- ³⁵N. Akopov, E. C. Aschenauer, K. Bailey, S. Bernreuther, N. Bianchi, G. P. Capitani, P. Carter, E. Cisbani, R. De Leo, E. De Sanctis, D. De Schepper, V. Djordjadze, B. W. Filippone, S. Frullani, F. Garibaldi, J. O. Hansen, B. Hommez, M. Iodice, H. E. Jackson, P. Jung, R. Kaiser, J. Kanesaka, R. Kowalczyk, L. Lagamba, A. Maas, V. Muccifora, E. Nappi, K. Negodaeva, W. D. Nowak, T. O'Connor, T. G. O'Neill, D. H. Potterveld, D. Ryckbosch, Y. Sakemi, F. Sato, A. Schwind, T. A. Shibata, K. Suetsugu, E. Thomas, M. Tytgat, G. M. Urciuoli, K. Van de Kerckhove, R. Van de Vyver, S. Yoneyama, H. Zohrabian, and L. F. Zhang, "The HERMES dual-radiator ring imaging Cherenkov detector," *Nucl. Instrum. Methods Phys. Res., Sect. A* **479**, 511–530 (2002).
- ³⁶G. Adams, V. Burkert, R. Carl, T. Carstens, V. Frolov, L. Houghtlin, G. Jacobs, M. Kossov, M. Klusman, B. Kross, M. Onuk, J. Napolitano, J. W. Price, C. Riggs, Y. Sharabian, A. Stavinsky, L. C. Smith, W. A. Stephens, P. Stoler, W. Tuzel, K. Ullrich, A. Vlassov, A. Weisenberger, M. Witkowski, B. Wojtkowski, P. F. Yergin, and C. Zorn, "The CLAS Cherenkov detector," *Nucl. Instrum. Methods Phys. Res., Sect. A* **465**, 414–427 (2001).
- ³⁷K. Nakamura, "Hyper-Kamiokande: A next generation water Cherenkov detector," *Int. J. Mod. Phys. A* **18**, 4053–4063 (2003).
- ³⁸K. Kleinknecht, "Particle detectors," *Phys. Rep.* **84**, 85–161 (1982).
- ³⁹A. Papanestis, "The LHCb RICH system; detector description and operation," *Nucl. Instrum. Methods Phys. Res. Sect. A* **766**, 14–18 (2014).
- ⁴⁰I. Carusotto and G. Rousseaux, "The Cherenkov effect revisited: From swimming ducks to zero modes in gravitational analogues," in *Analogous Gravity Phenomenology* (Springer, 2013), pp. 109–144.
- ⁴¹C. Pellegrini, A. Marinelli, and S. Reiche, "The physics of x-ray free-electron lasers," *Rev. Mod. Phys.* **88**, 015006 (2016).
- ⁴²J. D. Joannopoulos, S. G. Johnson, J. N. Winn, and R. D. Meade, *Photonic Crystals: Molding the Flow of Light*, 2nd ed. (Princeton University Press, 2011).
- ⁴³L. Novotny and B. Hecht, *Principles of Nano-Optics* (Cambridge University Press, 2009), Vol. 9781107005, pp. 1–564.
- ⁴⁴N. Yu and F. Capasso, "Flat optics with designer metasurfaces," *Nat. Mater.* **13**, 139–150 (2014).
- ⁴⁵E. Yablonovitch, "Photonic crystals," *J. Mod. Opt.* **41**, 173–194 (1994).

- ⁴⁶K. J. Vahala, "Optical microcavities," *Nature* **424**, 839–846 (2003).
- ⁴⁷D. K. Armani, T. J. Kippenberg, S. M. Spillane, and K. J. Vahala, "Ultra-high-Q toroid microcavity on a chip," *Nature* **421**(6926), 925–928 (2003).
- ⁴⁸N. Yamamoto, K. Araya, A. Toda, and H. Sugiyama, "Light emission from surfaces, thin films and particles induced by high-energy electron beam," *Surf. Interface Anal.* **31**, 79–86 (2001).
- ⁴⁹N. Yamamoto, M. Nakano, and T. Suzuki, "Light emission by surface plasmons on nanostructures of metal surfaces induced by high-energy electron beams," *Surf. Interface Anal.* **38**, 1725–1730 (2006).
- ⁵⁰A. Gektin and M. Korzhik, *Inorganic Scintillators for Detector Systems* (Springer, 2017).
- ⁵¹T. M. Shaffer, E. C. Pratt, and J. Grimm, "Utilizing the power of Cerenkov light with nanotechnology," *Nat. Nanotechnol.* **12**, 106–117 (2017).
- ⁵²X. Lin, H. Hu, S. Easo, Y. Yang, Y. Shen, K. Yin, M. P. Blago, I. Kaminer, B. Zhang, H. Chen, J. Joannopoulos, M. Soljačić, and Y. Luo, "A Brewster route to Cerenkov detectors," *Nat. Commun.* **12**(1), 5554 (2021).
- ⁵³X. Lin, S. Easo, Y. Shen, H. Chen, B. Zhang, J. D. Joannopoulos, M. Soljačić, and I. Kaminer, "Controlling Cerenkov angles with resonance transition radiation," *Nat. Phys.* **14**(8), 816–821 (2018).
- ⁵⁴U. Niedermayer, O. Boine-Frankenheim, and T. Egenolf, "Designing a dielectric laser accelerator on a chip," *J. Phys.: Conf. Ser.* **874**, 012041 (2017).
- ⁵⁵D. S. Black, K. J. Leedle, Y. Miao, U. Niedermayer, R. L. Byer, and O. Solgaard, "Laser-driven electron lensing in silicon microstructures," *Phys. Rev. Lett.* **122**, 104801 (2019).
- ⁵⁶A. Karnieli, N. Rivera, A. Arie, and I. Kaminer, "The coherence of light is fundamentally tied to the quantum coherence of the emitting particle," *Sci. Adv.* **7**, eabf8096 (2021).
- ⁵⁷A. Ben Hayun, O. Reinhardt, J. Nemirovsky, A. Karnieli, N. Rivera, and I. Kaminer, "Shaping quantum photonic states using free electrons," *Sci. Adv.* **7**, 4270–4280 (2021).
- ⁵⁸L. J. Wong, N. Rivera, C. Murdia, T. Christensen, J. D. Joannopoulos, M. Soljačić, and I. Kaminer, "Control of quantum electrodynamical processes by shaping electron wavepackets," *Nat. Commun.* **12**(1), 1700 (2021).
- ⁵⁹F. J. García De Abajo and V. D. Giulio, "Optical excitations with electron beams: Challenges and opportunities," *ACS Photonics* **8**, 945–974 (2021).
- ⁶⁰V. D. Giulio, O. Kfir, C. Ropers, and F. J. García De Abajo, "Modulation of cathodoluminescence emission by interference with external light," *ACS Nano* **15**, 7290–7304 (2021).
- ⁶¹I. Kaminer, M. Mutzafi, A. Levy, G. Harari, H. H. Sheinfux, S. Skirlo, J. Nemirovsky, J. D. Joannopoulos, M. Segev, and M. Soljačić, "Quantum Čerenkov radiation: Spectral cutoffs and the role of spin and orbital angular momentum," *Phys. Rev. X* **6**, 011006 (2016).
- ⁶²O. Kfir, V. D. Giulio, F. J. García de Abajo, and C. Ropers, "Optical coherence transfer mediated by free electrons," *Sci. Adv.* **7**, eabf6380 (2021).
- ⁶³N. Rivera and I. Kaminer, "Light-matter interactions with photonic quasiparticles," *Nat. Rev. Phys.* **2**(10), 538–561 (2020).
- ⁶⁴Y. Adiv, K. Wang, R. Dahan, P. Broaddus, Y. Miao, D. Black, K. Leedle, R. L. Byer, O. Solgaard, R. J. England, and I. Kaminer, "Quantum nature of dielectric laser accelerators," *Phys. Rev. X* **11**, 041042 (2021).
- ⁶⁵L. Schächter, "Periodic structures," in *Beam-Wave Interaction in Periodic and Quasi-Periodic Structures* (Springer Berlin Heidelberg, Berlin, Heidelberg, 1997), pp. 195–234.
- ⁶⁶Y. Kurman, A. Shultzman, O. Segal, A. Pick, and I. Kaminer, "Photonic-crystal scintillators: Molding the flow of light to enhance x-ray and γ -ray detection," *Phys. Rev. Lett.* **125**, 040801 (2020).
- ⁶⁷V. L. Ginzburg, "Quantum theory of radiation of electron uniformly moving in medium," *Zh. Eksp. Teor. Fiz.* **2**, 441 (1940).
- ⁶⁸R. T. Cox, "Momentum and energy of photon and electron in the Čerenkov radiation," *Phys. Rev.* **66**, 106 (1944).
- ⁶⁹C. W. Hsu, B. Zhen, J. Lee, S. L. Chua, S. G. Johnson, J. D. Joannopoulos, and M. Soljačić, "Observation of trapped light within the radiation continuum," *Nature* **499**, 188–191 (2013).
- ⁷⁰J. K. Hyun, M. Couillard, P. Rajendran, C. M. Liddell, and D. A. Muller, "Measuring far-ultraviolet whispering gallery modes with high energy electrons," *Appl. Phys. Lett.* **93**, 243106 (2008).
- ⁷¹Y. Auad, C. Hamon, M. Tencé, H. Lourenço-Martins, V. Mkhitarian, O. Stéphan, F. J. García de Abajo, L. H. Tizei, and M. Kociak, "Unveiling the coupling of single metallic nanoparticles to whispering-gallery microcavities," *Nano Lett.* **22**, 319–327 (2022).
- ⁷²N. L. Thomas, D. T. Alexander, M. Cantoni, W. Sigle, R. Houdré, and C. Hébert, "Imaging of high-Q cavity optical modes by electron energy-loss microscopy," *Phys. Rev. B: Condens. Matter Mater. Phys.* **87**, 155314 (2013).
- ⁷³N. Müller, V. Hock, H. Koch, N. Bach, C. Rathje, and S. Schäfer, "Broadband coupling of fast electrons to high-Q whispering-gallery mode resonators," *ACS Photonics* **8**, 1569–1575 (2021).
- ⁷⁴R. J. Glauber, "Time-dependent displacement correlations and inelastic scattering by crystals," *Phys. Rev.* **98**, 1692 (1955).
- ⁷⁵J. J. Earney, "Phonon scattering of fast electrons by crystals," *Philos. Mag.* **23**, 577–583 (1971).
- ⁷⁶P. Rez, "Is localized infrared spectroscopy now possible in the electron microscope?," *Microsc. Microanal.* **20**, 671–677 (2014).
- ⁷⁷B. D. Forbes and L. J. Allen, "Modeling energy-loss spectra due to phonon excitation," *Phys. Rev. B* **94**, 014110 (2016).
- ⁷⁸M. J. Lagos, A. Trügler, U. Hohenester, and P. E. Batson, "Mapping vibrational surface and bulk modes in a single nanocube," *Nature* **543**(7646), 529–532 (2017).
- ⁷⁹T. Liu, J. Y. Ou, E. Plum, K. F. MacDonald, and N. I. Zheludev, "Visualization of subatomic movements in nanostructures," *Nano Lett.* **21**, 7746–7752 (2021).
- ⁸⁰X. Li, G. Haberfehlner, U. Hohenester, O. Stéphan, G. Kothleitner, and M. Kociak, "Three-dimensional vectorial imaging of surface phonon polaritons," *Science* **371**, 1364–1367 (2021).
- ⁸¹Y. Kurman, R. Dahan, H. H. Sheinfux, K. Wang, M. Yannai, Y. Adiv, O. Reinhardt, L. H. Tizei, S. Y. Woo, J. Li, J. H. Edgar, M. Kociak, F. H. Koppens, and I. Kaminer, "Spatiotemporal imaging of 2D polariton wave packet dynamics using free electrons," *Science* **372**, 1181 (2021).
- ⁸²Á. Konečná, J. Li, J. H. Edgar, F. J. García De Abajo, J. A. Hachtel, A. Konečná, F. J. García De Abajo, J. Li, J. H. E. Tim Taylor, and J. A. Hachtel, "Revealing nanoscale confinement effects on hyperbolic phonon polaritons with an electron beam," *Small* **17**, 2103404 (2021).
- ⁸³E. J. Hall and A. J. Giaccia, *Radiobiology for the Radiologist*, 7th ed. (Lippincott Williams & Wilkins, 2012).
- ⁸⁴J. B. Birks, *The Theory and Practice of Scintillation Counting*, International Series of Monographs on Electronics and Instrumentation (Pergamon Press, 1967).
- ⁸⁵C. A. Klein, "Bandgap dependence and related features of radiation ionization energies in semiconductors," *J. Appl. Phys.* **39**, 2029 (1968).
- ⁸⁶P. Wurfel, "The chemical potential of radiation," *J. Phys. C: Solid State Phys.* **15**, 3967–3985 (1982).
- ⁸⁷J. J. Greffet, P. Bouchon, G. Brucoli, and F. Marquier, "Light emission by non-equilibrium bodies: Local Kirchhoff Law," *Phys. Rev. X* **8**, 021008 (2018).
- ⁸⁸M. Kociak and L. F. Zagonel, "Cathodoluminescence in the scanning transmission electron microscope," *Ultramicroscopy* **176**, 112–131 (2017).
- ⁸⁹S. Meuret, L. H. Tizei, T. Cazimajou, R. Bourrellier, H. C. Chang, F. Treussart, and M. Kociak, "Photon bunching in cathodoluminescence," *Phys. Rev. Lett.* **114**, 197401 (2015).
- ⁹⁰N. Varkentina, Y. Auad, S. Y. Woo, A. Zobelli, J.-D. Blazit, X. Li, M. Tencé, K. Watanabe, T. Taniguchi, O. Stéphan, M. Kociak, and L. H. G. Tizei, "Cathodoluminescence excitation spectroscopy: Nanoscale imaging of excitation pathways," *Sci. Adv.* **8**, 4947 (2022).
- ⁹¹B. J. Brenny, T. Coenen, and A. Polman, "Quantifying coherent and incoherent cathodoluminescence in semiconductors and metals," *J. Appl. Phys.* **115**, 244307 (2014).
- ⁹²F. J. García De Abajo, A. Rivacoba, N. Zabala, and N. Yamamoto, "Boundary effects in Čerenkov radiation," *Phys. Rev. B* **69**, 155420 (2004).
- ⁹³A. P. Potylitsyn, M. I. Ryazanov, M. N. Strikhanov, and A. A. Tishchenko, *Diffraction Radiation from Relativistic Particles*, Springer Tracts in Modern Physics Vol. 239 (Springer, 2010).
- ⁹⁴J. Yuan, X. Sang, C. Yu, Y. Han, G. Zhou, S. Li, and L. Hou, "Highly efficient and broadband Čerenkov radiation at the visible wavelength in the fundamental mode of photonic crystal fiber," *IEEE Photonics Technol. Lett.* **23**, 786–788 (2011).
- ⁹⁵G. Chang, L.-J. Chen, and F. X. Kärtner, "Highly efficient Čerenkov radiation in photonic crystal fibers for broadband visible wavelength generation," *Opt. Lett.* **35**(14), 2361–2363 (2010).

- ⁹⁶D. V. Skryabin, F. Luan, J. C. Knight, and P. S. J. Russell, "Soliton self-frequency shift cancellation in photonic crystal fibers," *Science* **301**, 1705–1708 (2003).
- ⁹⁷X. B. Zhang, X. Zhu, L. Chen, F. G. Jiang, X. B. Yang, J. G. Peng, and J. Y. Li, "Enhanced violet Cherenkov radiation generation in GeO₂-doped photonic crystal fiber," *Appl. Phys. B: Lasers Opt.* **111**, 273–277 (2013).
- ⁹⁸M. A. Belkin and F. Capasso, "New frontiers in quantum cascade lasers: High performance room temperature terahertz sources," *Phys. Scr.* **90**, 118002 (2015).
- ⁹⁹S. Vavilov, "On the possible causes of blue γ -glow of liquids," *C. R. Dokl. Akad. Nauk SSSR* **28**, 457 (1934).
- ¹⁰⁰I. Frank and I. Tamm, "Coherent visible radiation from fast electrons passing through matter," *Phys.-Usp.* **93**, 388 (1937).
- ¹⁰¹P. Cherenkov, "The visible light emitted by electrons moving with velocities exceeding that of light in a medium," *C. R. Acad. Sci. USSR* **14**, 101–105 (1937).
- ¹⁰²P. Cherenkov, "Spatial distribution of visible radiation produced by fast electrons," *C. R. (Dokl.) Acad. Sci. URSS* **21**, 319–321 (1938).
- ¹⁰³I. E. Tamm, "General characteristics of radiation emitted by systems moving with superlight velocities with some applications to plasma physics," Nobel Lectures, 1959.
- ¹⁰⁴V. Ginzburg and I. Frank, "To the theory of transition radiation," *Sov. Phys. JETP* **16**, 15 (1946).
- ¹⁰⁵G. Garibyan, "Transition radiation effects in particle energy losses," *Sov. Phys. J.* **37**, 372–376 (1960).
- ¹⁰⁶I. Frank, "Doppler effect in a refractive medium," *Izv. Akad. Nauk USSR, Ser. Fiz.* **6**, 3 (1942).
- ¹⁰⁷V. Ginzburg and I. Frank, "On the Doppler effect at the superluminal velocity," *Dokl. Akad. Nauk SSSR* **56**, 583–586 (1947).
- ¹⁰⁸G. Urbain, *La Phosphorescence Cathodique Des Terres Rares* (Gauthier-Villars, 1909).
- ¹⁰⁹W. C. Röntgen, "On a new kind of rays," *Science* **3**, 227–231 (1896).
- ¹¹⁰P. Lecoq, "Development of new scintillators for medical applications," *Nucl. Instrum. Methods Phys. Res. Sect. A* **809**, 130–139 (2016).
- ¹¹¹G. Remond, M. R. Phillips, and C. Roques-Carmes, "Importance of instrumental and experimental factors on the interpretation of cathodoluminescence data from wide band gap materials," in *Cathodoluminescence in Geosciences* (Springer, Berlin, Heidelberg, 2000), pp. 59–126.
- ¹¹²B. G. Yacobi and D. B. Holt, "Cathodoluminescence scanning electron microscopy of semiconductors," *J. Appl. Phys.* **59**, R1 (1986).
- ¹¹³G. F. Garlick, "Cathodoluminescence," *Adv. Electron. Electron Phys.* **2**, 151–184 (1950).
- ¹¹⁴S. E. Tsimring, *Electron Beams and Microwave Vacuum Electronics* (Wiley, 2006), pp. 1–573.
- ¹¹⁵M. C. Lampel, "Coherent Smith–Purcell radiation as a pulse length diagnostic," *Nucl. Instrum. Methods Phys. Res., Sect. A* **385**, 19–25 (1997).
- ¹¹⁶This review focuses on spontaneous emission from free electrons, which is why we do not display major achievements like the first operation of a free-electron laser,³⁴⁷ or work on dielectric laser accelerators³¹⁰ in the timeline (though we discuss their connection with nanophotonics in Sec. IV).
- ¹¹⁷H. Ishizuka, Y. Kawamura, K. Yokoo, H. Shimawaki, and A. Hosono, "Smith–Purcell experiment utilizing a field-emitter array cathode: Measurements of radiation," *Nucl. Instrum. Methods Phys. Res. A* **475**, 593–598 (2001).
- ¹¹⁸C. Roques-Carmes, S. Kooi, Y. Yang, A. Massuda, P. D. Keathley, A. Zaidi, Y. Yang, J. D. Joannopoulos, K. K. Berggren, I. E. Kaminer, and M. Soljačić, "Towards integrated tunable all-silicon free-electron light sources," *Nat. Commun.* **10**, 3176 (2019).
- ¹¹⁹D. Vick, H. Sahasrabudhe, M. Malac, P. Shekhar, R. Rahman, S. Pendharker, and Z. Jacob, "Extreme ultraviolet plasmonics and Cherenkov radiation in silicon," *Optica* **5**(12), 1590–1596 (2018).
- ¹²⁰X. Zhang, M. Hu, Z. Zhang, Y. Wang, T. Zhang, X. Xu, T. Zhao, Z. Wu, R. Zhong, D. Liu, Y. Wei, Y. Gong, and S. Liu, "High-efficiency threshold-less Cherenkov radiation generation by a graphene hyperbolic grating in the terahertz band," *Carbon* **183**, 225–231 (2021).
- ¹²¹S. A. Guerrero and A. I. Akinwande, "Silicon field emitter arrays with current densities exceeding 100 A/cm² at gate voltages below 75 V," *IEEE Electron Device Lett.* **37**, 96–99 (2016).
- ¹²²S. A. Guerrero and A. I. Akinwande, "Nanofabrication of arrays of silicon field emitters with vertical silicon nanowire current limiters and self-aligned gates," *Nanotechnology* **27**, 295302 (2016).
- ¹²³D. Temple, "Recent progress in field emitter array development for high performance applications," *Mater. Sci. Eng., R* **24**, 185–239 (1999).
- ¹²⁴Y. Yang, C. Roques-Carmes, S. E. Kooi, H. Tang, J. Beroz, E. Mazur, I. Kaminer, J. D. Joannopoulos, and M. Soljačić, "Photonic flatband resonances for free-electron radiation," *Nature* **613**, 42–47 (2023).
- ¹²⁵R. Remez, N. Shapira, C. Roques-Carmes, R. Tirole, Y. Yang, Y. Lereah, M. Soljačić, I. Kaminer, and A. Arie, "Spectral and spatial shaping of Smith–Purcell radiation," *Phys. Rev. A* **96**, 061801 (2017).
- ¹²⁶S. L. Chuang and J. A. Kong, "Enhancement of Smith–Purcell radiation from a grating with surface-plasmon excitation," *J. Opt. Soc. Am. A* **1**, 672 (1984).
- ¹²⁷T. Coenen, E. J. R. Vesseur, and A. Polman, "Angle-resolved cathodoluminescence spectroscopy," *Appl. Phys. Lett.* **99**, 143103 (2011).
- ¹²⁸Y. Yang, C. Roques-Carmes, I. Kaminer, A. Zaidi, A. Massuda, Y. Yang, S. E. Kooi, K. K. Berggren, and M. Soljačić, "Manipulating Smith–Purcell radiation polarization with metasurfaces," in Conference on Lasers and Electro-Optics, CLEO, 2018.
- ¹²⁹V. Veselago, "Electrodynamics of substances with simultaneously negative electrical and magnetic permeabilities," *Sov. Phys. Usp.* **10**, 509–514 (1968).
- ¹³⁰Y. U. Ye, F. Liu, M. Wang, L. Tai, K. Cui, X. Feng, W. Zhang, and Y. Huang, "Deep-ultraviolet Smith–Purcell radiation," *Optica* **6**, 592–597 (2019).
- ¹³¹K. Watanabe, T. Taniguchi, T. Niiyama, K. Miya, and M. Taniguchi, "Far-ultraviolet plane-emission handheld device based on hexagonal boron nitride," *Nat. Photonics* **3**, 591–594 (2009).
- ¹³²K. Watanabe and T. Taniguchi, "Hexagonal boron nitride as a new ultraviolet luminescent material and its application," *Int. J. Appl. Ceram. Technol.* **8**, 977–989 (2011).
- ¹³³K. Watanabe, T. Taniguchi, and H. Kanda, "Direct-bandgap properties and evidence for ultraviolet lasing of hexagonal boron nitride single crystal," *Nat. Mater.* **3**, 404–409 (2004).
- ¹³⁴J. Urata, M. Goldstein, M. F. Kimmitt, A. Naumov, C. Platt, and J. E. Walsh, "Superradiant Smith–Purcell emission," *Phys. Rev. Lett.* **80**, 516–519 (1998).
- ¹³⁵M. Goldstein, J. E. Walsh, M. F. Kimmitt, J. Urata, and C. L. Platt, "Demonstration of a micro far-infrared Smith–Purcell emitter," *Appl. Phys. Lett.* **71**, 452 (1998).
- ¹³⁶T. Coenen and N. M. Haegel, "Cathodoluminescence for the 21st century: Learning more from light," *Appl. Phys. Rev.* **4**, 031103 (2017).
- ¹³⁷R. Dahan, S. Neheemia, M. Shentcis, O. Reinhardt, Y. Adiv, X. Shi, O. Be'er, M. H. Lynch, Y. Kurman, K. Wang, and I. Kaminer, "Resonant phase-matching between a light wave and a free-electron wavefunction," *Nat. Phys.* **16**, 1123–1131 (2020).
- ¹³⁸Y. Morimoto and P. Baum, "Diffraction and microscopy with attosecond electron pulse trains," *Nat. Phys.* **14**, 252–256 (2018).
- ¹³⁹K. E. Priebe, C. Rathje, S. V. Yalunin, T. Hohage, A. Feist, S. Schäfer, and C. Ropers, "Attosecond electron pulse trains and quantum state reconstruction in ultrafast transmission electron microscopy," *Nat. Photonics* **11**, 793–797 (2017).
- ¹⁴⁰G. M. Vanacore, I. Madan, G. Berruto, K. Wang, E. Pomarico, R. J. Lamb, D. McGrouther, I. Kaminer, B. Barwick, F. J. García De Abajo, and F. Carbone, "Attosecond coherent control of free-electron wave functions using semi-infinite light fields," *Nat. Commun.* **9**(1), 2694 (2018).
- ¹⁴¹M. Kozák, N. Schönerberger, and P. Hommelhoff, "Ponderomotive generation and detection of attosecond free-electron pulse trains," *Phys. Rev. Lett.* **120**, 103203 (2018).
- ¹⁴²A. Feist, K. E. Echternkamp, J. Schauss, S. V. Yalunin, S. Schäfer, and C. Ropers, "Quantum coherent optical phase modulation in an ultrafast transmission electron microscope," *Nature* **521**, 200–203 (2015).
- ¹⁴³V. D. Giulio, M. Kociak, and F. J. G. de Abajo, "Probing quantum optical excitations with fast electrons," *Optica* **6**, 1524 (2019).
- ¹⁴⁴J. Lim, Y. S. Ang, L. K. Ang, and L. J. Wong, "Control of atom-photon interactions with shaped quantum electron wavepackets," *arXiv:2111.13317* (2021).
- ¹⁴⁵B. Barwick, D. J. Flannigan, and A. H. Zewail, "Photon-induced near-field electron microscopy," *Nature* **462**, 902–906 (2009).
- ¹⁴⁶S. T. Park, M. Lin, and A. H. Zewail, "Photon-induced near-field electron microscopy (PINEM): Theoretical and experimental," *New J. Phys.* **12**, 123028 (2010).

- ¹⁴⁷F. J. Garcia De Abajo, A. Asenjo-Garcia, and M. Kociak, "Multiphoton absorption and emission by interaction of swift electrons with evanescent light fields," *Nano Lett.* **10**, 1859–1863 (2010).
- ¹⁴⁸G. M. Vanacore, G. Berruto, I. Madan, E. Pomarico, P. Biagioni, R. J. Lamb, D. McGrouther, O. Reinhardt, I. Kaminer, B. Barwick, H. Larocque, V. Grillo, E. Karimi, F. J. Garcia de Abajo, and F. Carbone, "Ultrafast generation and control of an electron vortex beam via chiral plasmonic near fields," *Nat. Mater.* **18**, 573–579 (2019).
- ¹⁴⁹R. Dahan, A. Gorlach, U. Haeusler, A. Karnieli, O. Eyal, P. Yousefi, M. Segev, A. Arie, G. Eisenstein, P. Hommelhoff, and I. Kaminer, "Imprinting the quantum statistics of photons on free electrons," *Science* **373**, abj7128 (2021).
- ¹⁵⁰J. W. Henke, A. S. Raja, A. Feist, G. Huang, G. Arend, Y. Yang, F. J. Kappert, R. N. Wang, M. Möller, J. Pan, J. Liu, O. Kfir, C. Ropers, and T. J. Kippenberg, "Integrated photonics enables continuous-beam electron phase modulation," *Nature* **600**, 653–658 (2021).
- ¹⁵¹A. Feist, G. Huang, G. Arend, Y. Yang, J.-W. Henke, A. S. Raja, F. J. Kappert, R. N. Wang, H. Lourenço-Martins, Z. Qiu, and J. Liu, "Cavity-mediated electron-photon pairs," *Science* **377**(6607), 777–780 (2022).
- ¹⁵²Y. Adiv, H. Hu, S. Tsesses, R. Dahan, K. Wang, Y. Kurman, A. Gorlach, H. Chen, X. Lin, G. Bartal, and I. Kaminer, "Observation of 2D Cherenkov radiation," [arXiv:2203.01698](https://arxiv.org/abs/2203.01698) (2022).
- ¹⁵³J. D. Jackson, *Classical Electrodynamics* (John Wiley, 1999).
- ¹⁵⁴A. Szczepkiewicz, L. Schächter, and R. J. England, "Frequency-domain calculation of Smith–Purcell radiation for metallic and dielectric gratings," *Appl. Opt.* **59**, 11146 (2020).
- ¹⁵⁵D. L. C. Chan, M. Soljačić, and J. D. Joannopoulos, "Direct calculation of thermal emission for three-dimensionally periodic photonic crystal slabs," *Phys. Rev. E* **74**, 036615 (2006).
- ¹⁵⁶F. J. de Abajo, A. Rivacoba, N. Zabala, and P. M. Echenique, "Electron energy loss spectroscopy as a probe of two-dimensional photonic crystals," *Phys. Rev. B* **68**, 205105 (2003).
- ¹⁵⁷F. J. Garcia de Abajo and L. A. Blanco, "Electron energy loss and induced photon emission in photonic crystals," *Phys. Rev. B* **67**, 125108 (2003).
- ¹⁵⁸A. Losquin and M. Kociak, "Link between cathodoluminescence and electron energy loss spectroscopy and the radiative and full electromagnetic local density of states," *ACS Photonics* **2**, 1619–1627 (2015).
- ¹⁵⁹A. Losquin, L. F. Zagonel, V. Myroshnychenko, B. Rodríguez-González, M. Tencé, L. Scarabelli, J. Förstner, L. M. Liz-Marzán, F. J. Garcia De Abajo, O. Stéphane, and M. Kociak, "Unveiling nanometer scale extinction and scattering phenomena through combined electron energy loss spectroscopy and cathodoluminescence measurements," *Nano Lett.* **15**, 1229–1237 (2015).
- ¹⁶⁰C. Kremers, D. N. Chigrin, and J. Kroha, "Theory of Cherenkov radiation in periodic dielectric media: Emission spectrum," *Phys. Rev. A* **79**, 013829 (2009).
- ¹⁶¹C. Roques-Carmes, N. Rivera, J. D. Joannopoulos, M. Soljačić, and I. Kaminer, "Nonperturbative quantum electrodynamics in the Cherenkov effect," *Phys. Rev. X* **8**, 041013 (2018).
- ¹⁶²I. Kaminer, Y. T. Katan, H. Buljan, Y. Shen, O. Ilic, J. J. Lopez, L. J. Wong, J. D. Joannopoulos, and M. Soljacic, "Efficient plasmonic emission by the quantum Čerenkov effect from hot carriers in graphene," *Nat. Commun.* **7**, 11880 (2016).
- ¹⁶³W. W. Salisbury, "Generation of light from free electrons," *J. Opt. Soc. Am.* **60**(10), 1279–1284 (1970).
- ¹⁶⁴N. Yamamoto, F. Javier Garcia De Abajo, and V. Myroshnychenko, "Interference of surface plasmons and Smith–Purcell emission probed by angle-resolved cathodoluminescence spectroscopy," *Phys. Rev. B: Condens. Matter Mater. Phys.* **91**, 125144 (2015).
- ¹⁶⁵S. Tsesses, G. Bartal, and I. Kaminer, "Light generation via quantum interaction of electrons with periodic nanostructures," *Phys. Rev. A* **95**, 013832 (2017).
- ¹⁶⁶V. G. Baryshevsky, K. G. Batrakov, I. D. Feranchuk, A. O. Grubich, A. A. Gurinovich, A. S. Lobko, A. A. Rouba, P. F. Safronov, V. I. Stolyarsky, B. A. Tarnopolsky, and A. P. Ulyanenko, "Coherent bremsstrahlung and parametric x-ray radiation from nonrelativistic electrons in a crystal," *Tech. Phys. Lett.* **32**, 392–395 (2006).
- ¹⁶⁷V. G. Baryshevsky and I. D. Feranchuk, "Parametric x-rays from ultrarelativistic electrons in a crystal: Theory and possibilities of practical utilization," *J. Phys. Paris* **44**, 913–922 (1983).
- ¹⁶⁸H. Überall, "High-energy interference effect of Bremsstrahlung and pair production in crystals," *Phys. Rev.* **103**, 1055–1067 (1956).
- ¹⁶⁹Y. Korobochko, V. Kosmach, and V. I. Mineev, "On coherent electron Bremsstrahlung," *Sov. Phys. JETP* **21**, 1248–1256 (1965).
- ¹⁷⁰L. J. Wong and I. Kaminer, "Prospects in x-ray science emerging from quantum optics and nanomaterials," *Appl. Phys. Lett.* **119**, 130502 (2021).
- ¹⁷¹Y. J. Tan, P. Pitchappa, N. Wang, R. Singh, and L. J. Wong, "Space-time wave packets from Smith–Purcell radiation," *Adv. Sci.* **8**, 2100925 (2021).
- ¹⁷²A. Balanov, A. Gorlach, and I. Kaminer, "Temporal and spatial design of x-ray pulses based on free-electron–crystal interaction," *APL Photonics* **6**, 070803 (2021).
- ¹⁷³J. P. Bachheimer, "Experimental investigation of the interaction radiation of a moving electron with a metallic grating: The Smith–Purcell effect," *Phys. Rev. B* **6**, 2985–2994 (1972).
- ¹⁷⁴I. Kaminer, S. E. Kooi, R. Shiloh, B. Zhen, Y. Shen, J. J. López, R. Remez, S. A. Skirlo, Y. Yang, J. D. Joannopoulos, A. Arie, and M. Soljačić, "Spectrally and spatially resolved Smith–Purcell radiation in plasmonic crystals with short-range disorder," *Phys. Rev. X* **7**, 011003 (2017).
- ¹⁷⁵S. Huang, R. Duan, N. Pramanik, J. S. Herrin, C. Boothroyd, "Z. Liu, and L. J. Wong, Quantum recoil in free electron-driven spontaneous emission from van der Waals crystals," in Conference on Lasers and Electro-Optics (CLEO), 2022.
- ¹⁷⁶V. L. Ginzburg and V. N. Tsytovich, "Transition radiation and transition scattering: Some questions regarding the theory," *Moscow Izdatel. Nauka* **1984**, 360.
- ¹⁷⁷K. A. Barsukov, "Transition radiation in a waveguide," *Sov. Phys. JETP* **37**, 1106–1109 (1960).
- ¹⁷⁸K. Yamada, T. Hosokawa, and H. Takenaka, "Observation of soft x rays of single-mode resonant transition radiation from a multilayer target with a sub-micrometer period," *Phys. Rev. A* **59**, 3673 (1999).
- ¹⁷⁹B. Pardo and J. M. André, "Classical theory of resonant transition radiation in multilayer structures," *Phys. Rev. E* **63**, 016613 (2000).
- ¹⁸⁰O. Keller, "Electrodynamic surface dressing of a moving electron: Cherenkov–Landau surface shock waves," *Phys. Lett. A* **188**, 272–280 (1994).
- ¹⁸¹S. Liu, P. Zhang, W. Liu, S. Gong, R. Zhong, Y. Zhang, and M. Hu, "Surface polariton Cherenkov light radiation source," *Phys. Rev. Lett.* **109**, 153902 (2012).
- ¹⁸²F. J. Garcia De Abajo, "Multiple excitation of confined graphene plasmons by single free electrons," *ACS Nano* **7**, 11409–11419 (2013).
- ¹⁸³S. Gong, M. Hu, R. Zhong, X. Chen, P. Zhang, T. Zhao, and S. Liu, "Electron beam excitation of surface plasmon polaritons," *Opt. Express* **22**, 19252 (2014).
- ¹⁸⁴X. Lin, I. Kaminer, X. Shi, F. Gao, Z. Yang, Z. Gao, H. Buljan, J. D. Joannopoulos, M. Soljačić, H. Chen, and B. Zhang, "Splashing transients of 2D plasmons launched by swift electrons," *Sci. Adv.* **3**, e1601192 (2017).
- ¹⁸⁵H. Hu, X. Lin, L. J. Wong, Q. Yang, D. Liu, B. Zhang, and Y. Luo, "Surface Dyakonov–Cherenkov radiation," *eLight* **2**, 2 (2022).
- ¹⁸⁶P. Chao, B. Strekha, R. Kuate Defo, S. Molesky, and A. W. Rodriguez, "Physical limits on electromagnetic response," *Nat. Rev. Phys.* **4**(8), 543–559 (2022).
- ¹⁸⁷O. D. Miller, A. G. Polimeridis, M. T. Homer Reid, C. W. Hsu, B. G. DeLacy, J. D. Joannopoulos, M. Soljačić, and S. G. Johnson, "Fundamental limits to optical response in absorptive systems," *Opt. Express* **24**, 3329 (2016).
- ¹⁸⁸H. Shim, H. Chung, and O. D. Miller, "Maximal free-space concentration of electromagnetic waves," *Phys. Rev. Appl.* **10**, 14007 (2020).
- ¹⁸⁹J. Michon, M. Benzaouia, M. Benzaouia, W. Yao, O. D. Miller, and S. G. Johnson, "Limits to surface-enhanced Raman scattering near arbitrary-shape scatterers," *Opt. Express* **27**, 35189–35202 (2019).
- ¹⁹⁰H. Shim, L. Fan, S. G. Johnson, and O. D. Miller, "Fundamental limits to near-field optical response over any bandwidth," *Phys. Rev. X* **9**, 011043 (2019).
- ¹⁹¹N. Talebi, *Near-Field-Mediated Photon-Electron Interactions*, Springer Series in Optical Sciences, Vol. 228 (Springer International Publishing, Cham, 2019).
- ¹⁹²N. Talebi, "Strong interaction of slow electrons with near-field light visited from first principles," *Phys. Rev. Lett.* **125**, 080401 (2020).
- ¹⁹³M. Liebrau, M. Sivilis, A. Feist, H. Lourenço-Martins, N. Pazos-Pérez, R. A. Alvarez-Puebla, F. J. G. de Abajo, A. Polman, and C. Ropers, "Spontaneous

- and stimulated electron-photon interactions in nanoscale plasmonic near fields,” *Light: Sci. Appl.* **10**, 82 (2021).
- ¹⁹⁴C. Roques-Carmes, Z. Lin, R. E. Christiansen, Y. Salamin, S. E. Kooi, J. D. Joannopoulos, S. G. Johnson, and M. Soljačić, “Toward 3D-printed inverse-designed metaoptics,” *ACS Photonics* **9**, 43–51 (2022).
- ¹⁹⁵C. I. Osorio, T. Coenen, B. J. M. Brenny, A. Polman, and A. F. Koenderink, “Angle-resolved cathodoluminescence imaging polarimetry,” *ACS Photonics* **3**, 147–154 (2015).
- ¹⁹⁶M. Solà-García, K. W. Mauser, N. van Nielen, T. Coenen, S. Meuret, and A. Polman, “Pump-probe cathodoluminescence microscopy,” [arXiv:2112.03034](https://arxiv.org/abs/2112.03034) (2021).
- ¹⁹⁷S. Meuret, M. Solà García, T. Coenen, E. Kieft, H. Zeijlemaker, M. Lätzel, S. Christiansen, S. Y. Woo, Y. H. Ra, Z. Mi, and A. Polman, “Complementary cathodoluminescence lifetime imaging configurations in a scanning electron microscope,” *Ultramicroscopy* **197**, 28–38 (2019).
- ¹⁹⁸A. Massuda, C. Roques-Carmes, A. Solanki, Y. Yang, S. E. Kooi, F. Habbal, I. Kaminer, M. Soljačić, F. Habbal, I. Kaminer, and M. Soljačić, “High-order Smith–Purcell radiation in silicon nanowires,” in *Conference on Lasers and Electro-Optics* (OSA, 2017), p. JTh5B.8.
- ¹⁹⁹L. Piazza, T. T. Lummen, E. Quiñonez, Y. Murooka, B. W. Reed, B. Barwick, and F. Carbone, “Simultaneous observation of the quantization and the interference pattern of a plasmonic near-field,” *Nat. Commun.* **6**, 6407 (2015).
- ²⁰⁰N. Yamamoto, “Development of high-resolution cathodoluminescence system for STEM and application to plasmonic nanostructures,” *Microscopy* **65**, 282–295 (2016).
- ²⁰¹J. K. So, K. F. MacDonald, and N. I. Zheludev, “Fiber optic probe of free electron evanescent fields in the optical frequency range,” *Appl. Phys. Lett.* **104**, 201101 (2014).
- ²⁰²J.-K. So, F. J. García de Abajo, K. F. MacDonald, and N. I. Zheludev, “Amplification of the evanescent field of free electrons,” *ACS Photonics* **2**, 1236–1240 (2015).
- ²⁰³A. I. Denisyyuk, G. Adamo, K. F. MacDonald, J. Edgar, M. D. Arnold, V. Myroshnychenko, M. J. Ford, F. J. García De Abajo, and N. I. Zheludev, “Transmitting hertzian optical nanoantenna with free-electron feed,” *Nano Lett.* **10**, 3250 (2010).
- ²⁰⁴J. Scheffold, S. Meuret, N. Schilder, T. Coenen, H. Agrawal, E. C. Garnett, and A. Polman, “Spatial resolution of coherent cathodoluminescence super-resolution microscopy,” *ACS Photonics* **6**, 1067–1072 (2019).
- ²⁰⁵T. Han, S. Zu, Z. Li, M. Jiang, X. Zhu, and Z. Fang, “Reveal and control of chiral cathodoluminescence at subnanoscale,” *Nano Lett.* **18**, 567–572 (2018).
- ²⁰⁶S. J. Bauman, Q. Yan, M. Benamara, and J. B. Herzog, “Plasmonic nanogap structures studied via cathodoluminescence imaging,” *Proc. SPIE* **10346**, 1034607 (2017).
- ²⁰⁷A. C. Liu, J. Lloyd, T. Coenen, and D. E. Gómez, “Mapping local surface plasmon modes in a nanoplasmonic trimer using cathodoluminescence in the scanning electron microscope,” *Microsc. Microanal.* **26**, 808–813 (2020).
- ²⁰⁸R. Ron, M. S. Zielinski, and A. Salomon, “Cathodoluminescence nanoscopy of 3D plasmonic networks,” *Nano Lett.* **20**, 8205–8211 (2020).
- ²⁰⁹V. Myroshnychenko, J. Nelayah, G. Adamo, N. Geuquet, J. Rodríguez-Fernández, I. Pastoriza-Santos, K. F. MacDonald, L. Henrard, L. M. Liz-Marzán, N. I. Zheludev, M. Kociak, and F. J. García De Abajo, “Plasmon spectroscopy and imaging of individual gold nanodecahedra: A combined optical microscopy, cathodoluminescence, and electron energy-loss spectroscopy study,” *Nano Lett.* **12**, 4172 (2012).
- ²¹⁰J. Krehl, G. Guzzinati, J. Schultz, P. Potapov, D. Pohl, J. Martin, J. Verbeeck, A. Fery, B. Büchner, and A. Lubk, “Spectral field mapping in plasmonic nanostructures with nanometer resolution,” *Nat. Commun.* **9**, 2080 (2018).
- ²¹¹B. J. Brenny, D. M. Beggs, R. E. Van Der Wel, L. Kuipers, and A. Polman, “Near-infrared spectroscopic cathodoluminescence imaging polarimetry on silicon photonic crystal waveguides,” *ACS Photonics* **3**, 2112–2121 (2016).
- ²¹²N. Talebi, W. Sigle, R. Vogelgesang, M. Esmann, S. F. Becker, C. Lienau, and P. A. Van Aken, “Excitation of mesoscopic plasmonic tapers by relativistic electrons: Phase matching versus eigenmode resonances,” *ACS Nano* **9**, 7641–7648 (2015).
- ²¹³J. Yan, X. Fang, L. Zhang, Y. Bando, U. K. Gautam, B. Dierre, T. Sekiguchi, and D. Golberg, “Structure and cathodoluminescence of individual ZnS/ZnO biaxial nanobelt heterostructures,” *Nano Lett.* **8**, 2794–2799 (2008).
- ²¹⁴A. Prabaswara, D. J. Stowe, B. Janjua, T. K. Ng, D. H. Anjum, P. Longo, C. Zhao, R. T. Elafandy, X. Li, A. Y. Alyamani, M. M. El-Desouki, and B. S. Ooi, “Spatially resolved investigation of competing nanocluster emission in quantum-disks-in-nanowires structure characterized by nanoscale cathodoluminescence,” *J. Nanophotonics* **11**, 026015 (2017).
- ²¹⁵D. T. Vu, N. Matthaikakakis, H. Saito, and T. Sannomiya, “Exciton-dielectric mode coupling in MoS₂ nanoflakes visualized by cathodoluminescence,” *Nanophotonics* **11**, 2129–2137 (2022).
- ²¹⁶P. R. Edwards, R. W. Martin, B. J. Kowalski, A. Pieniek, A. Reszka, S. Rodt, and S. Reitzenstein, “High-performance deterministic in situ electron-beam lithography enabled by cathodoluminescence spectroscopy,” *Nano Express* **2**, 014007 (2021).
- ²¹⁷A. C. Atre, B. J. Brenny, T. Coenen, A. García-Etxarri, A. Polman, and J. A. Dionne, “Nanoscale optical tomography with cathodoluminescence spectroscopy,” *Nat. Nanotechnol.* **10**, 429–436 (2015).
- ²¹⁸S. Fiedler, P. E. Stamatopoulou, A. Assadillayev, C. Wolff, H. Sugimoto, M. Fujii, N. A. Mortensen, S. Raza, and C. Tserkezis, “Disentangling cathodoluminescence spectra in nanophotonics: Particle eigenmodes vs transition radiation,” *Nano Lett.* **22**, 2320–2327 (2022).
- ²¹⁹K. W. Mauser, M. Solà-García, M. Liebrau, B. Damilano, P. M. Coulon, S. Vézien, P. A. Shields, S. Meuret, and A. Polman, “Employing cathodoluminescence for nanothermometry and thermal transport measurements in semiconductor nanowires,” *ACS Nano* **15**, 11385–11395 (2021).
- ²²⁰S. Pochon, K. F. MacDonald, R. J. Knize, and N. I. Zheludev, “Phase coexistence in gallium nanoparticles controlled by electron excitation,” *Phys. Rev. Lett.* **92**, 145702 (2004).
- ²²¹A. I. Denisyyuk, F. Jonsson, K. F. MacDonald, N. I. Zheludev, and F. J. García De Abajo, “Luminescence readout of nanoparticle phase state,” *Appl. Phys. Lett.* **92**, 093112 (2008).
- ²²²N. J. Schilder, H. Agrawal, E. C. Garnett, and A. Polman, “Phase-resolved surface plasmon scattering probed by cathodoluminescence holography,” *ACS Photonics* **7**, 1476–1482 (2020).
- ²²³T. Sannomiya, A. Konečná, T. Matsukata, Z. Thollar, T. Okamoto, F. J. García De Abajo, and N. Yamamoto, “Cathodoluminescence phase extraction of the coupling between nanoparticles and surface plasmon polaritons,” *Nano Lett.* **20**, 592–598 (2020).
- ²²⁴T. Coenen, A. Polman, K. J. Klein Koerkamp, S. Enoch, F. B. Segerink, N. F. van Hulst, and L. Kuipers, “Polarization-sensitive cathodoluminescence Fourier microscopy,” *Opt. Express* **20**, 18679–18691 (2012).
- ²²⁵S. Meuret, T. Coenen, H. Zeijlemaker, M. Lätzel, S. Christiansen, S. Conesa-Boj, and A. Polman, “Photon bunching reveals single-electron cathodoluminescence excitation efficiency in InGaN quantum wells,” *Phys. Rev. B* **96**, 035308 (2017).
- ²²⁶S. Meuret, T. Coenen, S. Y. Woo, Y. H. Ra, Z. Mi, and A. Polman, “Nanoscale relative emission efficiency mapping using cathodoluminescence $g^{(2)}$ imaging,” *Nano Lett.* **18**, 2288–2293 (2018).
- ²²⁷R. Bourrellier, S. Meuret, A. Tararan, O. Stéphan, M. Kociak, L. H. Tizei, and A. Zobelli, “Bright UV single photon emission at point defects in h-BN,” *Nano Lett.* **16**, 4317–4321 (2016).
- ²²⁸M. Kuttge, E. J. Vesseur, A. F. Koenderink, H. J. Lezec, H. A. Atwater, F. J. De Abajo, and A. Polman, “Local density of states, spectrum, and far-field interference of surface plasmon polaritons probed by cathodoluminescence,” *Phys. Rev. B: Condens. Matter Mater. Phys.* **79**, 113405 (2009).
- ²²⁹S. Peng, N. J. Schilder, X. Ni, J. Van De Groep, M. L. Brongersma, A. Alù, A. B. Khanikaev, H. A. Atwater, and A. Polman, “Probing the band structure of topological silicon photonic lattices in the visible spectrum,” *Phys. Rev. Lett.* **122**, 117401 (2019).
- ²³⁰F. J. García De Abajo and M. Kociak, “Probing the photonic local density of states with electron energy loss spectroscopy,” *Phys. Rev. Lett.* **100**, 106804 (2008).
- ²³¹S. Mignuzzi, M. Mota, T. Coenen, Y. Li, A. P. Mihai, P. K. Petrov, R. F. M. Oulton, S. A. Maier, and R. Sapienza, “Energy-momentum cathodoluminescence spectroscopy of dielectric nanostructures,” *ACS Photonics* **5**, 1381–1387 (2018).

- ²³²J. Silver, X. Yan, G. R. Fern, and N. Wilkinson, "Cathodoluminescent images and spectra of single crystals of $Y_2O_3:S:Tb^{3+}$ and $Gd_2O_3:S:Tb_{3+}$ nanometer sized phosphor crystals excited in a field emission scanning transmission electron microscope," *J. Phys.: Conf. Ser.* **619**, 012049 (2015).
- ²³³M. Stöger-Pollach, L. Kachtik, B. Miesenberger, and P. Retzl, "Transition radiation in EELS and cathodoluminescence," *Ultramicroscopy* **173**, 31–35 (2017).
- ²³⁴M. Stöger-Pollach, K. Bukvišová, S. Schwarz, M. Kvapil, T. Šamořil, and M. Horák, "Fundamentals of cathodoluminescence in a STEM: The impact of sample geometry and electron beam energy on light emission of semiconductors," *Ultramicroscopy* **200**, 111–124 (2019).
- ²³⁵M. Stöger-Pollach, C. F. Pichler, T. Dan, G. A. Zickler, K. Bukvišová, O. Eibl, and F. Brandstätter, "Coherent light emission in cathodoluminescence when using GaAs in a scanning (transmission) electron microscope," *Ultramicroscopy* **224**, 113260 (2021).
- ²³⁶R. Remez, A. Karnieli, S. Trajtenberg-Mills, N. Shapira, I. Kaminer, Y. Lereah, and A. Arie, "Observing the quantum wave nature of free electrons through spontaneous emission," *Phys. Rev. Lett.* **123**, 060401 (2019).
- ²³⁷A. Horl, G. Haberfehlner, A. Trugler, F. P. Schmidt, U. Hohenester, and G. Kothleitner, "Tomographic imaging of the photonic environment of plasmonic nanoparticles," *Nat. Commun.* **8**, 37 (2017).
- ²³⁸B. Barwick and A. H. Zewail, "Photonics and plasmonics in 4D ultrafast electron microscopy," *ACS Photonics* **2**, 1391–1402 (2015).
- ²³⁹D. S. Yang, O. F. Mohammed, and A. H. Zewail, "Scanning ultrafast electron microscopy," *Proc. Natl. Acad. Sci. U. S. A.* **107**, 14993–14998 (2010).
- ²⁴⁰R. J. Moerland, I. Gerward, C. Weppelman, M. W. H. Garming, P. Kruij, and J. P. Hoogenboom, "Time-resolved cathodoluminescence microscopy with sub-nanosecond beam blanking for direct evaluation of the local density of states," *Opt. Express* **24**, 24760–24772 (2016).
- ²⁴¹P. Genevet, D. Wintz, A. Ambrosio, A. She, R. Blanchard, and F. Capasso, "Controlled steering of Cherenkov surface plasmon wakes with a one-dimensional metamaterial," *Nat. Nanotechnol.* **10**, 804–809 (2015).
- ²⁴²E. Yablonovitch, "Accelerating reference frame for electromagnetic waves in a rapidly growing plasma: Unruh-Davies-Fulling-DeWitt radiation and the nonadiabatic Casimir effect," *Phys. Rev. Lett.* **62**, 1742 (1989).
- ²⁴³J. Sloan, N. Rivera, J. D. Joannopoulos, and M. Soljačić, "Controlling two-photon emission from superluminal and accelerating index perturbations," *Nat. Phys.* **18**, 67–74 (2021).
- ²⁴⁴D. Oue, K. Ding, and J. B. Pendry, "Cherenkov radiation in vacuum from a superluminal grating," *Phys. Rev. Res.* **4**, 013064 (2021).
- ²⁴⁵A. Dikopoltsev, Y. Sharabi, M. Lyubarov, Y. Lumer, S. Tsesses, E. Lustig, I. Kaminer, and M. Segev, "Light emission by free electrons in photonic time-crystals," *Proc. Natl. Acad. Sci. U. S. A.* **119**, e2119705119 (2022).
- ²⁴⁶M. Henstridge, C. Pfeiffer, D. Wang, A. Boltasseva, V. M. Shalaev, A. Grbic, and R. Merlin, "Synchrotron radiation from an accelerating light pulse," *Science* **362**, 439–442 (2018).
- ²⁴⁷S. A. Mikhailov, "Graphene-based voltage-tunable coherent terahertz emitter," *Phys. Rev. B* **87**, 115405 (2013).
- ²⁴⁸H. Chen and M. Chen, "Flipping photons backward: Reversed Cherenkov radiation," *Mater. Today* **14**, 34–41 (2011).
- ²⁴⁹S. Xi, H. Chen, T. Jiang, L. Ran, J. Huangfu, B. I. Wu, J. A. Kong, and M. Chen, "Experimental verification of reversed Cherenkov radiation in left-handed metamaterial," *Phys. Rev. Lett.* **103**, 194801 (2009).
- ²⁵⁰L. Jing, X. Lin, Z. Wang, I. Kaminer, H. Hu, E. Li, Y. Liu, M. Chen, B. Zhang, and H. Chen, "Polarization shaping of free-electron radiation by gradient bianisotropic metasurfaces," *Laser Photonics Rev.* **15**, 2000426 (2021).
- ²⁵¹S. Antipov, L. Spentzouris, W. Liu, W. Gai, and J. G. Power, "Wakefield generation in metamaterial-loaded waveguides," *J. Appl. Phys.* **102**, 034906 (2007).
- ²⁵²S. Antipov, L. Spentzouris, W. Gai, M. Conde, F. Franchini, R. Konecny, W. Liu, J. G. Power, Z. Yusof, and C. Jing, "Observation of wakefield generation in left-handed band of metamaterial-loaded waveguide," *J. Appl. Phys.* **104**, 014901 (2008).
- ²⁵³J. F. Zhu, C. H. Du, Z. W. Zhang, F. H. Li, P. K. Liu, A. W. Cross, and L. Zhang, "Free-electron-driven orbital angular momentum emitter," in 13th UK-Europe-China Workshop on Millimetre-Waves and Terahertz Technologies, UCMMT, 2020.
- ²⁵⁴Z. W. Zhang, C. H. Du, J. F. Zhu, F. H. Li, P. K. Liu, A. W. Cross, and L. Zhang, "Orbital angular momentum generator based on super Smith–Purcell radiation," in 13th UK-Europe-China Workshop on Millimetre-Waves and Terahertz Technologies, UCMMT, 2020.
- ²⁵⁵Z. Wang, K. Yao, M. Chen, H. Chen, and Y. Liu, "Manipulating Smith–Purcell emission with babinet metasurfaces," *Phys. Rev. Lett.* **117**, 157401 (2016).
- ²⁵⁶Y. C. Lai, T. C. Kuang, B. H. Cheng, Y. C. Lan, and D. P. Tsai, "Generation of convergent light beams by using surface plasmon locked Smith–Purcell radiation," *Sci. Rep.* **7**(1), 11096 (2017).
- ²⁵⁷A. Karnieli, D. Roitman, M. Liebrau, S. Tsesses, N. Van Nielsen, I. Kaminer, A. Arie, and A. Polman, "Cylindrical metals for generation and focusing of free-electron radiation," *Nano Lett.* **22**, 5641–5650 (2022).
- ²⁵⁸Z. Su, F. Cheng, L. Li, and Y. Liu, "Complete control of Smith–Purcell radiation by graphene metasurfaces," *ACS Photonics* **6**, 1947–1954 (2019).
- ²⁵⁹G. Li, B. P. Clarke, J.-K. So, K. F. MacDonald, and N. I. Zheludev, "Holographic free-electron light source," *Nat. Commun.* **7**, 13705 (2016).
- ²⁶⁰N. Talebi, S. Meuret, S. Guo, M. Hentschel, A. Polman, H. Giessen, and P. A. van Aken, "Merging transformation optics with electron-driven photon sources," *Nat. Commun.* **10**, 599 (2019).
- ²⁶¹P. M. Van den Berg, "Smith–Purcell radiation from a point charge moving parallel to a reflection grating," *J. Opt. Soc. Am.* **63**, 1588 (1973).
- ²⁶²J. R. Saavedra, D. Castells-Graells, and F. J. García De Abajo, "Smith–Purcell radiation emission in aperiodic arrays," *Phys. Rev. B* **94**, 035418 (2016).
- ²⁶³T. Coenen, F. Bernal Arango, A. F. Koenderink, and A. Polman, "Directional emission from a single plasmonic scatterer," *Nat. Commun.* **5**, 3250 (2014).
- ²⁶⁴T. Coenen and A. Polman, "Energy-momentum cathodoluminescence imaging of anisotropic directionality in elliptical aluminum plasmonic bullseye antennas," *ACS Photonics* **6**, 573–580 (2019).
- ²⁶⁵A. A. Peshkov, "Spin-polarization effects in cherenkov radiation from electrons," *Can. J. Phys.* **98**, 660–663 (2020).
- ²⁶⁶W. Li, J. Liu, Y. Gao, K. Zhou, and S. Liu, "Circular polarization of Cherenkov radiation assisted by a metasurface on waveguides," *Opt. Lett.* **45**, 315–318 (2020).
- ²⁶⁷Y. Shibata, S. Sasaki, K. Ishi, T. Takahashi, T. Matsuyama, and K. Kobayashi, "Generation of circularly polarized light by superposition of coherent transition radiation in the millimeter wavelength region," *Rev. Sci. Instrum.* **72**, 3221 (2001).
- ²⁶⁸L. Liu, H. Chang, C. Zhang, Y. Song, and X. Hu, "Terahertz and infrared Smith–Purcell radiation from babinet metasurfaces: Loss and efficiency," *Phys. Rev. B* **96**, 165435 (2017).
- ²⁶⁹M. Wang, M. Wang, M. Wang, F. Liu, F. Liu, F. Liu, Y. Lin, Y. Lin, Y. Lin, K. Cui, K. Cui, K. Cui, X. Feng, X. Feng, X. Feng, W. Zhang, W. Zhang, W. Zhang, Y. Huang, Y. Huang, and Y. Huang, "Vortex Smith–Purcell radiation generation with holographic grating," *Photonics Res.* **8**, 1309–1315 (2020).
- ²⁷⁰S. N. Galyamin and A. V. Tyukhtin, "Dielectric concentrator for Cherenkov radiation," *Phys. Rev. Lett.* **113**, 064802 (2014).
- ²⁷¹S. N. Galyamin, A. V. Tyukhtin, and V. V. VorobeV, "Focusing the Cherenkov radiation using dielectric concentrator: Simulations and comparison with theory," *J. Instrum.* **13**, C02029 (2018).
- ²⁷²B. P. Clarke, K. F. MacDonald, and N. I. Zheludev, "Direction-division multiplexed holographic free-electron-driven light sources," *Appl. Phys. Lett.* **112**, 021109 (2018).
- ²⁷³B. P. Clarke, B. Gholipour, K. F. Macdonald, and N. I. Zheludev, "All-dielectric free-electron-driven holographic light sources," *Appl. Phys. Lett.* **113**, 241902 (2018).
- ²⁷⁴N. Van Nielsen, M. Hentschel, N. Schilder, H. Giessen, A. Polman, and N. Talebi, "Electrons generate self-complementary broadband vortex light beams using chiral photon sieves," *Nano Lett.* **20**, 5975–5981 (2020).
- ²⁷⁵N. Talebi, "Spectral interferometry with electron microscopes," *Sci. Rep.* **6**, 33874 (2016).
- ²⁷⁶S. Yamaguti, J. i Inoue, O. Haeblerl, and K. Ohtaka, "Photonic crystals versus diffraction gratings in Smith–Purcell radiation," *Phys. Rev. B* **66**, 195202 (2002).
- ²⁷⁷C. W. Hsu, B. Zhen, A. D. Stone, J. D. Joannopoulos, and M. Soljačić, "Bound states in the continuum," *Nat. Rev. Mater.* **1**, 16048 (2016).

- ²⁷⁸S. Zheng, J. K. So, F. Liu, Z. Liu, N. Zheludev, and H. J. Fan, "Giant enhancement of cathodoluminescence of monolayer transitional metal dichalcogenides semiconductors," *Nano Lett.* **17**, 6475–6480 (2017).
- ²⁷⁹A. Knapitsch and P. Lecoq, "Review on photonic crystal coatings for scintillators," *Int. J. Mod. Phys. A* **29**, 1430070 (2015).
- ²⁸⁰D. N. Basov, M. M. Fogler, and F. J. García De Abajo, "Polaritons in van der Waals materials," *Science* **354**, aag1992 (2016).
- ²⁸¹J. D. Caldwell, I. Aharonovich, G. Cassabois, J. H. Edgar, B. Gil, and D. N. Basov, "Photonics with hexagonal boron nitride," *Nat. Rev. Mater.* **4**, 552–567 (2019).
- ²⁸²C. Elias, P. Valvin, T. Pelini, A. Summerfield, C. J. Mellor, T. S. Cheng, L. Eaves, C. T. Foxon, P. H. Beton, S. V. Novikov, B. Gil, and G. Cassabois, "Direct band-gap crossover in epitaxial monolayer boron nitride," *Nat. Commun.* **10**, 2639 (2019).
- ²⁸³Q. Chen, J. Wu, X. Ou, B. Huang, J. Almutlaq, A. A. Zhumekenov, X. Guan, S. Han, L. Liang, Z. Yi, J. Li, X. Xie, Y. Wang, Y. Li, D. Fan, D. B. Teh, A. H. All, O. F. Mohammed, O. M. Bakr, T. Wu, M. Bettinelli, H. Yang, W. Huang, and X. Liu, "All-inorganic perovskite nanocrystal scintillators," *Nature* **561**, 88–93 (2018).
- ²⁸⁴E. M. Purcell, "Spontaneous emission probabilities at radio frequencies," *Phys. Rev.* **69**, 681 (1946).
- ²⁸⁵J.-J. Greffet, R. Carminati, K. Joulain, J.-P. Mulet, S. Mainguy, and Y. Chen, "Coherent emission of light by thermal sources," *Nature* **416**, 61–64 (2002).
- ²⁸⁶A. C. Overvig, S. A. Mann, and A. Alù, "Thermal metasurfaces: complete emission control by combining local and nonlocal light–matter interactions," *Phys. Rev. X* **11**, 021050 (2021).
- ²⁸⁷P. P. Iyer, R. A. DeCrescent, Y. Mohtashami, G. Lheureux, N. A. Butakov, A. Alhassan, C. Weisbuch, S. Nakamura, S. P. DenBaars, and J. A. Schuller, "Unidirectional luminescence from InGaN/GaN quantum-well metasurfaces," *Nat. Photonics* **14**, 543–548 (2020).
- ²⁸⁸S. Liu, A. Vaskin, S. Addamane, B. Leung, M. C. Tsai, Y. Yang, P. P. Vabishchevich, G. A. Keeler, G. Wang, X. He, Y. Kim, N. F. Hartmann, H. Htoon, S. K. Doorn, M. Zilk, T. Pertsch, G. Balakrishnan, M. B. Sinclair, I. Staude, and I. Brener, "Light-emitting metasurfaces: Simultaneous control of spontaneous emission and far-field radiation," *Nano Lett.* **18**, 6906–6914 (2018).
- ²⁸⁹B. Liu, H. Chen, J. Zhu, J. Liu, L. Chen, M. Gu, Q. Wu, X. Ouyang, X. Chen, and Z. Zhu, "Enhanced light extraction of plastic scintillator using large-area photonic crystal structures fabricated by hot embossing," *Opt. Express* **26**, 11438–11446 (2018).
- ²⁹⁰A. Knapitsch, E. Auffray, C. W. Fabjan, J. L. Leclercq, X. Letartre, R. Mazurczyk, and P. Lecoq, "Results of photonic crystal enhanced light extraction on heavy inorganic scintillators," *IEEE Trans. Nucl. Sci.* **59**, 2334–2339 (2012).
- ²⁹¹Z. Zhu, S. Wu, C. Xue, J. Zhao, L. Wang, Y. Wu, B. Liu, C. Cheng, M. Gu, H. Chen, and R. Tai, "Enhanced light extraction of scintillator using large-area photonic crystal structures fabricated by soft-x-ray interference lithography," *Appl. Phys. Lett.* **106**, 241901 (2015).
- ²⁹²P. Pignalosa, B. Liu, H. Chen, H. Smith, and Y. Yi, "Giant light extraction enhancement of medical imaging scintillation materials using biologically inspired integrated nanostructures," *Opt. Lett.* **37**, 2808 (2012).
- ²⁹³B. Liu, C. Zhang, F. Zhang, H. Tang, J. Liu, J. Xu, L. Chen, M. Gu, X. Ouyang, Z. Zhu, L. Chen, J. Liu, and X. Ouyang, "Improved light output from thick beta-Ga₂O₃ scintillation crystals via graded-refractive-index photonic crystals," *Opt. Express* **29**, 18646–18653 (2021).
- ²⁹⁴X. Ouyang, B. Liu, X. Xiang, L. Chen, M. Xu, X. Song, J. Ruan, J. Liu, C. Chen, Z. Zhu, and Y. Li, "Enhanced light output of CsI(Na) scintillators by photonic crystals," *Nucl. Instrum. Methods Phys. Res. Sect. A* **969**, 164007 (2020).
- ²⁹⁵N. Rivera, L. J. Wong, J. D. Joannopoulos, M. Soljačić, and I. Kaminer, "Light emission based on nanophotonic vacuum forces," *Nat. Phys.* **15**, 1284–1289 (2019).
- ²⁹⁶L. J. Wong, I. Kaminer, O. Ilic, J. D. Joannopoulos, and M. Soljačić, "Towards graphene plasmon-based free-electron infrared to x-ray sources," *Nat. Photonics* **10**, 46–52 (2015).
- ²⁹⁷Y. Yu, K. Lai, J. Shao, J. Power, M. Conde, W. Liu, S. Doran, C. Jing, E. Wisniewski, and G. Shvets, "Transition radiation in photonic topological crystals: Quasiresonant excitation of robust edge states by a moving charge," *Phys. Rev. Lett.* **123**, 057402 (2019).
- ²⁹⁸N. Talebi, "Schrödinger electrons interacting with optical gratings: Quantum mechanical study of the inverse Smith–Purcell effect," *New J. Phys.* **18**, 123006 (2016).
- ²⁹⁹G. Rosolen, L. J. Wong, N. Rivera, B. Maes, M. Soljačić, and I. Kaminer, "Metasurface-based multi-harmonic free-electron light source," *Light: Sci. Appl.* **7**, 64 (2018).
- ³⁰⁰L. Wong, X. Shi, A. Karnieli, I. Kaminer, and L. Wong, "Tailoring free electron spontaneous emission from graphene using shaped electron wavepackets," in *CLEO* (Optica Publishing Group, 2022), Paper No. JTh5P.3.
- ³⁰¹A. Gorlach, A. Karnieli, R. Dahan, E. Cohen, A. Pe'er, and I. Kaminer, "Ultrafast non-destructive measurement of the quantum state of light using free electrons," [arXiv:2012.12069](https://arxiv.org/abs/2012.12069) (2020).
- ³⁰²R. Shiloh, T. Chlouba, and P. Hommelhoff, "Quantum-coherent light-electron interaction in a scanning electron microscope," *Phys. Rev. Lett.* **128**, 235301 (2022).
- ³⁰³F. J. García de Abajo, "Interaction of radiation and fast electrons with clusters of dielectrics: A multiple scattering approach," *Phys. Rev. Lett.* **82**, 2776–2779 (1999).
- ³⁰⁴F. J. García De Abajo, R. J. Hernández, I. Kaminer, A. Meyerhans, J. Rosell-Llompard, and T. Sanchez-Elsner, "Back to normal: An old physics route to reduce SARS-CoV-2 transmission in indoor spaces," *ACS Nano* **14**, 7704–7713 (2020).
- ³⁰⁵S. Huang, R. Duan, N. Pramanik, C. Boothroyd, Z. Liu, and L. J. Wong, "Enhanced versatility of table-top x-rays from van der Waals structures," *Adv. Sci.* **9**, 2105401 (2022).
- ³⁰⁶X. Shi, Y. Kurman, M. Shentcis, L. J. Wong, F. J. G. de Abajo, and I. Kaminer, "Free-electron-driven x-ray caustics from strained van der Waals materials," in *CLEO: QELS Fundamental Science* (Optica Publishing Group, 2022), Paper No. FTh4A-5.
- ³⁰⁷K. Takahashi, A. Yoshikawa, A. Sandhu, Y. Ishitani, and Y. Kawakami, *Wide Bandgap Semiconductors: Fundamental Properties and Modern Photonic Electronic Devices* (Springer, 2007), pp. 1–460.
- ³⁰⁸A. Pizzi, G. Rosolen, L. J. Wong, R. Ischebeck, M. Soljačić, T. Feurer, and I. Kaminer, "Graphene metamaterials for intense, tunable, and compact extreme ultraviolet and x-ray sources," *Adv. Sci.* **7**, 1901609 (2020).
- ³⁰⁹T. Plettner and R. L. Byer, "Proposed dielectric-based microstructure laser-driven undulator," *Phys. Rev. Spec. Top.—Accel. Beams* **11**, 030704 (2008).
- ³¹⁰R. J. England, R. J. Noble, K. Bane, D. H. Dowell, C.-K. Ng, J. E. Spencer, S. Tantawi, Z. Wu, R. L. Byer, E. Peralta, K. Soong, C.-M. Chang, B. Montazeri, S. J. Wolf, B. Cowan, J. Dawson, W. Gai, P. Hommelhoff, Y.-C. Huang, C. Jing, C. McGuinness, R. B. Palmer, B. Naranjo, J. Rosenzweig, G. Travish, A. Mizrahi, L. Schachter, C. Sears, G. R. Werner, and R. B. Yoder, "Dielectric laser accelerators," *Rev. Mod. Phys.* **86**, 1337–1389 (2014).
- ³¹¹J. Breuer and P. Hommelhoff, "Laser-based acceleration of nonrelativistic electrons at a dielectric structure," *Phys. Rev. Lett.* **111**, 134803 (2013).
- ³¹²E. A. Peralta, K. Soong, R. J. England, E. R. Colby, Z. Wu, B. Montazeri, C. McGuinness, J. Mcneur, K. J. Leedle, D. Walz, E. B. Sozer, B. Cowan, B. Schwartz, G. Travish, and R. L. Byer, "Demonstration of electron acceleration in a laser-driven dielectric microstructure," *Nature* **503**, 91 (2013).
- ³¹³R. Shiloh, J. Illmer, T. Chlouba, P. Yousefi, N. Schönenberger, U. Niedermayer, A. Mittelbach, and P. Hommelhoff, "Electron phase-space control in photonic chip-based particle acceleration," *Nature* **597**, 498–502 (2021).
- ³¹⁴Z. Zhao, D. S. Black, R. J. England, T. W. Hughes, Y. Miao, O. Solgaard, R. L. Byer, and S. Fan, "Design of a multichannel photonic crystal dielectric laser accelerator," *Photonics Res.* **8**(10), 1586–1598 (2020).
- ³¹⁵S. Molesky, Z. Lin, A. Y. Piggott, W. Jin, J. Vucković, and A. W. Rodriguez, "Inverse design in nanophotonics," *Nat. Photonics* **12**, 659–670 (2018).
- ³¹⁶J. Jensen and O. Sigmund, "Topology optimization for nano-photonics," *Laser Photonics Rev.* **5**, 308–321 (2011).
- ³¹⁷W. Jin, W. Li, M. Orenstein, and S. Fan, "Inverse design of lightweight broadband reflector for relativistic lightsail propulsion," *ACS Photonics* **7**, 2350 (2020).
- ³¹⁸Z. Lin, B. Groever, F. Capasso, A. W. Rodriguez, and M. Lončar, "Topology-optimized multilayered metaoptics," *Phys. Rev. Appl.* **9**, 044030 (2018).

- ³¹⁹A. Y. Piggott, J. Lu, K. G. Lagoudakis, J. Petykiewicz, T. M. Babinec, and J. Vucković, “Inverse design and demonstration of a compact and broadband on-chip wavelength demultiplexer,” *Nat. Photonics* **9**, 374–377 (2015).
- ³²⁰Z. Lin, X. Liang, M. Lončar, S. G. Johnson, A. W. Rodriguez, and J. A. Paulson, “Cavity-enhanced second-harmonic generation via nonlinear-overlap optimization,” *Optica* **3**, 233–238 (2016).
- ³²¹A. M. Hammond, A. Oskooi, A. Oskooi, S. G. Johnson, and S. E. Ralph, “Photonic topology optimization with semiconductor-foundry design-rule constraints,” *Opt. Express* **29**, 23916–23938 (2021).
- ³²²U. Haeusler, M. Seidling, P. Yousefi, and P. Hommelhoff, “Boosting the efficiency of Smith–Purcell radiators using nanophotonic inverse design,” *ACS Photonics* **9**, 664–671 (2022).
- ³²³J. R. Fontana and R. H. Pantell, “A high-energy, laser accelerator for electrons using the inverse Cherenkov effect,” *J. Appl. Phys.* **54**, 4285 (1998).
- ³²⁴L. Schächter and A. Ron, “Smith–Purcell free-electron laser,” *Phys. Rev. A* **40**, 876 (1989).
- ³²⁵J. R. Pierce, “Traveling-wave tubes,” *Bell Syst. Tech. J.* **29**, 189–250 (1950).
- ³²⁶W. Xu and H. Xu, “Review of the high-power vacuum tube microwave sources based on Cherenkov radiation,” [arXiv:2003.04288](https://arxiv.org/abs/2003.04288) (2020).
- ³²⁷S. Fisher, C. Roques-Carmes, N. Rivera, L. J. Wong, I. Kaminer, and M. Soljačić, “Monochromatic x-ray source based on scattering from a magnetic nanoundulator,” *ACS Photonics* **7**, 1096–1103 (2020).
- ³²⁸H. L. Andrews and C. A. Brau, “Gain of a Smith–Purcell free-electron laser,” *Phys. Rev. Spec. Top.—Accel. Beams* **7**, 22–28 (2004).
- ³²⁹N. Rivera, C. Roques-Carmes, I. Kaminer, and M. Soljačić, “Toward nanophotonic free-electron lasers,” in *Conference on Lasers and Electro-Optics* (Optical Society of America, 2020), p. FM2Q.3.
- ³³⁰V. Kumar and K. J. Kim, “Analysis of Smith–Purcell free-electron lasers,” *Phys. Rev. E* **73**, 026501 (2006).
- ³³¹B. I. Wu, J. Lu, J. A. Kong, and M. Chen, “Left-handed metamaterial design for Čerenkov radiation,” *J. Appl. Phys.* **102**, 114907 (2007).
- ³³²R. Matloob and A. Ghaffari, “Čerenkov radiation in a causal permeable medium,” *Phys. Rev. A* **70**, 052116 (2004).
- ³³³L. Lu, J. D. Joannopoulos, and M. Soljačić, “Topological photonics,” *Nat. Photonics* **8**, 821–829 (2014).
- ³³⁴T. Ozawa, H. M. Price, A. Amo, N. Goldman, M. Hafezi, L. Lu, M. C. Rechtsman, D. Schuster, J. Simon, O. Zilberberg, and I. Carusotto, “Topological photonics,” *Rev. Mod. Phys.* **91**, 015006 (2019).
- ³³⁵Y. Song, N. Jiang, L. Liu, X. Hu, and J. Zi, “Cherenkov radiation from photonic bound states in the continuum: Towards compact free-electron lasers,” *Phys. Rev. Appl.* **10**, 064026 (2018).
- ³³⁶R. Yu, R. Alaei, R. W. Boyd, and F. J. G. De Abajo, “Ultrafast topological engineering in metamaterials,” *Phys. Rev. Lett.* **125**, 037403 (2020).
- ³³⁷A. Fallah, Y. Kiasat, M. G. Silveirinha, and N. Engheta, “Nonreciprocal guided waves in the presence of swift electron beams,” *Phys. Rev. B* **103**, 214303 (2021).
- ³³⁸Z. Wang, Y. Chong, J. D. Joannopoulos, and M. Soljačić, “Observation of unidirectional backscattering-immune topological electromagnetic states,” *Nature* **461**, 772–775 (2009).
- ³³⁹L. Lu, Z. Wang, D. Ye, L. Ran, L. Fu, J. D. Joannopoulos, and M. Soljačić, “Experimental observation of Weyl points,” *Science* **349**, 622–624 (2015).
- ³⁴⁰C. A. Spindt, C. E. Holland, A. Rosengreen, and I. Brodie, “Field-emitter arrays for vacuum microelectronics,” *IEEE Trans. Electron Devices* **38**, 2355–2363 (1991).
- ³⁴¹C.-M. Tang, T. A. Swyden, K. A. Thomason, L. N. Yadon, D. Temple, C. A. Ball, W. D. Palmer, J. E. Mancusi, D. Vellenga, and G. E. McGuire, “Emission measurements and simulation of silicon field-emitter arrays with linear planar lenses,” *J. Vac. Sci. Technol. B* **14**, 3455 (1996).
- ³⁴²H. Ishizuka, Y. Kawamura, K. Yokoo, H. Shimawaki, and A. Hosono, “Smith–Purcell radiation experiment using a field-emission array cathode,” *Nucl. Instrum. Methods Phys. Res. Sect. A* **445**, 276–280 (2000).
- ³⁴³Y. Neo, H. Shimawaki, T. Matsumoto, and H. Mimura, “Smith–Purcell radiation from ultraviolet to infrared using a Si field emitter,” *J. Vac. Sci. Technol. B* **24**, 924 (2006).
- ³⁴⁴U. Niedermayer, J. Lautenschläger, T. Egenolf, and O. Boine-Frankenheim, “Design of a scalable integrated nanophotonic electron accelerator on a chip,” *Phys. Rev. Appl.* **16**, 024022 (2021).
- ³⁴⁵D. Lemoine, “Vacuum packaging at the wafer level for the monolithic integration of MEMS and CMOS,” Master’s thesis (McGill University, 2009).
- ³⁴⁶M. Behnam, G. V. Kaigala, M. Khorasani, P. Marshall, C. J. Backhouse, and D. G. Elliott, “An integrated CMOS high voltage supply for lab-on-a-chip systems,” *Lab Chip* **8**, 1524–1529 (2008).
- ³⁴⁷D. A. Deacon, L. R. Elias, J. M. Madey, G. J. Ramian, H. A. Schwettman, and T. I. Smith, “First operation of a free-electron laser,” *Phys. Rev. Lett.* **38**, 892–894 (1977).
- ³⁴⁸G. Doucas, J. H. Mulvey, M. Otori, J. Walsh, and M. F. Kimmitt, “First observation of Smith–Purcell radiation from relativistic electrons,” *Phys. Rev. Lett.* **69**, 1761 (1992).